UNIVERSITY OF CALIFORNIA, SAN DIEGO

Histone acetylation dynamics play a critical role in co-transcriptional spliceosome assembly and spliceosomal rearrangements

A dissertation submitted in partial satisfaction of the requirements for the degree Doctor of Philosophy

in

Biology

by

Felizza F. Gunderson

Committee in charge:

Professor Tracy Johnson, Chair
Professor Gourisankar Ghosh
Professor Jim Kadonaga
Professor Lorraine Pillus
Professor Jim Wilhelm

2010

The Dissertation of Felizza F. Gunderson is approved, and it is acceptable in quality and form for publication on microfilm and electronically:

_____

_____

_____

_____

_____

Chair

University of California, San Diego

2010

DEDICATION

I would like to dedicate this dissertation to my parents.
Gracias por todo el amor y apoyo que me han dado.
Los quiero mucho.

To my husband, Carl, thank you for putting up with me during the craziness that is graduate school. I love you

EPIGRAPH

“Te deso lo major de la vida, la vida misma” ~ Fernando “Freddy” Quiñones

“Imagination is more important than knowledge."~ Albert Einstein

“This chamber has NO windows and NO doors, which offers you this chilling challenge - to find a way OUT! Of course, there's always my way.'
Vincent Price, Haunted Mansion, Disneyland

TABLE OF CONTENTS

LIST OF FIGURES

LIST OF TABLES

ACKNOWLEDGEMENTS

I would like to acknowledge Professor Tracy Johnson for guidance and direction throughout the course of this project.

I would like to acknowledge my dissertation committee for their helpful suggests and support throughout this process.

I would like to acknowledge the members of the T. Johnson lab (past and present) for scientific discussions and for making lab a fun environment to work in.

Portions of Chapter 2 were published as: Gunderson, Felizza Q and Johnson,Tracy L, 2009. Acetylation by the transcriptional coactivator Gcn5 plays a novel role in co-transcriptional spliceosome assembly. PLoS Genetics 5 (10) e1000682.

Portions of Chapter 3 have been submitted for publication as: Gunderson, Felizza Q and Johnson, Tracy L, 2010. Histone acetylation dynamics play a critical role in co-transcriptional spliceosome assembly and spliceosomal rearrangements.

VITA

Education

University of California, San Diego

PhD., Biology

September, 2010

San Diego State University

BS. Microbiology

May, 2003

Publications

Gunderson, FQ and Johnson, TL. 2010. Histone acetylation dynamics play a critical role in co-transcriptional spliceosome assembly and spliceosomal rearrangements. Submitted PNAS.

Gunderson, FQ and Johnson, TL. 2009. Acetylation by the transcriptional coactivator Gcn5 plays a novel role in co-transcriptional spliceosome assembly. *PLoS Genet 5:e*1000682 .

Layton T, Stalens C, **Gunderson F**, Goodison S, Silletti S. 2009. The Nonreceptor Tyrosine Kinase Syk acts as a Pancreatic Adenocarcinoma Tumor Suppressor via Regulation of Gene Expression and Cellular Invasion. *Am J Pathol 175:*2625-2636.

Becker E, Herrera NC, **Gunderson FQ**, Derman AI, Dance AL, Sims J, Larsen RA, Pogliano J. 2006. DNA segregation by the bacterial actin AlfA during *Bacillus subtilis* growth and development. *Embo J 25*:5919-5931.

Layton T, **Gunderson F**, Stalens C, Lee CY, Silletti S. 2009. Kinase activity is required for growth regulation but not invasion suppression by syk kinase in pancreatic adenocarcenoma cells. Submitted IJC.

Research Experience

Graduate Student *September 2004- 2010*
UCSD, Biological Sciences Ph.D. Program. In the laboratory of Dr. Tracy Johnson. My thesis project involves elucidating the interaction between specific splicing factors and histone modifying enzymes to coordinate transcription and pre-mRNA splicing in *Sacchromyces cerevisiae*.

Staff Research Associate I *June 2003- August 2004*
UCSD Cancer Center. In the laboratory of Dr. Steven Silletti: Cellular Interactions in Tumor Development, Melanoma, Metastasis, Pancreatic Cancer.

Undergraduate Research Assistant *January 2002 – May 2003*
San Diego State University. In the laboratory of Dr. Anca Segall: Biochemical analysis of TDP inhibitors, and researching the existence of TDP activity in prokaryotes.

Undergraduate Research Assistant *January 1999 - January 2002*
San Diego State University / Rees- Stealy Research Foundation. In the laboratory of Dr. Paul Paolini: Determining the effects of laminin and LPS on contractility of adult rat cardiomyocytes and the effect of a Lipid A analog on TLR4 expression in adult cardiomyocytes.

Summer Undergraduate Research Fellow *Summer 2000*
University of California, San Francisco. In the laboratory of Dr. Thomas Kornberg: Co-localization of Patch and Smoothened in the presence of Hedgehog in *Drosophila* wing development.

Teaching Experience

University of California, San Diego, La Jolla, CA
Teaching Assistant, Undergraduate Molecular Biology Lecture
September 2007 to December 2007

University of California, San Diego, La Jolla, CA
Teaching Assistant, Upper Division Structural Biochemistry Lecture
September 2006 to December 2006

University of California, San Diego, La Jolla, CA
Teaching Assistant, Undergraduate Microbiology Laboratory
January 2006 to March 2006

Presentations

2009, Annual Meeting of the RNA Society. “Acetylation by the Transcriptional Coactivator Gcn5 Plays a Novel Role in Co-transcriptional Spliceosome Assembly.” Talk

2006, Annual Meeting of the RNA Society. “Identification of Novel Interactions between Histone Acetyltransferases and *S cerevisiae* U2 snRNP Proteins” Poster

Awards:

2009-2010	University of California President’s Dissertation Year Fellowship
2006-2010	NIH F31 Predoctoral Research Service Award
2004-2006	San Diego Fellowship
2001-2003	Minority Biomedical Research Scholar
1999-2001	Minority Access to Research Careers Scholar
2000	CSU Sally Cassanova Predoctoral Fellowship
2000	Doris Howell Women’s Research Foundation Young Investigator Fellowship

ABSTRACT OF THE DISSETATION

Histone acetylation dynamics play a critical role in co-transcriptional spliceosome assembly and spliceosomal rearrangements

by

Felizza F. Gunderson

Doctor of Philosophy in Biology

University of California, San Diego, 2010

Professor Tracy Johnson, Chair

In the last several years, a number of studies have shown that spliceosome assembly and splicing catalysis can occur co-transcriptionally. However, it has been unclear which specific transcription factors play key roles in coupling splicing to transcription and the mechanisms through which they act. Here we report the discovery that Gcn5, which encodes the histone acetyltransferase (HAT) activity of the SAGA complex, has HAT-dependent genetic interactions with the genes encoding the heterodimeric U2 snRNP proteins Msl1 and Lea1, suggesting a functional relationship between Gcn5 HAT activity and Msl1/Lea1 function. To understand this relationship, we carried out an analysis of Gcn5's role in co-transcriptional recruitment of Msl1 and Lea1 to

pre-mRNA and find that Gcn5 HAT activity is required for co-transcriptional recruitment of the U2 snRNP (and subsequent snRNP) components to the branchpoint. Although previous studies suggested that transcription elongation can alter co-transcriptional pre-mRNA splicing, we do not observe evidence of defective transcription elongation for these genes in the absence of Gcn5, while Gcn5-dependent histone acetylation is enriched in the promoter regions. While all these data suggest a role for *histone* acetylation in co-transcriptional spliceosome assembly. A closer examination of the functional interactions between histone mutants and the U2 snRNP and the effects of histone mutants and histone deacetylation on spliceosome assembly provide convincing evidence of the functional coordination of histone deaceylation and splicing. Mutations in histone residues targeted by Gcn5 show genetic interactions with the U2 snRNP and splicing defects that mirror *GCN5* deletion. Furthermore, not only is Gcn5 associated throughout intron-containing genes, but deletion of multiple HDACs reveals peaks in acetylation in these regions, and this results in defects in spliceosome assembly. Finally, we present data that support a model whereby the Gcn5-dependent U2 snRNP recruitment facilitates HDAC recruitment, suggesting that splicing factors can, in fact, affect histone acetylation. These studies show that co-transcriptional spliceosome rearrangements are driven by dynamic changes in the acetylation state of histones and provide a model whereby spliceosome assembly is tightly coupled to histone modification.

Chapter 1: Introduction

Section 1.1: Pre-messenger RNA splicing is catalyzed by the Spliceosome

Eukaryotic genes contain introns that must be removed from the RNA-polymerase II transcribed pre-messenger RNA in order to produce a mature mRNA. The spliceosome is a macromolecular complex made up of over 100 proteins and five small nuclear RNAs (U1, U2, U4, U5, and U6). The snRNAs and their associated proteins form small ribonucleoprotein sub complexes (snRNPs) that recognize sequences in the pre-mNRA and are responsible for the removal of introns (reviewed in (Brow, 2002, Rino & Carmo-Fonseca, 2009). *In vitro* complex gel studies were used to elucidate the spliceosome assembly pathway. Using this assay, it was found that four splicing-specific snRNP complexes assemble together on the RNA to make a yeast spliceosome (Cheng & Abelson, 1987), and similar spliceosome assembly occurred in mammalian extracts (Konarska & Sharp, 1987, Lamond *et al.*, 1988). These *in vitro* experiments helped describe the spliceosome assembly pathway.

Spliceosome assembly begins with the association of the U1 snRNP with the 5' splice site of the pre-mRNA through base pairing of the 5' end of the U1 snRNA with the pre-mRNA (Rosbash & Seraphin, 1991). Subsequently, two splicing factors, BBP (branchpoint binding protein) and Mud2 recognize the branchpoint region to form the commitment complex. This is followed by the ATP-dependent addition of the U2 snRNP to the branchpoint and, destabilization

of Mud2/BBP to the form the pre-spliceosome (Ares, 1986, Parker *et al.*, 1987, Seraphin & Rosbash, 1989). A second ATP-dependent step leads to the additions of a pre-assembled tri-snRNP consisting of U4, U5 and U6 snRNPs to form a mature spliceosome (Figure 1.1). Through a series of rearrangements, U1 and U4 are released from this complex to create an active spliceosome competent to undergo the first catalytic step of splicing (Cheng & Abelson, 1987, Konarska & Sharp, 1987, Weidenhammer *et al.*, 1997). In the second catalytic step, additional rearrangements occur in the presence of ATP in order to release the various snRNPs from the spliced pre-mRNA (reviewed in (Konarska *et al.*, 2006, Staley & Guthrie, 1998, Wahl *et al.*, 2009).

The coordination of this assembly occurs via changes in RNA:RNA and RNA:Protein interactions. Interestingly, it is believed that many of these interactions are mutually exclusive; the formation of one requires the disruption of others (Staley & Guthrie, 1998). It is known that the U1 snRNA base pairs with the 5' splice site (Rosbash & Seraphin, 1991). However, this base pairing changes and is replaced by U6 snRNA base pairing with the 5' splice site to allow for the progression of spliceosome assembly (Konforti *et al.*, 1993, Staley & Guthrie, 1999). Additionally, the U2 snRNA undergoes changes in base pairing to allow for base pairing with the branchpoint and then with the U6 snRNA (Staley & Guthrie, 1998).

There are a number of other U2 snRNP rearrangements that facilitate spliceosome formation. For example, the activity of the U2 snRNP is modulated

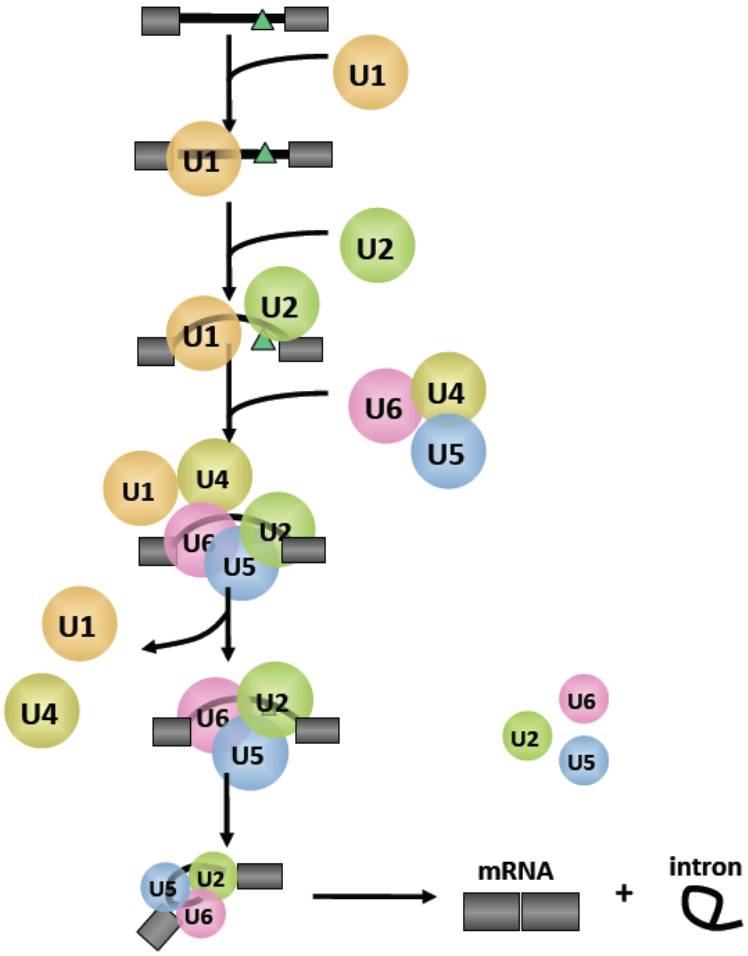

Figure 1.1: Pre-messenger RNA splicing is a dynamic process.
Pre-messenger RNA splicing is catalyzed by the spliceosome. The spliceosome is comprised of 5 small nuclear RNA's; U1, U2, U4, U5 and U6 and U snRNP and a multitude of different splicing factors. Spliceosome assembly occurs in a step-wise manner. In which U1 recognizes the 5' splice site, then U2 is recruited to the branchpoint sequence within the intron and a dynamic exchange in which U1 and U2 are released and the triple snRNP consisting of U4-U5-U6 complete the catalysis and the intron is released and remaining exons are ligated together.

via a switch between competing U2 conformations, which involves the release of factors such as Cus2 (Zavanelli *et al.*, 1994). Additionally, base pair changes within the triple snRNP lead to the disruption of U4 snRNA and U6 snRNA base pairing to allow for U6 snRNA to base pair with the U2 snRNA (Johnson & Abelson, 2001, Xu *et al.*, 1996, Yean & Lin, 1991).

A number of RNA:RNA and RNA:Protein rearrangements that occur during spliceosome assembly are ATP-dependent. The DEAD (Asp-Glu-Ala-Asp, or DEAD in one-letter code) or DExH/D- box family of RNA helicases use ATP hydrolysis to catalyze the rearrangements that occur during spliceosome assembly and splicing. For example, Prp5 is one of the first DEAD box proteins required in spliceosome assembly. Prp5 and ATP hydrolysis are required for stable association of the U2 snRNP with the pre-mRNA (Liao *et al.*, 1992, Ruby *et al.*, 1993). The helicase Brr2 which is a component of the U5 snRNP, is required for the removal of the U4 snRNP from the spliceosome (Maeder *et al.*, 2009). Additionally, the RNA helicase Prp28 has been shown to have the ability to disrupt RNA:Protein interactions during spliceosome assembly (Chen *et al.*, 2001, Jankowsky *et al.*, 2001). These helicases therefore play an important role in the necessary rearrangements for spliceosome assembly.

While spliceosomal proteins are critical for forming the catalytic spliceosome, the chemistry of the reaction is quite straightforward and is likely to be catalyzed by the RNA components of the catalytic center (Huppler *et al.*, 2002, Yean *et al.*, 2000, Valadkhan & Manley, 2001). The snRNPs assemble onto the pre-mRNA in a coordinated series of movements by binding to

sequences that are located on the 5’ and 3’ ends of introns (Figure 1.2). Introns are removed via two sequential transesterification reactions (Cech *et al.*, 1983, Zaug *et al.*, 1983). First, the 5’ splice site (SS) is attacked by the 2’ hydorxyl of the branchpoint adenosine. This generates a free 5’ hydroxyl and an intron-lariat connected to the 3’ exon. Next, the 3’ hydroxyl of the 5’ exon attacks the phosphodiester bond at the 3’SS, which leads to exon ligation and excision of the intron-lariat (Figure 1.2).

All of these studies demonstrate that the assembly of the spliceosome onto pre-mRNA is a very dynamic process that has to be precisely timed in order to ensure proper assembly and accurate splicing. Disruptions in the process can have a detrimental affect on the cell or an organism as a whole.

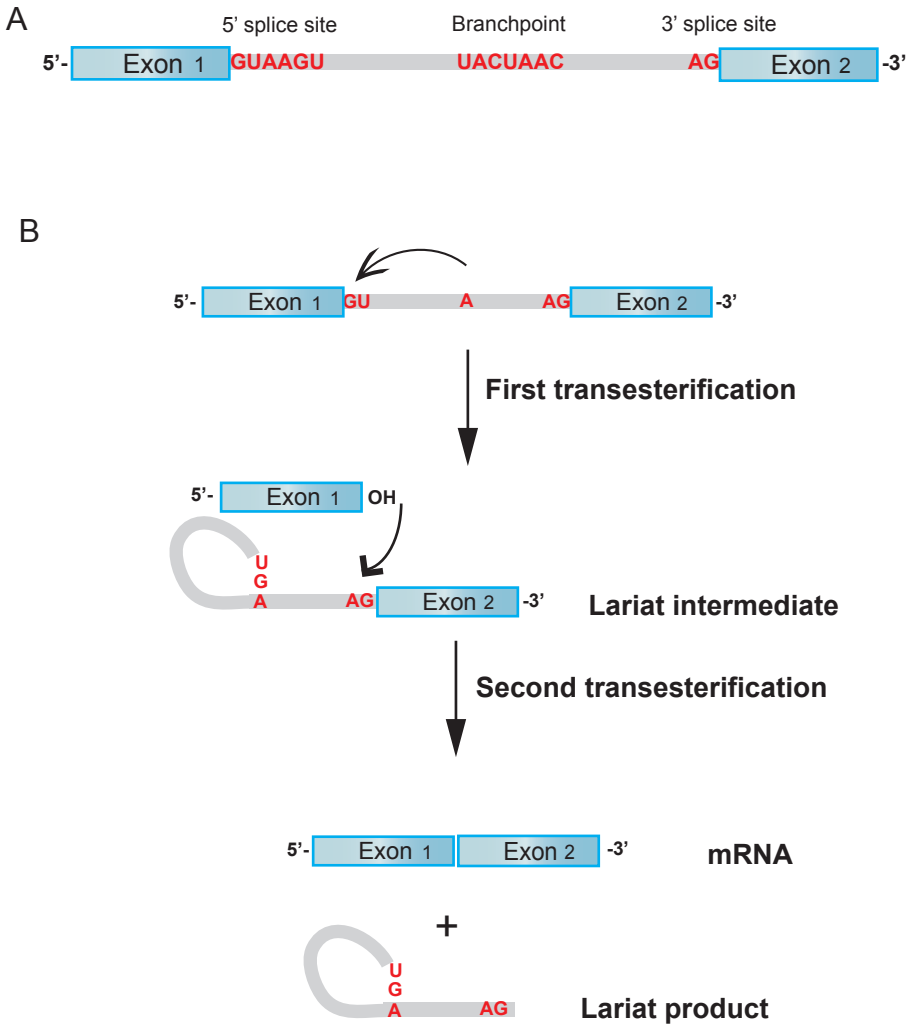

Figure 1.2: Pre-messenger RNA splicing occurs in two transesterification steps. A) Schematic of an intron-containing gene. Red font represents the 5' splice site, branchpoint and 3' splice site. Blue boxes represent exons. B) Splicing of intron and ligation of exons occurs in two transesterification steps. The 5' splice site is attacked by the 2' hyrdoxyl of the branchpoint adenosine. This generates a free 5' hydroxyl and an intron-lariat intermediate that is connected to the 3' exon. Subsequently, the 3' hydroxyl attacks the 3' splice site, which then releases the lariat intermediate, and ligation of the exons. (Adapted from Ritchie et al., 2009).

Section 1.2: Splicing and alternative splicing lead to protein diversity

Upon complete sequencing of the human genome, it was found that it contained far fewer genes than originally predicted (Venter *et al.*, 2001), suggesting that there were important mechanisms by which the proteome was expanded from the primary genome sequence. Remarkably, it was found that most human genes contained multiple exons with the average length of 50-250 basepairs (bp) and multiple introns (on average 10-12) that were thousands of basepairs long (Hawkins, 1988, Kalari *et al.*, 2006). Hence, through the process of alternative splicing, one transcript can produce a variety of different mature RNA (reviewed in (Black, 2000, Nilsen & Graveley, 2010).

The process of alternative splicing involves the differential use of splice sites to create protein diversity. There are four basic models of alternative splicing, alternative 5' splice site choice, and alternative 3' splice site choice, exon inclusion and exon skipping. Alternative splicing is facilitated by a family of proteins called SR (Ser-Arg) proteins (reviewed in (Chen & Manley, 2009, Shepard & Hertel, 2009). These proteins are involved in many steps during both constitutive splicing and alternative splicing and can influence splice site choice by facilitating or interfering with the binding of U1 or U2 snRNP to the splice sites (Cote *et al.*, 1999, Eperon *et al.*, 2000).

An example of how alternative splicing contributes to protein diversity is the human gene *KCNMA1.* This gene contains a variety of alternative 5' splice

sites and 3' splice sites and from this one gene, more than 500 mRNA isoforms can be generated (Navaratnam *et al.*, 1997, Rosenblatt *et al.*, 1997). Additionally, the best-known example of the power alternative splicing to create protein diversity is the *Drosophila melanogaster* gene *Dscam.* This one gene can produce up to 38,016 different isoforms (Schmucker *et al.*, 2000). Therefore, alternative splicing plays an important role in protein diversity in a variety of different organisms.

Many human genes express more than one mRNA by alternative splicing, a process that results in functionally diverse protein isoforms to be expressed. Since the majority of human genes contain introns and the majority of pre-mRNAs undergo alternative splicing, it is no surprise that defects in splicing can cause or modify human disease. It is estimated that 15-20% of point mutations that cause human disease cause splicing defects. Additionally, it is estimated that as many as 50% of disease causing mutations affect splicing (Lopez-Bigas *et al.*, 2005, Pan *et al.*, 2008, Wang *et al.*, 2008). However, it is not just mutations in alternative splicing that can lead to disease. Mutations in constitutive splicing can lead to disfunctional proteins that can have severe consequences on human health. A splicing error that adds or removes even 1 nucleotide will disrupt the open reading frame of an mRNA (Faustino & Cooper, 2003). Some mutations that disrupt splicing are single nucleotide changes within the intron or exon segments of the classical splice sites (Faustino & Cooper, 2003). Other mutations inactivate normally used splice signals, generate cryptic splice sites, or alter alternative splicing by mutation of regulatory sequences. One of the major

challenges the spliceosome faces is the ability to recognize correct splice sites from pseudo splice sites. Pseudo splice sites can outnumber canonical splice sites within the pre-mRNA by an order of magnitude (Sun & Chasin, 2000). Diseases caused by mutations in splicing include, Fraiser Syndrome, atypical cystic fibrosis, and spinal muscular atrophy, and a large number of human cancers (Faustino & Cooper, 2003). Therefore, knowledge of the mechanism by which splicing occurs within the cell can lead to a better understanding of human disease and possibly new treatments for human disease.

Section 1.3: Coupling transcription and pre-mRNA splicing: A critical role for chromatin

Transcription and RNA processing have been studied as biochemically separate reactions. However, it is clear that these processes are spatially and temporally linked (Maniatis, 2002). In fact, since the 1960's, imaging studies have clearly shown that RNA splicing is co-transcriptional. By electron microscopy, RNP particles are detected on the emerging nascent RNA (Beyer & Osheim, 1988, Osheim *et al.*, 1985). The functional implication of this coupling is only now becoming clear. Because of the close coordination, changes in transcription can affect spliceosome recognition of splice sites. In mammals, it has been shown that a slow RNA Polymerase II (RNAPII) can alter alternative splicing by

enhancing exon inclusion (de la Mata *et al.*, 2003, Howe *et al.*, 2003). Additionally, in mammals, it has been shown that nearly all splicing occurs while the pre-mRNA is attached to the chromatin template (Pandya-Jones & Black, 2009).

Since splicing occurs co-transcriptionally this suggests that spliceosome assembly must also occur co-transcriptionally, and this has been demonstrated in mammals and in yeast. It has been shown that the mammalian U1 and U5 snRNP are recruited co-transcriptionally (Listerman *et al.*, 2006). In *Sacchromyces cerevisiae,* co-transcriptional spliceosome assembly has also been reported (Kotovic *et al.*, 2003, Gornemann *et al.*, 2005, Gunderson & Johnson, 2009, Lacadie & Rosbash, 2005, Tardiff & Rosbash, 2006). In these studies, it was shown using Chromatin IP (ChIP) that each of the snRNPs were co-transcriptionally recruited in a stepwise manner.

Since co-transcriptional splicing occurs in the context of a chromatin DNA template, there are likely to be functional links between splicing factors and chromatin. Chromatin is comprised of nuclesomes, a complex of four core histone proteins that form an octomeric complex around which DNA is wrapped. These nuclesomes allow DNA to be highly compacted and organized. The N-terminal tails of histone proteins undergo a variety of post-translation modifications including, phosphorylation, ubiquitination, methylation, and the best characterized, acetylation. The details of these modifications, especially acetylation, will be described below. Nonetheless, mammalian studies have confirmed that chromatin structure of DNA can, indeed, influence splicing. One

of the first indications of this link was that the human U2 snRNP protein, SAP130 copurified with the human STAGA complex containing hGCN5, a histone acetyltransferase and transcriptional activator (Martinez, 2001). Additionally, in flies it was demonstrated that the histone acetyltransferase p2D10 co-transcriptionally associates with actin, the pre-mRNA, and the mRNP component hrp65 (Sjolinder *et al.*, 2005). Also, studies in mammals revealed that methylation of histone H3 facilitates pre-mRNA splicing (Sims *et al.*, 2007). Furthermore, the catalytic subunit of the human chromatin-remodeling complex, SWI/SNF regulated alternative splicing (Batsche *et al.*, 2006). Recently, histone modifications have been shown to influence splice site choice. In fact, modulation of histone modifications affects splicing by influencing the recruitment of splicing factors via a chromatin-binding protein (Luco *et al.*, 2010). These studies were primarily mammalian studies, so finding a functional connection between chromatin and splicing in yeast would be powerful, suggesting a fundamental, conserved role, for histone modifications in splicing. It would also be interesting since these modifications are reversible; thus, addition and removal of histone marks could influence the dynamics of spliceosome assembly. The histone code may not be providing instructions for transcription, but rather, directing mRNA processing.

While little mechanistic analysis has been carried out to show a functional relationship between chromatin and splicing in *S. cerevisiae*, a large scale yeast two-hybrid analysis revealed interactions between the yeast chromatin-remodeling factor, Swi1, and several splicing factors involved in pre-spliceosome

formation including*, MUD2, MSL5, MSL1*, and *CUS1* (Fromont-Racine *et al.*, 1997). Most notably, these factors are involved in U2 snRNP recognition of the branchpoint.

The work described in Chapter 2 provides the first clear evidence of a relationship between chromatin and splicing in yeast and the first indication of how a factor that affects chromatin can affect splicing of a constitutive gene. The fact that these interactions are seen in yeast, *Drosophila,* and humans suggest that model eukaryotic systems, which allow us to carry out detailed genetic and biochemical analysis, will provide important mechanistic insights into these processes.

It is likely that the genome-wide pattern of histone modifications and nucleosome occupancy are important for RNA splicing. Recently, reports that examined nucleosome occupancy throughout the mammalian genome have found that nucleosome occupancy was enriched in exons and depleted in introns (Schwartz *et al.*, 2009, Tilgner *et al.*, 2009). Other studies examined the role of histone modifications and found distinct patterns of histone modification to be enriched at intron-exon junctions (Kolasinska-Zwierz *et al.*, 2009). These studies provide fascinating hints that (1) nucleosome position and histone modifcations could affect splicing and (2) splicing factors may even contribute to histone marks. Studies described in Chapters two, three, and four provide strong indications that in yeast, at specific genes, chromatin can have significant effects on splicing and vice versa.

Section 1.4: Histone acetylation plays a critical role in gene expression

RNA polymerase II (RNAPII) transcribes protein-coding genes, many of which contain introns, and many non-coding RNAs. The largest subunit of the RNAPII, *RPB1* consists of a c-terminal domain (CTD), which is comprised of a hexapeptide consensus sequence that can undergo a variety of post-translation modifications. These modifications dictate the functional state of the polymerase and can also influence co-transcriptional events. For example, the phosphorylation state of the CTD changes during the transcription cycle leading recruitment of factors that modulate chromatin and RNA processing (reviewed in (Brookes & Pombo, 2009).

As mentioned in the previous section, eukaryotic cells package genetic material into higher order structures of histones and genomic DNA called chromatin. Chromatin is composed of 147 bp of DNA wrapped twice around a histone octomer that contains a histone H3/H4 tetramer and two H2A/H2B dimers (Figure 1.3). The structure of chromatin varies throughout the genome providing a means to regulate the access of the transcriptional machinery to the genes (reviewed in (Rando & Chang, 2009). Chromatin can adopt a more highly compacted structure called heterochromatin. When in the heterchromatic state, genes are less accessible to the RNA polymerase and in some cases are transcriptionally silenced. The uncondensed form of chromatin, termed euchromatin, provides greater accessibility to genes, and contains the majority of actively transcribed genes. The compact structure of chromatin is dynamic and

must be altered in order for the RNA polymerase to gain access to the DNA template to synthesize mRNA. Therefore, to regulate gene expression, post-translational modifications of histones, such as acetylation and methylation, phosphorylation, ubiquitination alter the chromatin structure allowing transcription to occur (reviewed in (Rando & Chang, 2009, Wu & Grunstein, 2000).

One of the best-characterized histone modifications is the reversible acetylation of lysine-residues on the N-terminal tails of histone H2B, H3 and H4. Histone acetylation is a positive mark of transcription. Acetylation neutralizes the charge on the basic histone proteins leading to the relaxation of the DNA and associated protein interactions. Acetylation of histone tails can also serve as binding sites for factors that regulate transcription (reviewed in (MacDonald & Howe, 2009), such as CHD1 that binds to methylated histones and Swi/Snf that binds to acetylated histones (see section 1.3 above).

Histone acetylation is carried out by several histone acetyltransferases (HATs). Histone acetyltransferases regulate the transcriptional activity of genes by determining the level of acetylation of the amino terminal tails of nucelosomal histones. Hyperacetylation of histones typically indicates active transcription. Whereas, hypoacteylation of histones is often indicative of transcriptional repression (Kristjuhan, 2002). The best characterized of the histone acetyltransferases is the yeast SAGA complex.

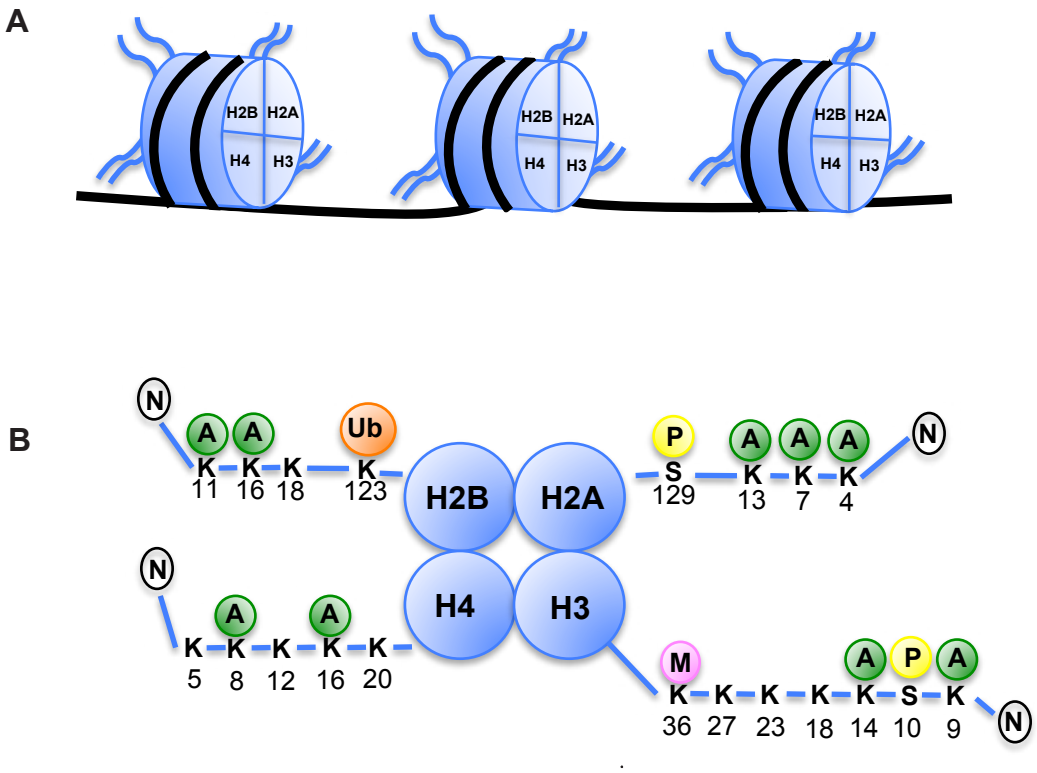

Figure 1.3: Schematic of the structure of histones in nucelosomes.
A) Nuclesomes are comprised of four core histone proteins H2A (histone 2A), histone H2B (histone 2B), histone H3 (histone 3), and histone H4 (histone 4). Each histone is present in two copies and the DNA (black) wraps around a histone octomer to make up a core nucleosome. B) The amino-terminal tails of histone proteins undergo a variety of different post-translational modifications. These modifications are catalyzed by histone modifying enzymes. Lysine residues in these amino-terminal tails are either methylated (M), acetylated (A), or ubiquitiated (Ub). In some instances, serine (S) residues are phosphorylated (P). Histone modifications that have been characterized in yeast are highlighted. (Adapted from Marks et al., 2001).

The *S. cerevisiae* SAGA complex is comprised of **S**pt- **A**da- **G**cn5 **a**cetyltrasferase (Figure 1.4), in which Gcn5 carries out the catalytic activity. There are two mammalian homologs of Gcn5; PCAF and Gcn5L. These homologs have been identified to be part of different SAGA-like complexes (Baker & Grant, 2007, Sterner & Berger, 2000). Similarly, in yeast, Gcn5 (**g**eneral **c**ontrol **n**onderepressible-5) is also part of different complexes, like SLIK/ SALSA. Gcn5 is the best characterized of the HAT's both structurally and functionally, *in vivo* and *in vitro*.

Gcn5 is comprised of a C-terminal bromodomain, an Ada2 interaction domain and the HAT domain. The HAT domain is where its catalytic activity resides and is required for adaptor mediated transcriptional activation *in vivo*. Truncation or point mutations of the HAT domain abolishes transcriptional activation (Candau & Berger, 1996, Kuo *et al.*, 1998). The bromodomain recognizes acetylated lysines and has been shown to promote SAGA retention on acetylated chromatin (Hassan *et al.*, 2007, Li & Shogren-Knaak, 2009, Syntichaki *et al.*, 2000).

Within the SAGA complex, there are several different subcomplexes. The catalytic core of SAGA is comprised of Ada2, Ada3 and Gcn5. Ada2 and Ada3 regulate Gcn5 catalytic activity via interaction with the Ada2 domain of Gcn5 (Candau *et al.*, 1997, Sermwittayawong & Tan, 2006). In addition to the catalytic core, there are a variety of different modules that are responsible for the structural integrity of the complex, TATA binding protein (TBP) targeting, histone deubiquititation, and mRNA export. The proteins Ada1, Spt7 and Spt20 have

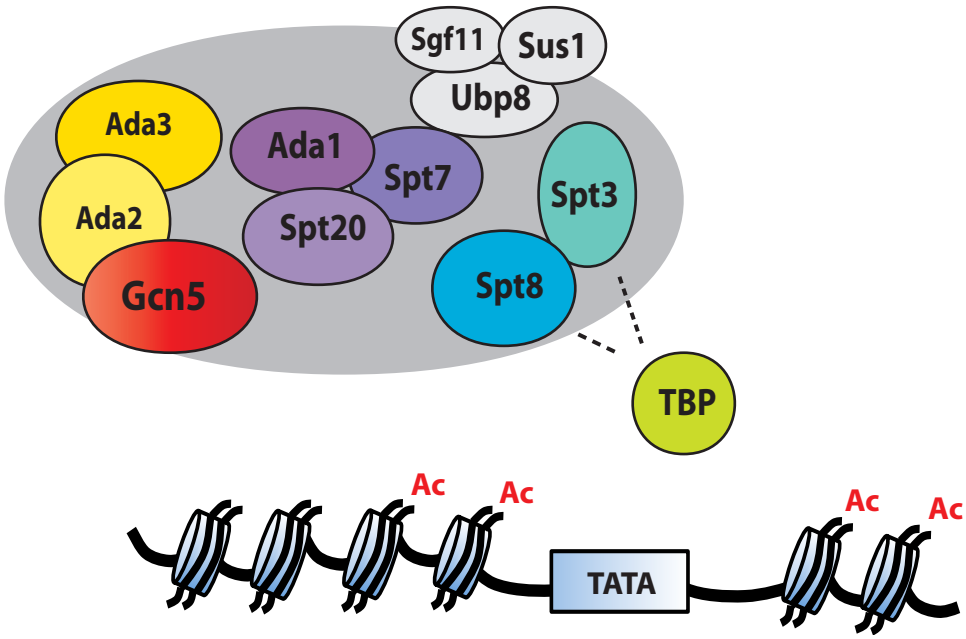

Figure 1.4: Schematic of the transcriptional coactivator complex, SAGA.
The SAGA complex (**S**pt- **A**da- **G**cn5) is a complex comprised of fifteen or more subunits. Some of the important modules of the complex are highlighted here. The histone acetyltransferase (HAT) Gcn5 (red) is the catalytic component of this complex. It acetylates histones on their N-terminal tails. Acetylation of histone tails opens the chromatin to expose binding sites for transcription factors (indicated by red font). Other components of the catalytic core of the SAGA complex are depicted in yellow. Factors that are involved in maintaining the structural integrity of the complex are represented in purple. Factors that are implicated in targeting the TATA binding protein to sites of transcription initiation are represented in green and cyan respectively. The histone ubiquititation/mRNA export module of the complex is represented in light grey.

been shown to be important for the structural integrity of the SAGA complex because when any of these factors is deleted, structural integrity is compromised (Sterner *et al.*, 1999, Wu & Winston, 2002). Spt3 and Spt8 are SAGA components that have been implicated in the recruitment of TBP to the TATA box of actively transcribed genes (Eisenmann *et al.*, 1992, Laprade *et al.*, 2007, Mohibullah & Hahn, 2008). The histone deubiquitination module is comprised of Ubp8, Sgf11, Sgf73 and Sus1, and it removes ubiquitin from histone H2B on lysine 123 (Henry *et al.*, 2003, Ingvarsdottir *et al.*, 2005, Kohler *et al.*, 2010). The catalytic component of this complex is Ubp8 (Henry et al., 2003). Interestingly, Sus1 has been implicated in mRNA export (Kohler *et al.*, 2006). The rest of the SAGA complex is comprised of a variety of different TAF (TBP-associated) transcription factors as reviewed in (Timmers & Tora, 2005).

Gcn5 is not only the catalytic core of the SAGA complex; it is also the catalytic core of the closely related complexes, SLIK (SAGA-like)/ SALSA (SAGA-altered) complexes (Pray-Grant *et al.*, 2002, Sterner *et al.*, 2002a). These complexes are distinguishable from SAGA in that SALSA and SLIK lack Spt 8 and have truncated versions of Spt7 (Pray-Grant et al., 2002, Sterner et al., 2002a). To date, these complexes have not been shown to acetylate histones within nucleosomes.

Substrate specificity studies of Gcn5 have revealed that *in vitro*, recombinant Gcn5 can acetylate histone H3 strongly and histone H4 weakly in a free histone mixture (Kuo, 1996). Protein sequence analysis of these reactions revealed that the primary sites of acetylation were lysine 14 on histone H3 and

lysine 8 and 16 on histone H4 (Kuo, 1996). Purified Gcn5 is unable to acetylate nucleosomal histones *in vitro*. Other factors are required to allow this level of substrate specificity. The SAGA complex gives Gcn5 the ability to acetylate nucleosomes, primarily at histone H3 and to a lesser extent H2B and histone H4 (Grant, 1997). *In vivo*, Gcn5 preferentially acetylates histone H3 (K9, K14) and H2B (K11, K16) and to some extent histone H4 (K8, K16) (Grant *et al.*, 1999, Suka *et al.*, 2001).

The SAGA complex was initially characterized for its ability to affect the histone acetylation state at sites of transcription initiation and to influence the ability of Pol II to initiate transcription (Biswas *et al.*, 2004, Imoberdorf *et al.*, 2006). Subsequent studies have demonstrated that the SAGA complex can also have an affect on transcription elongation by increasing histone H3 acetylation in the coding region (Govind *et al.*, 2007, Kristjuhan, 2004). In the fission yeast, *Schizosacchromyces pombe*, Gcn5 is found in the transcribed region of highly expression genes (Johnsson *et al.*, 2009). These results suggest that Gcn5 in the context of the SAGA complex not only affects histone acetylation at the promoter but in the coding region as well.

Section 1.5: Specific Aims

The hypothesis underlying the research presented in this thesis is that specific splicing factors interact with histone modifying enzymes to coordinate transcription and pre-mRNA splicing. The use of the genetically and biochemically tractable organism, *S. cerevisiae*, has allowed us to elucidate the role of this coordination in regulating gene expression.

To start this project I took a genetic approach to determine which non-essential splicing factors had functional interactions with transcription factors. From that directed screen, I found a functional interaction between *GCN5* and the U2 snRNP. From these results, came the first specific aim, which was to characterize the role of *GCN5* in co-transcriptional splicing. These results are described in Chapter two.

Upon investigating the role of Gcn5 in co-transcriptional splicing, I discovered that Gcn5-dependent histone H3 acetylation was important for co-trascriptional splicing. From these results, the second specific aim for this study emerged: determine the mechanism of how histone acetylation affects co-transcriptional splicing. I addressed this aim using a combination of genetic techniques and chromatin immunoprecipitation (ChIP). The results of this study have lead to a model whereby the dynamics of histone acetylation affect co-transcriptional splicing via alterations of the rearrangements of the spliceosome that are described in Chapter three.

Since splicing occurs within the context of a chromatin template and I observed that histone acetylation affected co-transcriptional splicing, I examined how splicing factors might, in turn, affect transcription. This emerged as my third specific aim and the results from this are described in chapter four.

Lastly, from these results I wanted to address the bigger question of the importance of co-transcriptional splicing for cellular function. We hypothesized that under certain stress conditions co-transcriptional splicing is essential. To address this aim I developed an experimental approach. I am employing a microfluidics analysis to examine at a single-cell level how co-transcriptional splicing can affect the cells's ability to respond to an environmental stress. While these studies are ongoing, I will describe how they open the door to the use of this tool in future studies of pre-mRNA splicing (Appendix 1).

Chapter 2: Acetylation by the transcriptional coactivator Gcn5 plays a novel role in co-transcriptional spliceosome assembly

Section 2.1: Introduction

Eukaryotic genes are interrupted by stretches of noncoding sequence (introns), which are removed from the newly-synthesized RNA by the spliceosome, a dynamic ribonucleoprotein complex made up of 5 highly structured snRNAs and over a hundred snRNA-associated proteins.

Although RNA synthesis and RNA splicing have been analyzed as biochemically separate reactions, recent studies demonstrate that these processes are spatially and temporally coordinated (Maniatis, 2002). *In vivo*, recognition of splice sites within the pre-mRNA by the spliceosome can occur while the polymerase is actively engaged with the DNA template (Beyer & Osheim, 1988, Beyer & Osheim, 1991, Bauren & Wieslander, 1994, Huang & Spector, 1996, Bauren *et al.*, 1996), and recent chromatin IP studies (in yeast and in mammals) suggest that this recruitment, or at least the *stable* association of snRNPs with the transcription complex, occurs in response to synthesis of specific signals in the pre-messenger RNA (Kotovic et al., 2003, Gornemann et al., 2005, Lacadie & Rosbash, 2005, Listerman et al., 2006). The regulatory implications of this coordination are suggested by studies showing that changes in transcription elongation caused by changes in the activity of specific transcription factors or the presence of transcriptional inhibitors can affect the

spliceosome's recognition of splice sites (de la Mata et al., 2003, Howe et al., 2003). These studies focus on the spliceosome's use of alternative splice sites in response to transcription signals, but they raise the possibility that constitutive splicing signals are also affected by conditions or factors that modulate transcription. Despite the evidence that co-transcriptional spliceosome assembly occurs, there is much to learn about the mechanism whereby splicing factors are co-transcriptionally recruited.

Transcription of DNA is strongly influenced by its packaging. The core histone proteins, H2A, H2B, H3, and H4 form an octameric complex that DNA is wrapped around to form the nucleosome, which is further compacted into chromatin—a general repressor of transcription. However, histones undergo extensive post-translational modifications on their N-terminal tails including acetylation, ubiquitination, methylation, and phosphorylation, which alter the chromatin and, in turn, affect transcription. One of the best-characterized histone modifications is the reversible acetylation of lysine residues on the N-terminal tails of histones H2B, H3, and H4. Histone acetylation, which is a positive mark of transcription, neutralizes the charge on the basic histone proteins leading to relaxation of the protein/DNA interactions, and the acetylated histone tails can serve as binding sites for proteins that regulate transcription.

Histone acetylation is carried out by several different acetyltransferases, the best characterized of which is the protein Gcn5, a component of the multi-subunit transcription co-activating SAGA (Spt/Ada/Gcn5/Ada) complex (STAGA in mammals). Gcn5 primarily acetylates histones H3 and H2B, and these

modifications are thought to loosen chromatin for specific transcription factor binding. Furthermore, association between the SAGA complex and general transcription factors, such as TBP, facilitate preinitiation complex formation (Sterner et al., 1999, Roberts & Winston, 1997). Gcn5 affects global acetylation of histones throughout the genome (Vogelauer *et al.*, 2000), but is typically found at the promoter and within coding regions and can influence elongation in addition to events at the promoter (Govind et al., 2007).

The co-transcriptional nature of pre-messenger RNA splicing raises the intriguing possibility that proteins involved in transcription and histone modification might affect splicing and its regulation. In fact, biochemical studies using mammalian cells indicate that histone-modifying enzymes that regulate histone acetylation physically interact with splicing factors. Prp4K, a U5 snRNP-associated kinase, copurifies with N-CoR, a nuclear hormone corepressor complex that mediates histone deacetylase activity and the mammalian chromatin remodeling protein Brg1 (Dellaire *et al.*, 2002). In an independent affinity purification/mass spectrometry analysis, N-CoR was also found associated with SAP130 and SF3a120, components of the U2 snRNP that stabilize U2 snRNP-branchpoint interactions (Dybkov *et al.*, 2006). Interestingly, SAP130 also copurifies with the human STAGA complex containing hGcn5 (Martinez, 2001). These studies suggest that mammalian complexes that regulate histone acetylation and chromatin remodeling have physical interactions with splicing factors, although the nature of these interactions remains unclear.

Based upon the spatial and temporal proximity of chromatin, chromatin-modifying enzymes (such as Gcn5), and pre-mRNA splicing complexes during gene expression, we undertook an analysis of genetic interactions between *GCN5* and genes encoding nonessential splicing factors. Here we show that deletion of the gene encoding Gcn5 (and not other yeast lysine acetyltransferases that target histones) is synthetically lethal when combined with deletion of either gene encoding the U2 snRNP proteins Lea1 and Msl1 (mammalian U2A'/U2B"). A mutation in *GCN5* that eliminates the protein's catalytic activity is sufficient to confer the synthetic lethality. Co-transcriptional recruitment of the U2 snRNP to the branchpoint and subsequent steps in spliceosome assembly are dependent on Gcn5 HAT activity. While previous studies indicate that transcription elongation can alter co-transcriptional spliceosome assembly, chromatin IP results reveal no obvious changes in elongation in the absence of Gcn5's HAT activity. Moreover, we observe a dramatic peak in Gcn5-dependent acetylation of histone H3 in the promoters of these intron-containing genes. Unexpectedly, we also find recruitment of Msl1 at the promoter region, indicating that Msl1 recruitment during active transcription can occur independently of its association at the branchpoint region. These results demonstrate a novel role for acetylation by SAGA in co-transcriptional recruitment of the U2 snRNP and recognition of the intron branchpoint.

Section 2.2: Results

The genes encoding the U2 snRNP components Msl1 and Lea1 interact genetically with the gene encoding the histone acetyltransferase Gcn5.

In order to characterize interactions between the non-essential histone acetyltransferase *GCN5* and genes encoding factors involved in pre-mRNA splicing, a targeted genetic screen was performed to identify synthetic lethal interactions between null alleles of non-essential splicing factors and *GCN5*. In this analysis, we uncovered genetic interactions between *GCN5* and the splicing factors *MSL1 and LEA1* (Figure 2.1 A).

Msl1 and Lea1 are the yeast homologs of the human U2 snRNP proteins U2A'/B" and, like their mammalian counterparts, are components of the U2 snRNP that bind to a conserved stem-loop structure in the U2 snRNA (Stem-loop IV) (Tang *et al.*, 1996). *In vitro,* spliceosome assembly is blocked prior to addition of the U2 snRNP in the absence of either Lea1 or Msl1, indicating a role for these proteins in U2 snRNA association with the pre-mRNA. Cells deleted of either gene also have a mild growth defect, which is observable in the strain background used here.

To determine if Gcn5's catalytic activity is required for the interactions with the genes encoding Msl1 and Lea1, we analyzed specific mutants in the HAT domain of Gcn5. A previously characterized mutation in *GCN5* which changes amino acids 126-128 (KQL) in domain I to alanines eliminates the histone acetyltransferase activity of Gcn5 (Wang *et al.*, 1998). The effect of this allele

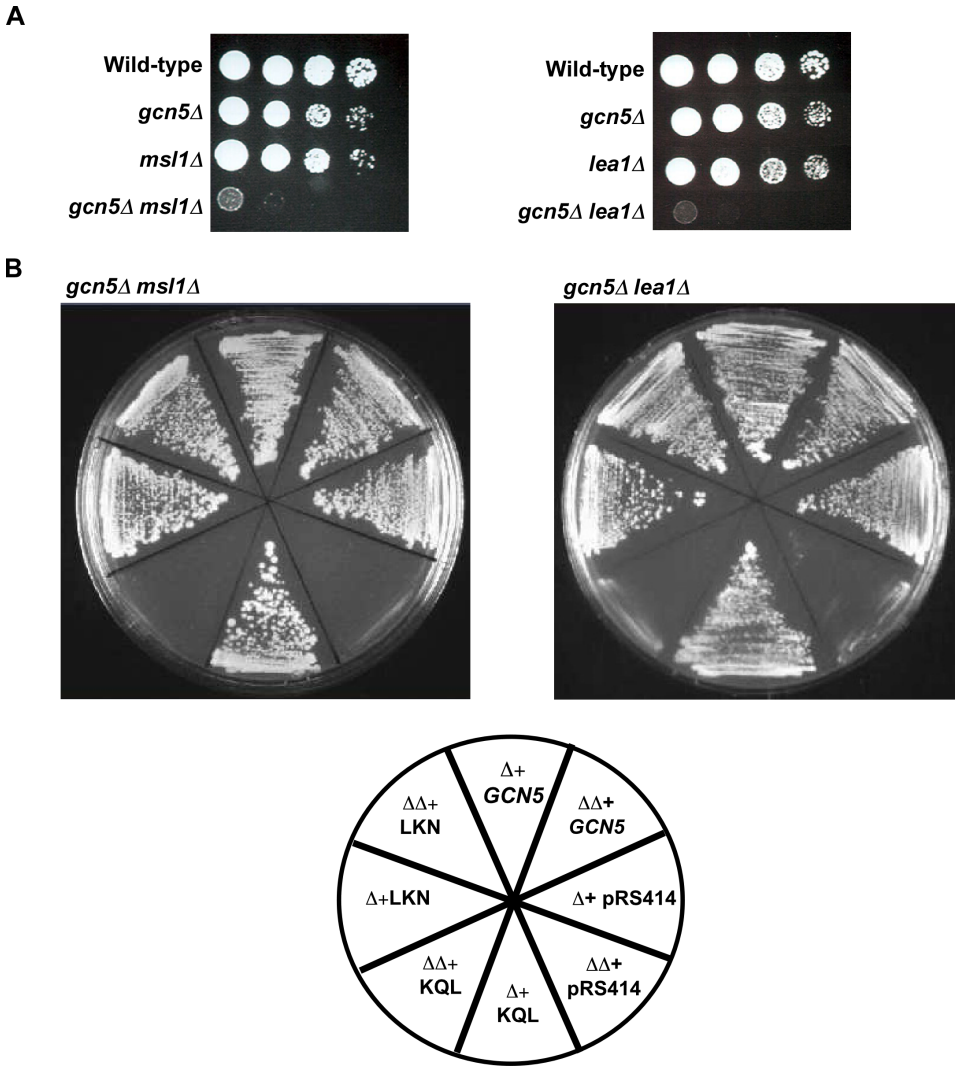

Figure 2.1: *GCN5* interacts with the genes encoding the non-essential U2 snRNP proteins, *MSL1* and *LEA1.*
A) Dilution series of double mutants, *gcn5*Δ *msl1*Δ, *gcn5*Δ *lea1*Δ. Cells were grown at 30°C in YPD liquid medium until the desired $O.D._{600}$ was obtained. Cells were spotted onto YPD plates as a ten-fold serial dilution, and the plates were incubated at 30°C for two days. B) Viability analysis of the double mutants, *gcn5*Δ *msl1*Δ and *gcn5*Δ *lea1*Δ in the presence of Gcn5 HAT mutants (*TRP* plasmids, pRS314) and then streaked onto 5-FOA-TRP to select for the ability to lose the wild type copy of *GCN5* on a *URA3*-marked plasmid. Plates were incubated at 30°C for two days. Δ indicates deletion of *GCN5*; ΔΔ indicates deletion of *GCN5* and either *MSL1* or *LEA1*.

was tested in the double mutants, and the KQL mutant is unable to support growth of either *gcn5*Δ *msl1*Δ or *gcn5*Δ *lea1*Δ double mutant (Figure 2.1 B). By contrast, a mutation in the same domain that changes amino acids 120-122 (LKN) to alanines and does not affect Gcn5 HAT activity (Wang et al., 1998) supports growth of the double mutants (Figure 2.1 B). These results demonstrate that the acetyltransferase activity of Gcn5 is critical for the functional interactions with Msl1 and Lea1.

We also tested other factors that have interactions with Msl1 and Lea1 and are involved in branchpoint recognition, including the commitment complex protein Mud2, and the U2 snRNP proteins Cus2 and Cus1, and found no genetic interactions between these factors and *GCN5* (Figure 2.2 A). These results demonstrate specificity in the interaction between *GCN5* and *MSL1* or *LEA1*. While we cannot exclude the possibility that there are other essential components of the U2 snRNP that interact with *GCN5*, the effect is not general for all splicing factors acting at the prespliceosome formation step.

In addition to Gcn5, there are several other HATs that affect gene expression in yeast, including Elp3, the catalytic component of the elongator complex, and Sas3, a component of the NuA3 complex. While both histone acetyltransferases share substrates with Gcn5, and deletion of either gene is synthetically lethal when combined with deletion of *GCN5* (Wittschieben *et al.*, 2000), neither *ELP3* deletion nor *SAS3* deletion has a synthetic interaction with *LEA1* or *MSL1* (Figure 2.2 B), suggesting that the interactions between *GCN5*

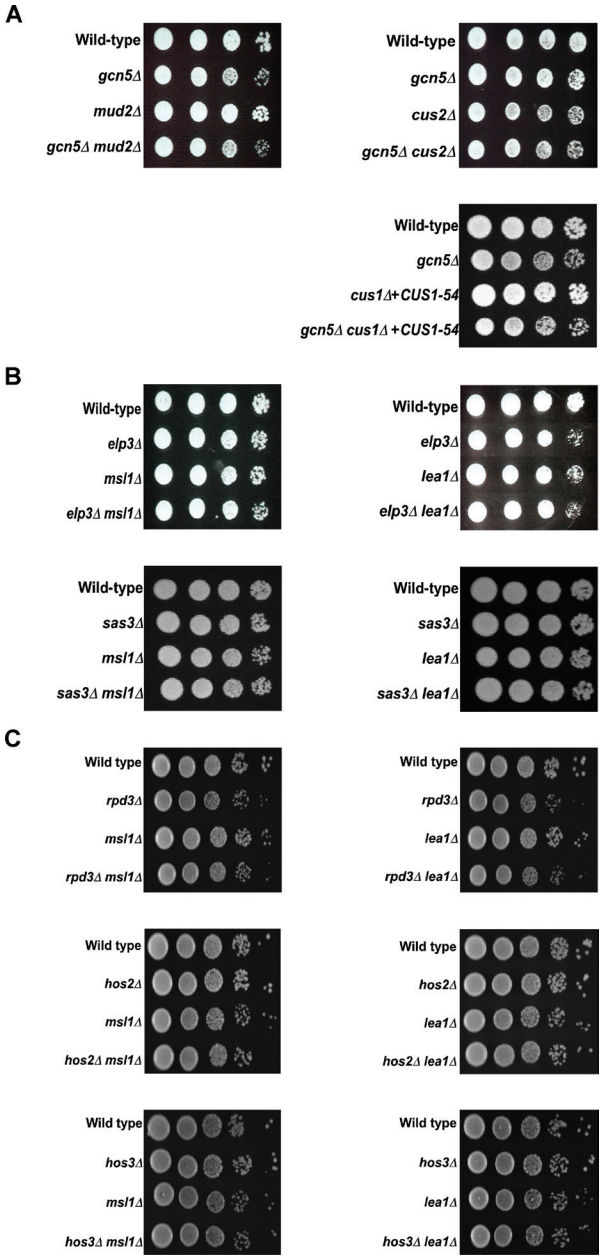

Figure 2.2: *GCN5* genetic interactions with *MSL1* and *LEA1* are specific.
A) Dilution series of double mutants *gcn5*Δ *mud2*Δ, *gcn5*Δ *cus2*Δ, and *gcn5*Δ *cus1*Δ + *CUS1-54*. Cells were grown at 30°C in YPD liquid medium until the desired $O.D._{600}$ was obtained. Cells were spotted onto YPD plates as a ten- fold serial dilution. Plates were incubated at 30°C for two days. B) Dilution series of the double mutants, *elp3*Δ *msl1*Δ, *elp3*Δ *lea1*Δ, *sas3*Δ *msl1*Δ, *sas3*Δ *lea1*Δ. Cells were treated as described in A. C) Dilution series of the double mutants *rpd3*Δ *msl1*Δ, *rpd3*Δ *lea1*Δ, *hos2*Δ *msl1*Δ, *hos2*Δ *lea1*Δ, *hos3*Δ *msl1*Δ, *hos3*Δ *lea1*Δ. Cells were treated as described in A.

.and *MSL1* and *LEA1* are specific to the activity of Gcn5 and are not a general feature of all histone acetyltransferases.

In addition to acetyltransferases, several deacetylases have been shown to act on the same histone residues as Gcn5. The histone deacetylase Rpd3 regulates transcription and silencing, and has genetic interactions with Gcn5 (Lin *et al.*, 2008b). Additionally, Hos2 and Hos3 are involved in gene activation and have been shown to deacetylate histones within the body of genes (Wang *et al.*, 2002, Govind et al., 2007). Mutation of *HOS2* suppresses *gcn5*Δ *elp3*Δ phenotypes (Wittschieben et al., 2000). When deletion of *RPD3*, *HOS2*, or *HOS3* is combined with deletion of *MSL1* or *LEA1,* cells grow indistinguishably from either deletion alone (Figure 2.2 C), suggesting that the acetylation activity of Gcn5 is functionally related to the activities of Msl1/Lea1, while the removal of acetyl groups from histones probably is not.

MSL1 and _LEA1_ have genetic interactions with structural components of SAGA.

SAGA is a 1.8 MDa, multisubunit complex comprised of five domains containing distinct sets of subunits [(Wu *et al.*, 2004)]. Interactions between Msl1 and Lea1 and these other components of the complex were also analyzed and are summarized in Table 2.1. Ada2 and Ada3 directly interact with Gcn5, are required for Gcn5 catalytic activity, and direct Gcn5's histone acetylation activity toward nucleosomes (Marcus *et al.*, 1994, Horiuchi *et al.*, 1995, Candau & Berger, 1996, Balasubramanian *et al.*, 2002). We hypothesized that, since

Table 2.1: Summary of genetic interactions between U2 snRNP factors, Msl1/Lea1 and SAGA components

	Double Mutant	Phenotype
SAGA Catalytic Module	*ada2Δ msl1Δ*	dead
	ada2Δ lea1Δ	dead
	ada3Δ msl1Δ	Severe growth defect
	ada3Δ lea1Δ	Severe growth defect
SAGA Structural Integrity	*spt7Δ msl1Δ*	Severe growth defect
	spt7Δ lea1Δ	Severe growth defect
TBP Recruitment	*spt3Δ msl1Δ*	Severe growth defect
	spt3Δ lea1Δ	Severe growth defect
	spt8Δ msl1Δ	Severe growth defect
	spt8Δ lea1Δ	Severe growth defect
Ubiquitination	*ubp8Δ msl1Δ*	No growth defect
	ubp8Δ lea1Δ	No growth defect
	sgf11Δ msl1Δ	No growth defect
	sgf11Δ lea1Δ	No growth defect

The genotype of each spore was confirmed by PCR, as described in Chapter 6.

abrogation of the catalytic activity of *GCN5* leads to synthetic lethality in cells deleted of *MSL1* and *LEA1*, a similar synthetic growth defect would be evident in the *ada2*Δ *msl1*Δ or the *ada2*Δ *lea1*Δ mutants, and indeed, this is what is observed. Furthermore, deletion of *SPT7*, which is required for the structural integrity of the SAGA complex (Grant, 1997, Sterner et al., 2002a, Wu et al., 2004), is lethal when combined with deletion of either *MSL1 or LEA1*, indicating that the interactions occur within the context of a functional complex. Two components of SAGA that target the complex to the promoter, Spt3 and Spt8 (Eisenmann et al., 1992, Sterner et al., 2002a, Sermwittayawong & Tan, 2006), also have genetic interactions with Msl1 and Lea1. Spt8 is unique to the SAGA complex and is missing from the other Gcn5 containing complexes, SALSA and SILK (Belotserkovskaya *et al.*, 2000), suggesting that the interactions between *GCN5* and *MSL1* and *LEA1* occur within the context of the SAGA and not the SALSA or SILK complexes. Deletion of genes encoding other components of SAGA that do not contribute to SAGA's HAT activity, such as Ubp8 or Sgf11, show no synthetic growth defects when combined with deletion of *GCN5*. Taken together, these data strongly suggest that the intact SAGA complex, with its catalytic activity targeted to nucleosomes, has a functional interaction with Msl1 and Lea1.

The best-characterized substrates of Gcn5 are lysine residues on histone tails, suggesting a model in which chromatin modification has some overlapping function with pre-mRNA splicing factors. Nonetheless, we considered the

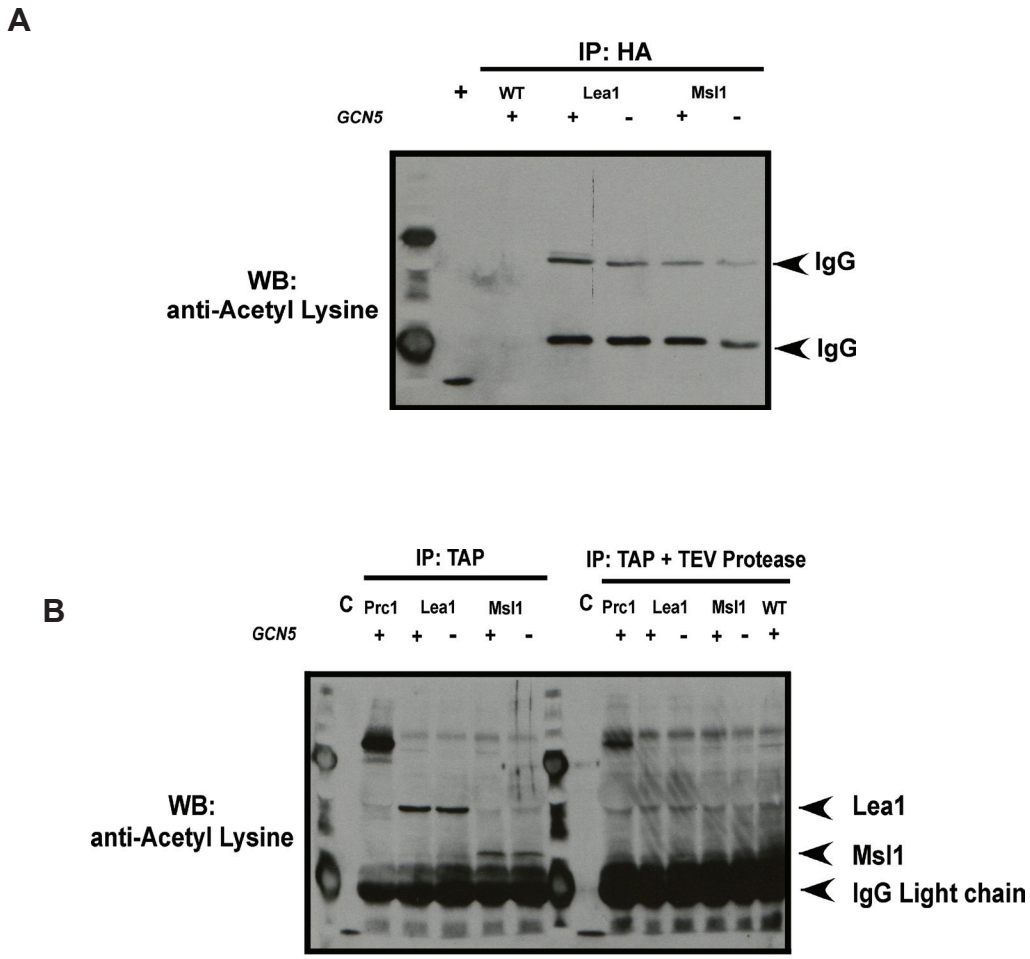

Figure 2.3: Gcn5 does not acetylate the U2 snRNP proteins, Msl1 or Lea1.
A) Gcn5 does not acetylate Lea1-HA or Msl1-HA. Lea1 and Msl1 were immunoprecipitated from whole cell extracts and separated by SDS-PAGE and probed with anti-Acetyl Lysine antibody as in panel C. Arrowheads indicate light and heavy IgG chains. +, represents purified histone control. B) Gcn5 does not acetylate Msl1 or Lea1 proteins. Lea1-TAP +/- *GCN5* and Msl1-TAP +/- *GCN5* were immunoprecipitated from whole cell extracts and separated by SDS-PAGE and probed with anti-Acetyl Lysine (K-103, Cell Signaling). For right side of gel, samples were incubated with TEV protease (Invitrogen) prior to separation by SDS-PAGE. Arrowheads indict were Msl1 and Lea1 migration. Prc1-TAP, a cytosolic protein was used as a control. C represents acid-butyrate treated purified histones (Upstate).

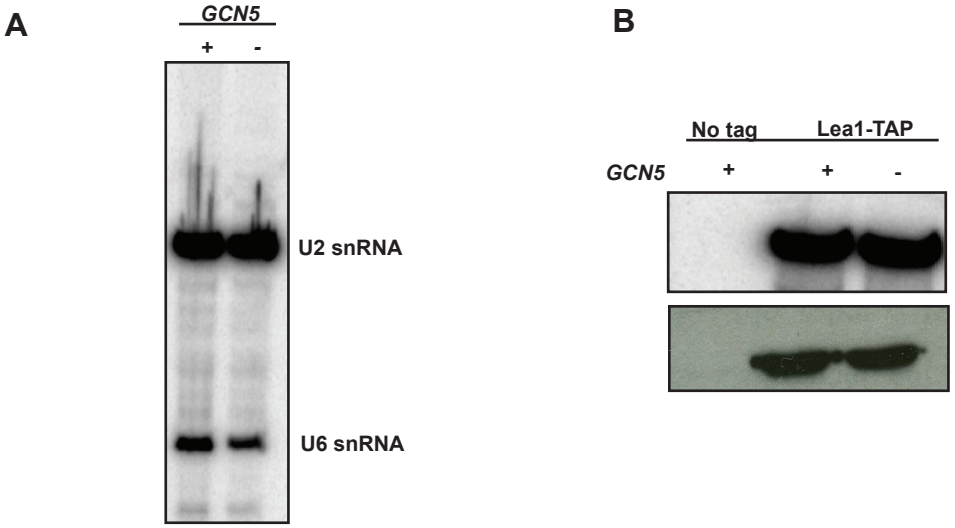

Figure 2.4: Deletion of *GCN5* does not alter the endogenous levels of U2 snRNA or Lea1 ability to bind the U2 snRNA.
A) Primer extension analysis of total RNA isolated from *gcn5*Δ and wild type strains. A U2 snRNA specific primer was used as depicted by U2. U6 snRNA was used as a loading control as depicted by U6. Primer extension products were separated on a 6% denaturing gel. B) Immunoprecipitation of TAP tagged Lea1 in the presence or absence of *GCN5* or Gcn5 in the presence and absence of *LEA1*, followed by primer extension from immunoprecipitated RNA using a U2snRNA specific primer. Bottom panel depicts analysis (anti-TAP) of TAP tagged samples used in the immunoprecipitation shown in panel A to ensure that equal amounts of protein were used in the immunoprecipitation step (refer to material and methods).

possibility that the genetic interactions we observed between *GCN5* and *MSL1* and *LEA1* are due to Gcn5's catalytic activity being directed toward one of these non-histone substrates. Using an antibody that recognizes acetylated lysine residues we probed an immunoprecipitated Lea1-HA and Msl1-HA samples to detect acetylation of these proteins in the presence or absence of Gcn5 and do not detect acetylation of either protein or associated U2 snRNP proteins (Figure 2.3 A). As a control, we immunoprecipitated Lea1-TAP and Msl1-TAP in the presence and absence of Gcn5. Previous studies I had done with these strains revealed that the TAP tag is acetylated. Cleavage of the TAP tag with TEV protease resulted in loss of acetylation (Figure 2.3 B). While this does not rule out the possibility that Gcn5 acetylates some other splicing factor, these data do suggest that the genetic interactions between *GCN5* and *MSL1* and *LEA1* are probably not due to acetylation of the U2 snRNP proteins by Gcn5, and indicate a novel functional interaction between the transcriptional co-activator complex, SAGA, and core components of the spliceosome.

We also wanted to determine whether the synthetic lethality that we observed when cells were deleted of *GCN5* and *MSL1/LEA1* was due to Gcn5's role in transcription. Since the U2 snRNA is a RNAPII transcript, we examined whether a deletion of *GCN5* altered the endogenous levels of U2 sRNA. Using primer extension with a primer specific to U2 snRNA, we did not observed a difference in endogenous U2snRNA levels when *GCN5* was deleted (Figure 2.4 A). In order for the U2 snRNA to properly associate with the spliceosome, both Lea1 and Msl1 have to be bound to stem loop IV of the U2 snRNA (Caspary &

Seraphin, 1998). To eliminate the possibility the Gcn5 is altering Lea1 or Msl1 ability to bind the U2 snRNA, we examined Lea1 binding to the U2 snRNA by immmunoprecipitation followed by primer extension with a primer specific to the U2 snRNA (Figure 2.4 B). From these experiments, a deletion of *GCN5* does alter the ability of Lea1 to bind to the U2 snRNA. These results suggest that the synthetic lethality we observed is not simply due to alteration in U2 snRNA levels or the ability of these proteins to bind the U2 snRNA.

Deletion of *GCN5* abrogates co-transcriptional recruitment of Lea1 and Msl1.

Recent studies in yeast demonstrate that *in vivo* spliceosome recruitment to pre-mRNA occurs while the nascent RNA is actively engaged with the transcription complex (Gornemann et al., 2005). Chromatin immunoprecipitation provides a powerful tool for detecting this co-transcriptional recruitment. The individual snRNPs can be formaldehyde crosslinked to the transcription complex or to the nascent RNA and immunoprecipitated (Figure 2.5). When the associated DNA is amplified, the signal is enriched in regions of the gene where the snRNPs would be predicted to associate, in a stepwise manner, with the corresponding pre-mRNA (Gornemann et al., 2005). To determine if co-transcriptional recruitment of either Msl1 or Lea1 is affected by deletion of *GCN5,* we analyzed the well-characterized intron-containing gene *DBP2* with an extended exon 2 (Figure 2.6). In strains in which *GCN5* is present, we detect

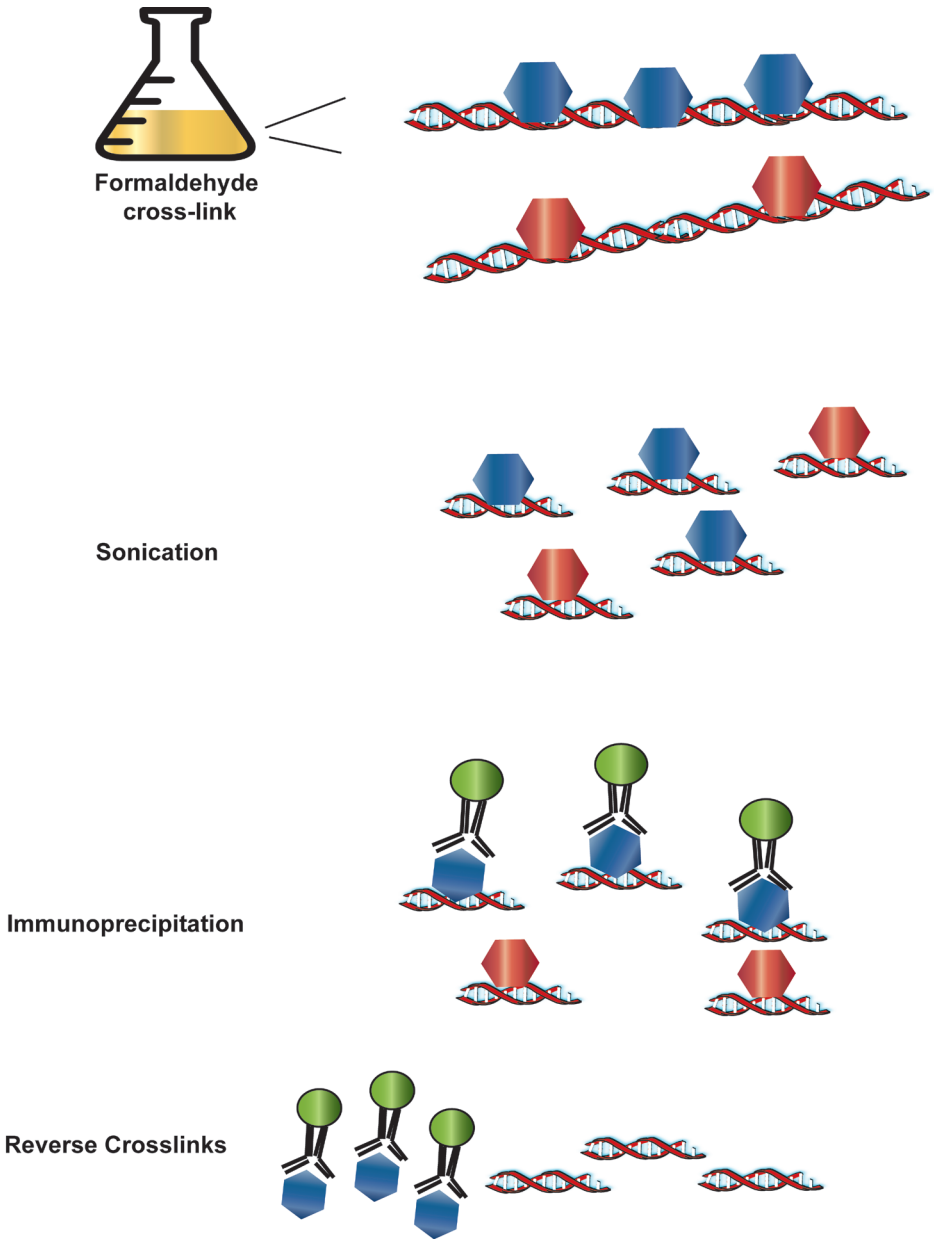

Figure 2.5: Schematic of Chromatin Immunoprecipitation (ChIP).
Cells are grown to mid-log and cross-linked with formaldehyde. This captures protein DNA (or protein-RNA) interactions. Following cross-linking, samples are sonicated to shear the protein-DNA complexes into small fragments (300-600bp). Once sheared, samples are then immunoporecipitated with an antibody specific to your protein. Ternary complexes containing chromatin-RNA are also immunoprecipitated with antibodies that recognize RNA binding proteins (data not shown) Then samples are heated to reverse the formaldehyde cross-linking releasing the corresponding DNA from the protein. The DNA is then purified quantitated by PCR.

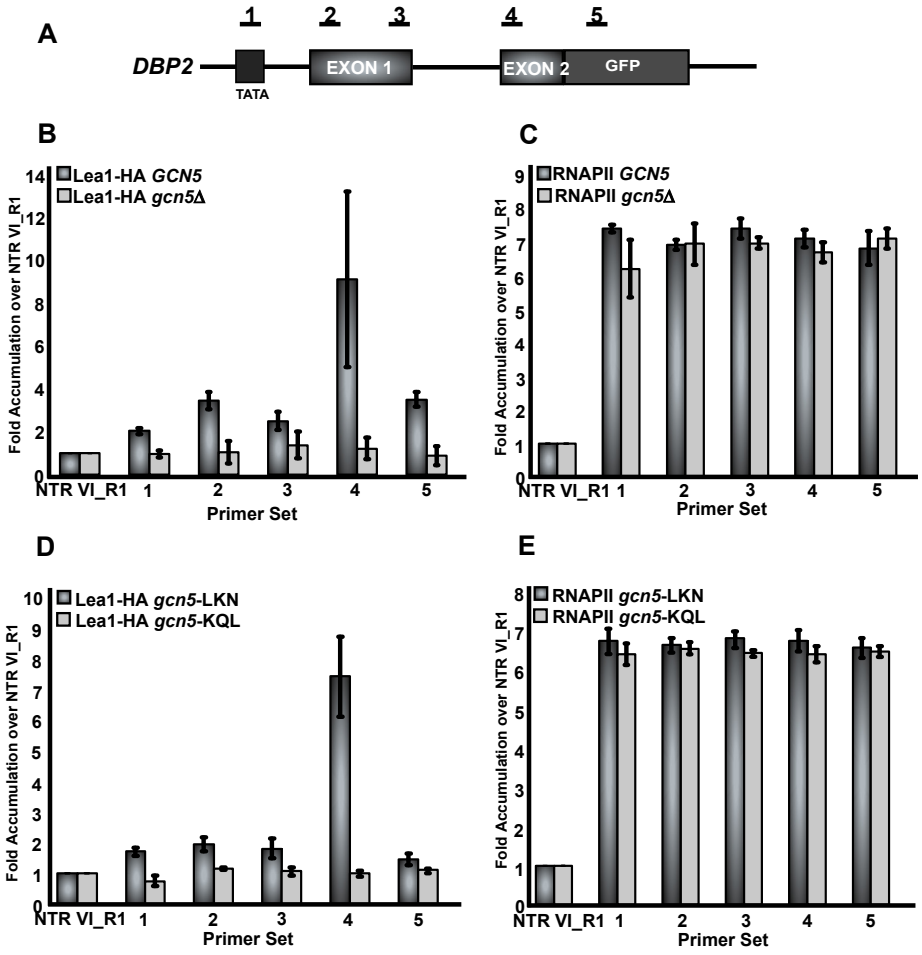

Figure 2.6: Deletion of *GCN5* affects co-transcriptional recruitment of Lea1 to *DBP2*. A) Schematic of the intron-containing gene, *DBP2*. Underlined numbers represent amplicons generated from each primer set used in the study. B) Graph depicting the occupancy of Lea1 at each region of *DBP2* relative to the non-transcribed region, in wild type or gcn5Δ. Dark grey bars represent Lea1 with wild type *GCN5* and light grey bars represent Lea1 levels in the gcn5Δ strain. C) Bar graph depicting RNA pol II occupancy within *DBP2* relative to the non-transcribed control. Dark grey bars represent RNAP II occupancy in the LEA1-HA strain and light grey bars represent RNAP II occupancy in the *LEA1-HA gcn5*Δ strain. D) Graph depicting the occupancy of Lea1 with the Gcn5 HAT mutants, LKN and KQL. Dark grey bars represent Lea1 with the Gcn5 LKN mutation, light grey bars represent Lea1 with the Gcn5 KQL mutation. E) Bar graph depicting RNA pol II occupancy in the presence of the Gcn5 HAT mutants. Dark grey bars represent RNA pol II occupancy with the Gcn5 LKN mutation and light grey bars represent RNAP II with the Gcn5 KQL mutant. All graphs depict the average of at least three independent experiments, and error bars represent the standard deviation.

Lea1 recruitment after synthesis of the pre-mRNA branchpoint sequence (Figure 2.6 B), a result consistent with what has been reported by others (Gornemann et al., 2005). However, when *GCN5* is deleted, there is a dramatic decrease in Lea1 association with *DBP2* (Figure 2.6 B). RNA polymerase association along *DBP2* was also examined, and no significant difference between the levels of RNA polymerase at the 5' and 3' ends of *DBP2* are apparent when *GCN5* was deleted. In fact, the polymerase distribution along the gene remains relatively unchanged for *GCN5* deleted cells relative to wild type cells (Figure 2.6 C). To determine if *DBP2* exon 2 length influences co-transcriptional Lea1 recruitment, we tested the recruitment of Lea1 to *DBP2* lacking the extension on exon 2. We find that the GFP extension has only a mild effect on the overall signal strength observed in the presence of *GCN5* with the primer sets used here, and recruitment of Lea1 is eliminated when *GCN5* is deleted regardless of whether exon 2 is extended (Figure 2.7).

Our discovery of an essential requirement for Gcn5's HAT activity in its interaction with Lea1/Msl1 led to the prediction that its HAT activity would also be required for the co-transcriptional recruitment of Lea1, and this is what is observed. When Gcn5's HAT activity is abrogated by the KQL mutation, no co-transcriptional recruitment of Lea1 is observed, whereas Lea1's association is unaffected by the LKN mutation (Figure 2.6 D). Pol II occupancy is not significantly affected by either mutation (Figure 2.6 E).

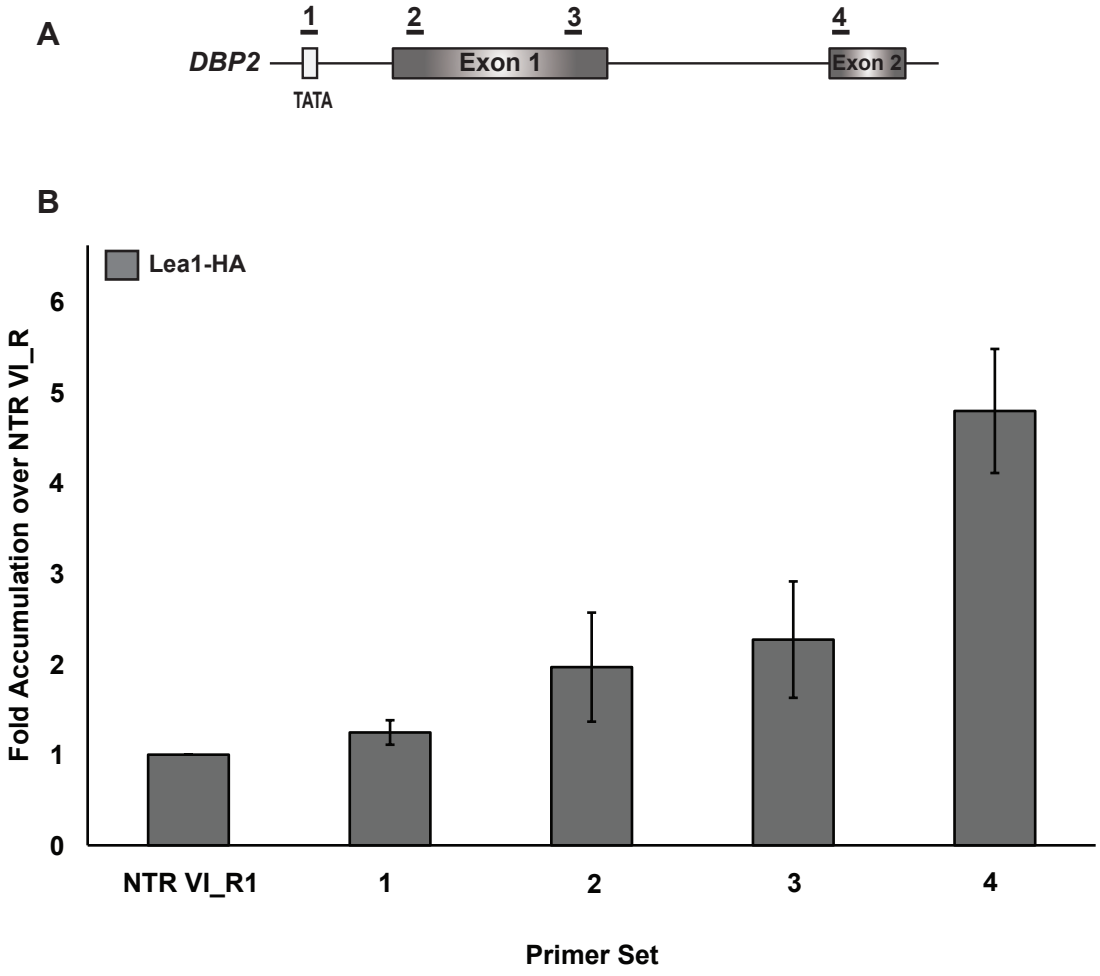

Figure 2.7: Second exon length does not affect co-transcriptional recruitment of Lea1 to *DBP2*.

A) Schematic of the intron-containing gene, *DBP2*. Underlined numbers represent amplicons from each primer set used in this study. B) Graph represents occupancy of Lea1 at each region of *DBP2* relative to the non-transcribed region.Graphs depict the average of three independent experiments, +/- 1 standard deviation.

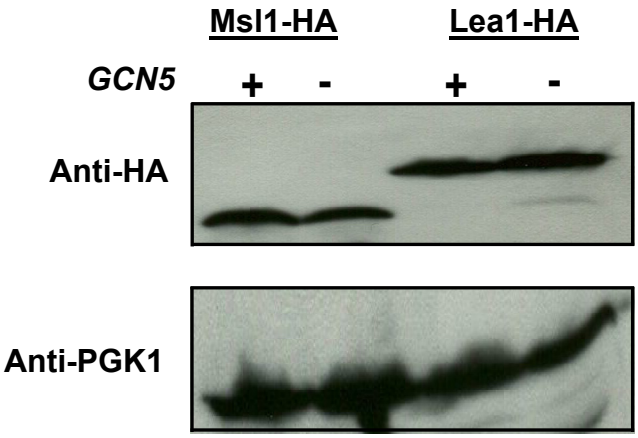

Figure 2.8: Deletion of *GCN5* does not alter the endogenous protein levels of Lea1 or Msl1.
Protein immunoblot of strains used for ChIP assays. Wild type and gcn5Δ cultures were gorwn in YPD liquid medium and whole cell extracts were prepared (see Chapter 6) and probed with anti-HA 12CA5 (Roche), in the top panel. Extracts were also probed with anti-Pgk1 (Invitrogen) as a loading control (bottom panel).

A somewhat trivial explanation of these results is that *GCN5* deletion or elimination of its HAT activity decreases the amount of Lea1, leading to a decrease in its association with the gene. However, total Lea1 protein levels are unchanged in the absence of Gcn5. Msl1 proteins levels are were unaffected (Figure 2.8).

Co-transcriptional recruitment of Msl1 to *DBP2* was also examined. As previously described, Msl1 association with *DBP2* is also enriched in regions downstream of the branchpoint sequence. This enrichment is abrogated when *GCN5* is deleted or when Gcn5 HAT activity is eliminated (Figures 2.9 B and 2.9 D, respectively). Consistent with previous studies, we routinely observe that the fold enrichment of Msl1 near the branchpoint (primer set 4) relative to the nontranscribed control is lower than for Lea1. Again RNA polymerase II occupancy was not significantly altered in the strain deleted of *GCN5* or HAT activity is mutated (Figure 2.9 C and D, respectively). To examine the specificity of the enrichment of Msl1 within *DBP2*, we examined the recruitment of Msl1 (and Lea1) to a region further upstream of the promoter of *DBP2* and find that neither protein is significantly recruited to these regions in the presence or absence of *GCN5* (Figure 2.10 B), suggesting that recruitment of Lea1 and Msl1 is transcription dependent. Additionally, we tested whether we can rescue recruitment of Lea1 and Msl1 by expressing *GCN5* from a plasmid and we observed that recruitment was rescued (Figure 2.11). These data demonstrate that co-transcriptional Msl1 and Lea1 recruitment to the branchpoint region of the pre-mRNA is dependent upon *GCN5*.

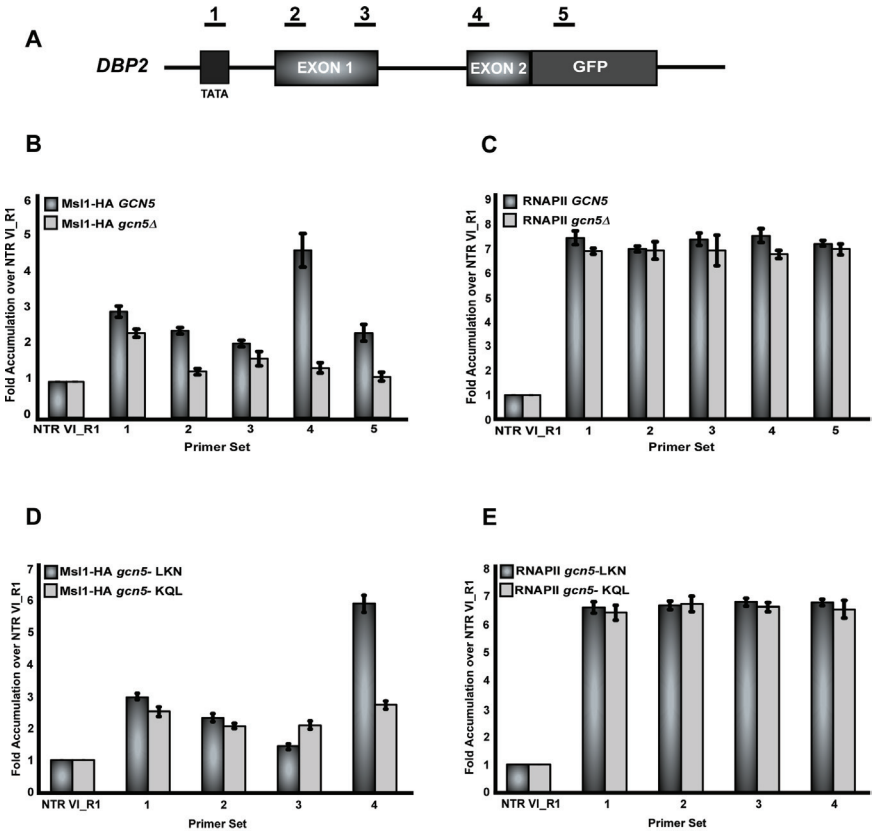

Figure 2.9: Deletion of *GCN5* affects co-transcriptional recruitment of Lea1 to *DBP2*. A) Schematic of the intron-containing gene, *DBP2.* Underlined numbers represent amplicons generated from each primer set used in the study. B) Graph depicting the occupancy of Lea1 at each region of *DBP2* relative to the non-transcribed region, in wild type or *gcn5*Δ. Dark grey bars represent Lea1 with wild type *GCN5* and light grey bars represent Lea1 levels in the *gcn5*Δ strain. C) Bar graph depicting RNA pol II occupancy within DBP2 relative to the non-transcribed control. Dark grey bars represent RNAP II occupancy in the *LEA1-HA* strain and light grey bars represent RNAP II occupancy in the *LEA1-HA gcn5*Δ strain. D) Graph depicting the occupancy of Lea1 with the Gcn5 HAT mutants, LKN and KQL. Dark grey bars represent Lea1 with the Gcn5 LKN mutation, light grey bars represent Lea1 with the Gcn5 KQL mutation. E) Bar graph depicting RNA pol II occupancy in the presence of the Gcn5 HAT mutants. Dark grey bars represent RNA pol II occupancy with the Gcn5 LKN mutation and light grey bars represent RNAP II with the Gcn5 KQL mutant. All graphs depict the average of at least three independent experiments, and error bars represent the standard deviation.

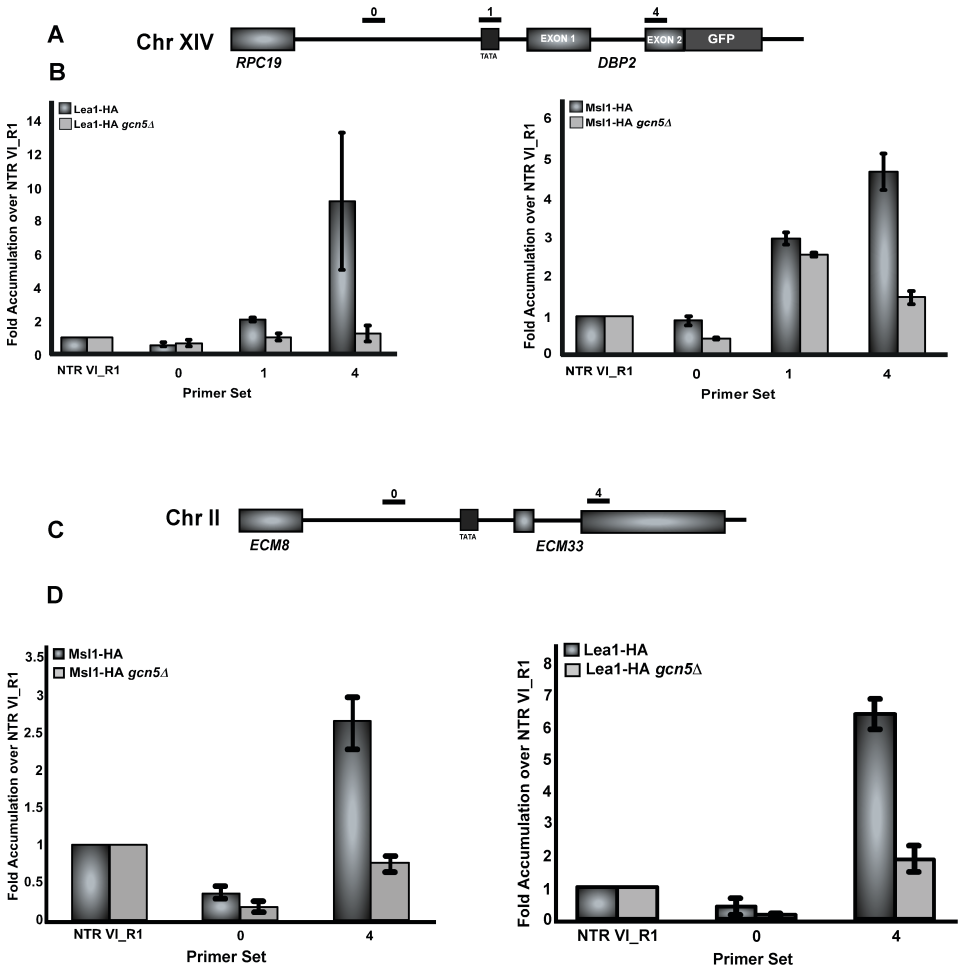

Figure 2.10: Recruitment of Msl1 and Lea1 to *DBP2* and *ECM33* is dependent on transcription.

A) Schematic of chromosome XIV and relative location of *DBP2*. Underlined numbers represent amplicons from each primer set used in this study. B) Graph represents occupancy of Lea1 and Msl1 at each region of *DBP2* relative to the non-transcribed region in the presence and absence of *GCN5*. Dark grey bars represent Lea1/Msl1 recruitment in the presence of *GCN5* and light grey bars represent recruitment of Lea1/Msl1 in the absence of *GCN5*. C) Schematic of chromosome II and the relative location of *ECM33*. Underlined numbers represent amplicons from each primer set used in this study. D) Occupancy of Lea1 and Msl1 at *ECM33* relative to the non-transcribed region. Dark Grey bars represent Lea1/Msl1 recruitment in the presence of *GCN5* and light grey bars represent Lea1/Msl1 recruitment in the absence. Graphs depict the average of three independent experiments, +/- 1 standard deviation.

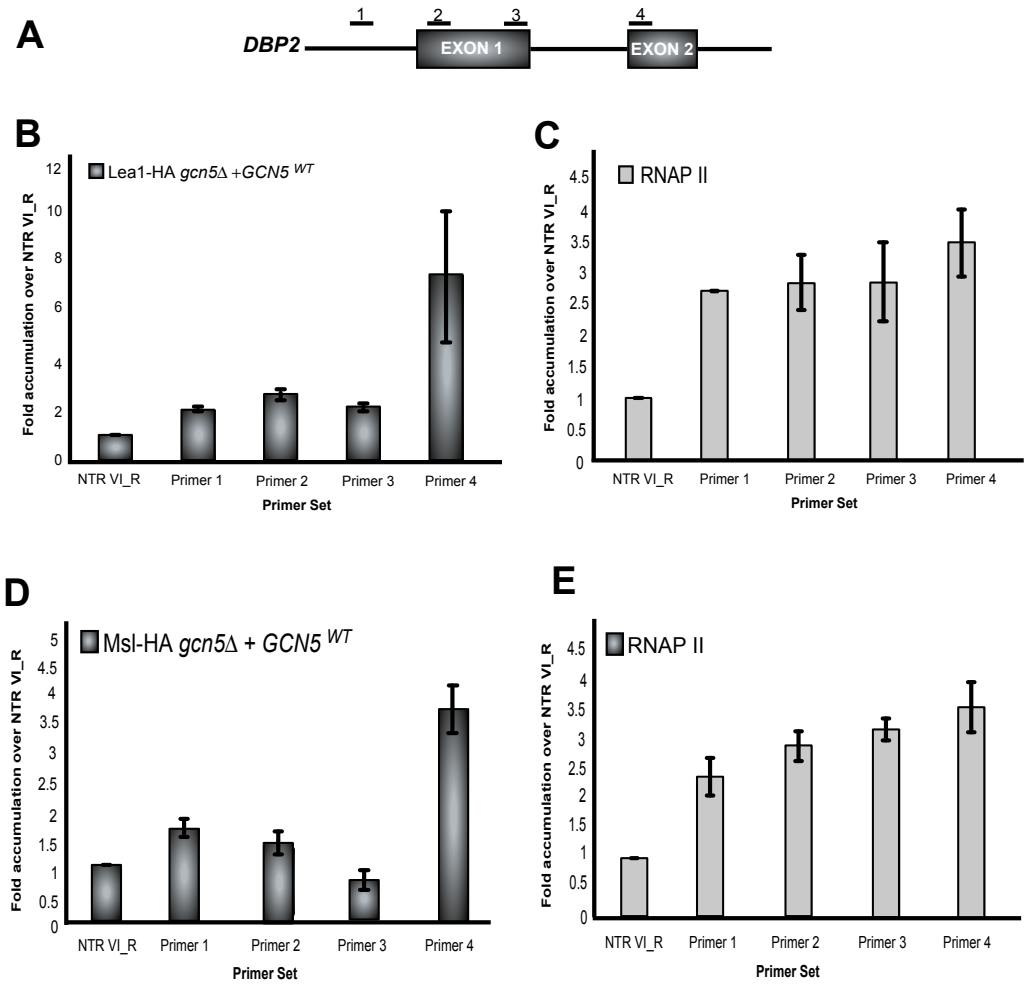

Figure 2.11: Recruitment of Msl1 and Lea1 are recovered when *GCN5* is provided on a plasmid.

A) Schematic of the intron-containing gene, *DBP2* and underlined numbers represent the location of each primer set used in the study. B) Graph measures the recruitment of Lea1 in the presence of *GCN5* on plasmid to *DBP2* normalized to the non-transcribed control. C) Bar graph measures the amount of RNAPII recruitment to *DBP2*. Data represented as fold accumulation over the non-transcribed region, +/- 1 standard deviation. D) Graph measures the recruitment of Msl1 in the presence of *GCN5* on a plasmid. Recruitment is measured as fold accumulation over the non-transcribed control. E) Representative graphs of RNAPII ChIP. Bar graph measures the recruitment of RNAPII normalized to the non-transcribed region. Graphs represent average of three independent experiments +/- 1 standard deviation.

To determine if Gcn5 affects splicing of *DBP2*, we performed qRT-PCR to determine the ratio of unspliced pre-mRNA to total *DBP2* RNA. Using this analysis, we reproducibly detect an approximately two-fold increase in the Precursor/Total RNA ratio in *GCN5* deleted cells compared to WT cells (Figure 2.12 A). When the genes encoding the splicing factors Msl1 and Lea1 are deleted, we observe a 10-15 fold increase in Precursor/Total RNA ratio relative to WT (approximately 5-9% total unspliced) (Figure 2.12 B). While deletion of *GCN5* leads to a moderate increase in intron accumulation when compared to deletion of a bona fide splicing factor, this reproducible increase indicates that splicing of *DBP2* is sensitive to the absence of Gcn5. While it is clear that post-transcriptional splicing can occur (Gornemann et al., 2005), at least under optimal growth conditions, when co-transcriptional splicing is abrogated, it is likely that the additive effect of disrupting co-transcriptional splicing across the genome has important implications for optimal cellular function, particularly under conditions in which optimal splicing of particular genes is required for cell viability. This hypothesis is currently being tested using experiments described in Appendix 1.

Interestingly, we consistently observe enrichment of Msl1 upstream of exon 1, within the promoter region of *DBP2,* which is illustrated by the amplification observed with primer set 1 (Figure 2.9 B, compare to primer set 4, which depicts peak enrichment within the gene). The level of Msl1 in this region is only mildly decreased when *GCN5* is deleted or its catalytic activity is eliminated. This result is surprising since it suggests that the protein is

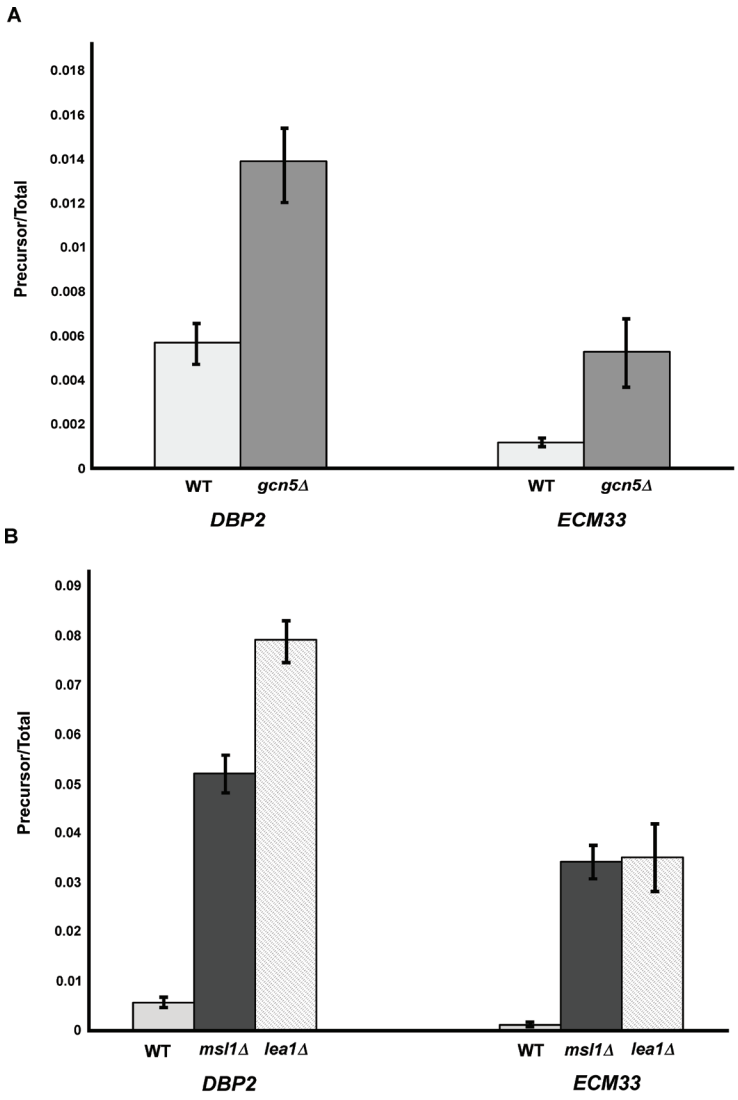

Figure 2.12: Deletion of *GCN5* alters splicing of *DBP2* and *ECM33* transcripts. Quantitative RT-PCR of *DBP2* and *ECM33* in the absence of *GCN5*, *MSL1*, or *LEA1*. A) Graph represents the ratio of precursor *DBP2* or *ECM33* transcript relative to mature message in a wild type and *GCN5* deleted cells. Data is represented as a ratio of precursor (unspliced) RNA to total message. B) Graph represents the ratio of precursor (unspliced) RNA to total *DBP2* or *ECM33* message in wild type, *MSL1* deleted, and *LEA1* deleted cells. Error bars represent +/- 1 standard deviation. The ratio of precursor to total message is calculated as described for 3A.

associated with the chromatin before synthesis of the appropriate RNA signal and that the crosslinking step has captured branchpoint-independent interactions between Msl1 and the transcription complex.

Msl1, but not Lea1, has been shown by yeast two-hybrid to interact with Ssl2, a component of TFIIH, and Tra1, a SAGA subunit that interacts with acidic activators (Fromont-Racine et al., 1997). Furthermore, Msl1, but not Lea1, affinity purifies with TAF4, a subunit of the TFIID complex (Sanders *et al.*, 2002). These unique interactions between Msl1 and components of the transcription machinery that are predicted to act at or near the promoter suggest that Msl1 may be recruited early during transcription initiation and could form a bridge between transcription and U2 snRNP recruitment.

Gcn5 affects acetylation of *DBP2*-bound histones.

The finding that Gcn5 HAT activity is required for co-transcriptional recruitment of the U2 snRNP to *DBP2* leads to the prediction that acetylation of *DBP2*-bound histones is also Gcn5 dependent. To test this prediction, ChIP was performed using an antibody that recognizes diacetylated histone H3. Histone H3 acetylation peaks at the promoter region of *DBP2* (Figure 2.13) with little evidence of enriched acetylation in the body of the gene. This acetylation drops dramatically when *GCN5* is deleted, demonstrating that *DBP2*-bound histones are acetylated in a Gcn5-dependent manner. Since histone deacetylases (HDACs) have been shown to affect rapid/dynamic histone acetylation patterns we examined histone acetylation in the absence of the individual HDACs shown

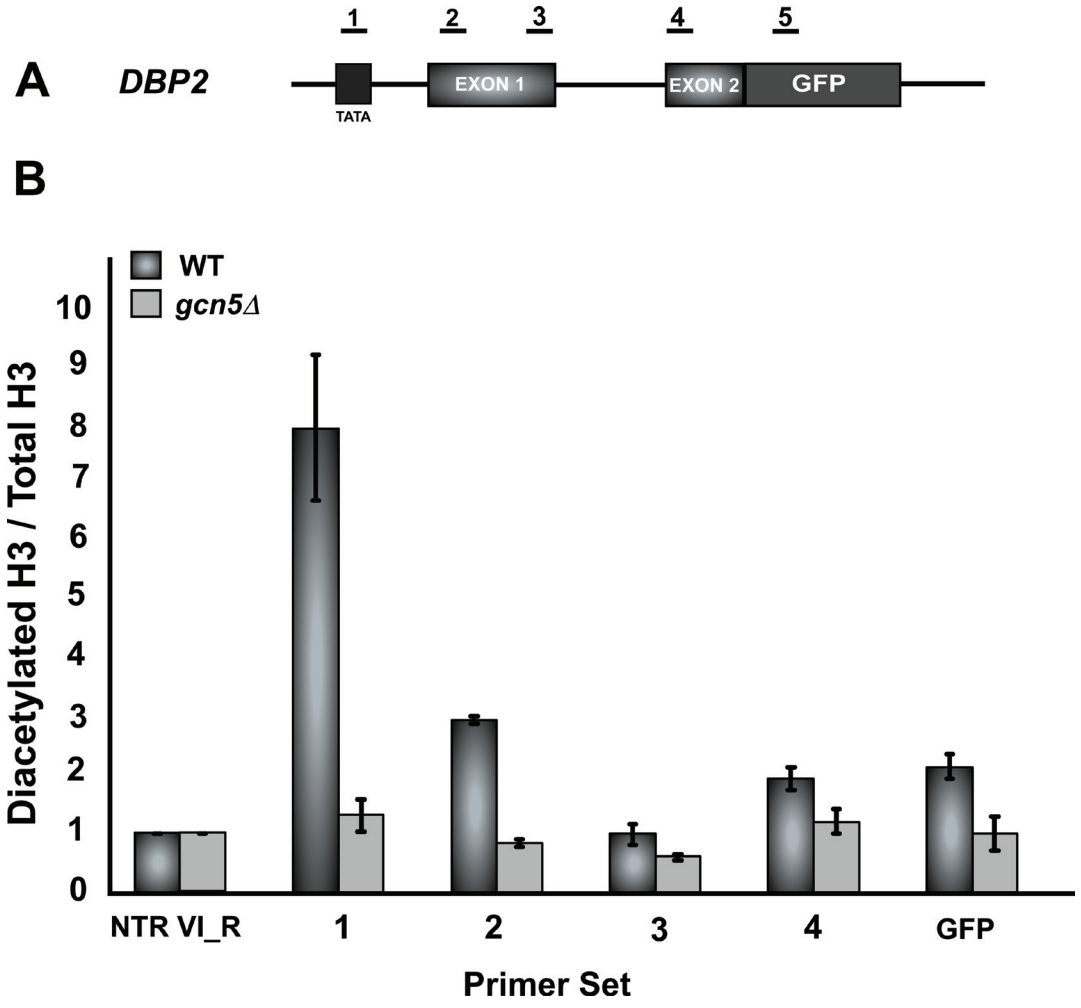

Figure 2.13: *DBP2*–bound histones are acetylated in a Gcn5-dependent manner. A) Schematic of the intron-containing gene, *DBP2.* Underlined numbers represent amplicons generated from each primer set used in this study. B) ChIP analysis of histone H3 K9/14 acetylation within *DBP2* in wild type and *gcn5*Δ strains using an antibody directed against diacetylated histone H3 (Upstate). Dark grey bars represent wild type and light grey bars represent histone acetylation in a *gcn5*Δ strain. Data are represented as diacetylated histone H3 normalized to the total amount of histone H3 (Total H3). Graph depicts the average of at least three independent experiments, and error bars represent the standard deviation.

in Figure 2.2 C, namely Hos2, and Hos3. We found that deletion of these HDACs did not significantly affect acetylation at the promoter or in the body of the gene (Figure 2.14). It remains possible that other deacetylases or some combination of HDACs may contribute to regulation of histone marks involved in co-transcriptional splicing. This is explored in Chapter three. It is also possible that histones are being rapidly exchanged such that the relevant marks within the body of the gene that facilitate co-transcriptional recruitment of Msl1 and Lea1 are difficult to detect. Nonetheless, Gcn5's acetylation activity, most likely toward histones, appears to be a critical determinant of Msl1 and Lea1 recruitment to the branchpoint. The precise role of Gcn5-mediated acetylation of lysine residues on either histone (H3, H2B, or H4) or non-histone substrates is currently under investigation.

Co-transcriptional recruitment of the U1 snRNP, but not the U5 snRNP, occurs in the absence of Gcn5.

Co-transcriptional recruitment of the spliceosome to the emerging pre-mRNA has been shown to occur in a stepwise fashion (Gornemann et al., 2005, Lacadie & Rosbash, 2005). Here we show that deletion of *GCN5* severely abrogates the co-transcriptional recruitment of the U2 snRNP. Combined with our genetic analysis, these results strongly suggest a specific role for Gcn5 activity in U2 snRNP function. Nonetheless, it is possible that deletion of *GCN5* acts generally to disrupt co-transcriptional recruitment of all snRNPs. To address this, recruitment of a representative component of the U1 snRNP and triple

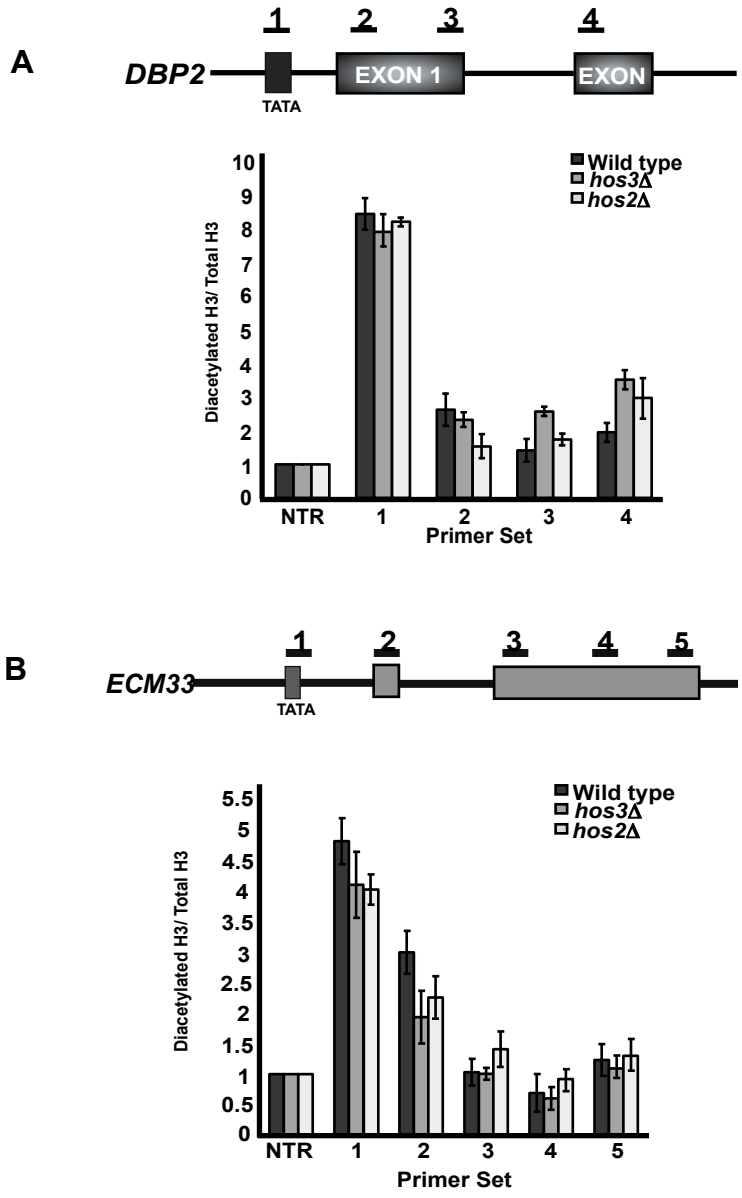

Figure 2.14: Deletion of *HOS2* or *HOS3* does not severely affect histone acetylation in the promoter of intron-containing genes.
A) Schematic of *DBP2*. Underlined numbers represent amplicons from each primer set used in this study. Histone H3 acetylation profile of *DBP2* in the presence and absence of *HOS2* and *HOS3.* Data is represented as diacetylated histone H3 relative to total histone H3. C) Schematic of ECM33. Underlined numbers represent amplicons from each primer set used in this study. D) Histone H3 acetylation profile of ECM33 in the presence and absence of *HOS2* and *HOS3*. Data is represented as diacetylated histone H3 relative to total histone H3. Each graph depicts an average of three independent experiments, +/- standard deviation.

snRNP was examined. Chromatin IP of Prp42 has been shown to be an indicator of U1 snRNP recruitment to intron-containing genes (Kotovic et al., 2003, Gornemann et al., 2005). To determine if recruitment of the U1 snRNP is altered in the absence of *GCN5*, Prp42 association with *DBP2* was analyzed. The U1 snRNP associates with the *DBP2* pre-mRNA shortly after synthesis of the 5' splice site, consistent with reports by others (Figure 2.15 B) (Kotovic et al., 2003, Gornemann et al., 2005). Unlike its effect on U2 snRNP recruitment, deletion of *GCN5* does not abrogate the recruitment of the U1 snRNP, demonstrating that the U1 snRNP is still being actively recruited to the pre-mRNA in a co-transcriptional manner (Figure 2.15 B). Hence, the observed disruption of co-transcriptional recruitment of the U2 snRNP in the absence of Gcn5's catalytic activity is specific, and *GCN5* deletion does not abrogate all early steps in spliceosome assembly.

Since co-transcriptional spliceosome assembly occurs in a stepwise fashion, the prediction is that disruption of U2 snRNP recruitment due to deletion of *GCN5* would affect co-transcriptional spliceosome assembly downstream of the U2 snRNP. Snu114 is a U5 snRNP protein that is involved in the destabilization of U1 and U4 snRNAs during spliceosome assembly (Bartels *et al.*, 2003, Bartels *et al.*, 2002, Brenner & Guthrie, 2006). Chromatin IP of Snu114 shows that the U5 snRNP is enriched downstream of the 3' splice site, a result consistent with previous observations (Figure 2.15 C) (Gornemann et al., 2005). However, deletion of *GCN5* eliminates the co-transcriptional recruitment of U5 snRNP (Figure 2.15 C), indicating that the lack of U2 snRNP recruitment does

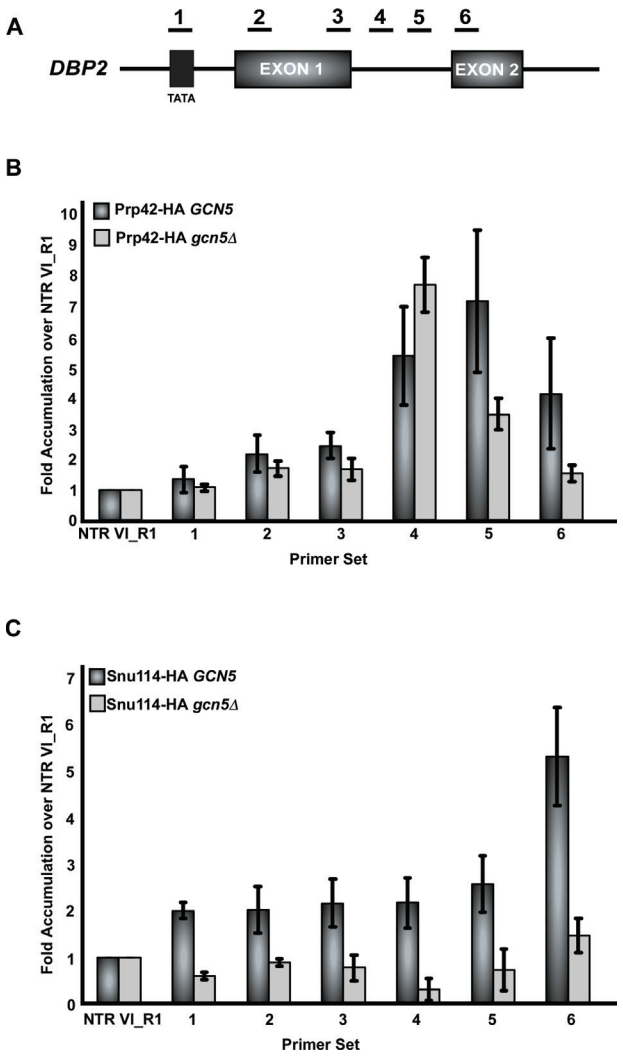

Figure 2.15: Co-transcriptional recruitment of U1 snRNP and U5 snRNP in the presence and absence of *GCN5*.

A) Schematic of the intron-containing gene, *DBP2*. Underlined numbers represent the amplicons generated from each primer set used in the study. B) Bar graph depicting recruitment of U1 snRNP (Prp42-HA) in the presence and absence of *GCN5*. Dark grey bars represent the occupancy of Prp42-HA in the presence of wild type *GCN5* and light grey bars represent Prp42-HA in the absence of *GCN5*. Occupancy is measured as fold accumulation over the non-transcribed region. C) Bar graph depicting the recruitment of U5 snRNP (Snu114-HA) in the presence and absence of *GCN5*. Dark grey bars represent the Snu114-HA in the presence of *GCN5*, and light grey bars represent Snu114-HA occupancy in the absence of *GCN5*. Graphs represent the average of at least three independent experiments, and error bars represent the standard deviation.

alter the recruitment of downstream factors and cripples spliceosome assembly. Although this is consistent with the ordered assembly model of co-transcriptional splicing (Gornemann et al., 2005, Lacadie & Rosbash, 2005), we cannot rule out the possibility of an independent effect by Gcn5 on U5 recruitment.

Gcn5 affects co-transcriptional recruitment of Lea1 and Msl1 to *ECM33* and acetylation of its promoter bound histones.

DBP2 was chosen for these studies because of its previously-characterized suitability for chromatin IP studies. *DBP2*'s long intron (~1Kb) and long first exon (~1Kb) allow for resolution of protein association throughout the gene. We wanted to examine a second well-characterized, intron-containing gene to determine if Gcn5's role in co-transcriptional recruitment of Lea1 and Msl1 is more general. *ECM33* has previously been described by others to be a gene to which splicing factors, including the U2 snRNP, are co-transcriptionally recruited (Gornemann et al., 2005). Examination of the co-transcriptional recruitment of Msl1 and Lea1 to *ECM33* in the presence of Gcn5 revealed that Lea1 and Msl1 recruitment occurred after the formation of the branchpoint (Figures 2.16 B and 2.16 C, respectively), consistent with what we observed with *DBP2*. In the absence of *GCN5*, recruitment of Lea1 and Msl1 was abolished (Figures 2.16 B and 2.16 C, respectively). Two other genes *YRA1* and *PFY1* show a similar Gcn5-dependent pattern of Msl1 and Lea1 recruitment (Figure 2.17 and Figure 2.18, respectively). As with *DBP2*, when recruitment of Msl1 and Lea1 to a region further upstream of the promoter of *ECM33* was examined

in the presence and absence of *GCN5, we* find that neither protein is significantly recruited to this region, reinforcing the transcription-dependence of their recruitment (Figure 2.10). Also similar to *DBP2*, deletion of *GCN5* leads to an increase in the Precursor/Total RNA ratio when compared to WT cells (approximately 4-5 fold) (Figure 2.12).

We next examined the acetylation pattern of *ECM33*-bound histones by ChIP. Consistent with what we observed with *DBP2*, a strong Gcn5-dependent peak in acetylation was observed at the promoter of *ECM33*, (Figure 2.16 D) and little change in this pattern was observed when the HDACs were deleted.

As with *DBP2*, Msl1 recruitment peaks after synthesis of the branchpoint of *ECM33* (Figure 2.16C, primer sets 3-4). Additionally, analysis of the upstream region of *ECM33* shows some early association of Msl1 relative to the non-transcribed control (Figure 2.16 C) and especially relative to the peak in signal with primer sets 3 and 4. This early association of Msl1 is most evident using primer set 2, although the short distance between amplicons 1 and 2 (around 300 base pairs) is likely too small to completely resolve. Nonetheless, the early recruitment of Msl1 to *ECM33* is less pronounced than what we observe with *DBP2.* A possible explanation for this is the transcriptional frequency of the individual genes. For example, *DBP2* generates about 4 times the number of mRNA molecules as *ECM33*, and the transcriptional frequency is approximately 7 times greater (Holstege *et al.*, 1998). It is possible that the increase in transcription of *DBP2* allows for more recruitment of Msl1 to the promoter.

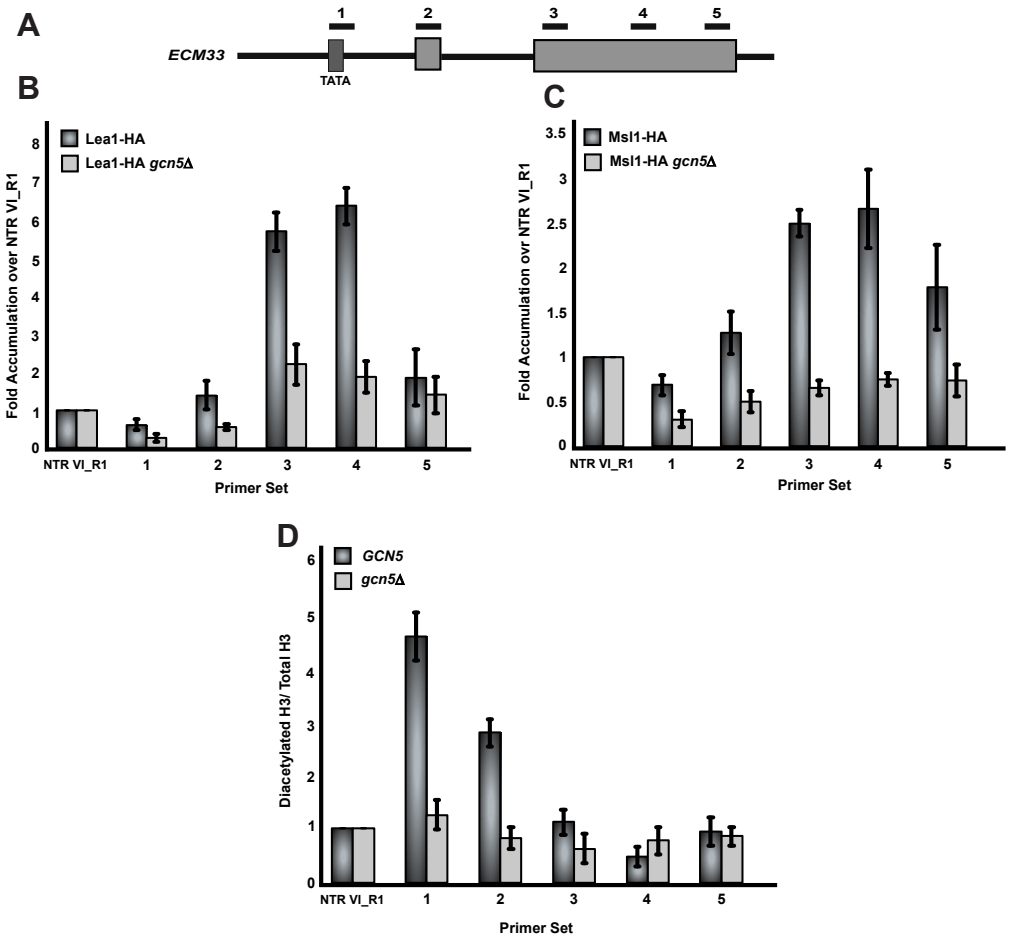

Figure 2.16: Deletion of *GCN5* affects co-transcriptional recruitment of Msl1 and Lea1 to ECM33 and histone H3 acetylation.

A) Schematic of the intron-containing gene, *ECM33*. Underlined numbers represent the amplicons generated from each primer set used in the study. B) Graph depicting the occupancy of Lea1 at each region of *ECM33* relative to the non-transcribed region, in wild type or *gcn5*Δ cells . Dark grey bars represent Lea1 with wild type *GCN5*, and light grey bars represent Lea1 levels in the *gcn5*Δ strain. C) Bar graph depicting Msl1-HA occupancy within *ECM33* relative to the non-transcribed control. Dark grey bars represent Msl1-HA with wild type *GCN5* and light grey bars represent Msl1-HA occupancy in the *gcn5*Δ strain. Data are represented as fold accumulation over the non-transcribed region. D) ChIP analysis of histone H3 K9/14 acetylation in *ECM33* of wild type and *gcn5*Δ strains using an antibody against diacetylated histone H3. Dark grey bars represent wild type and light grey bars represent histone acetylation in a *gcn5*Δ strain. Data are represented as diacetylated histone H3 normalized to the total amount of histone H3 (Total H3). Graphs depict the average of three independent experiments, and error bars represent the standard deviation.

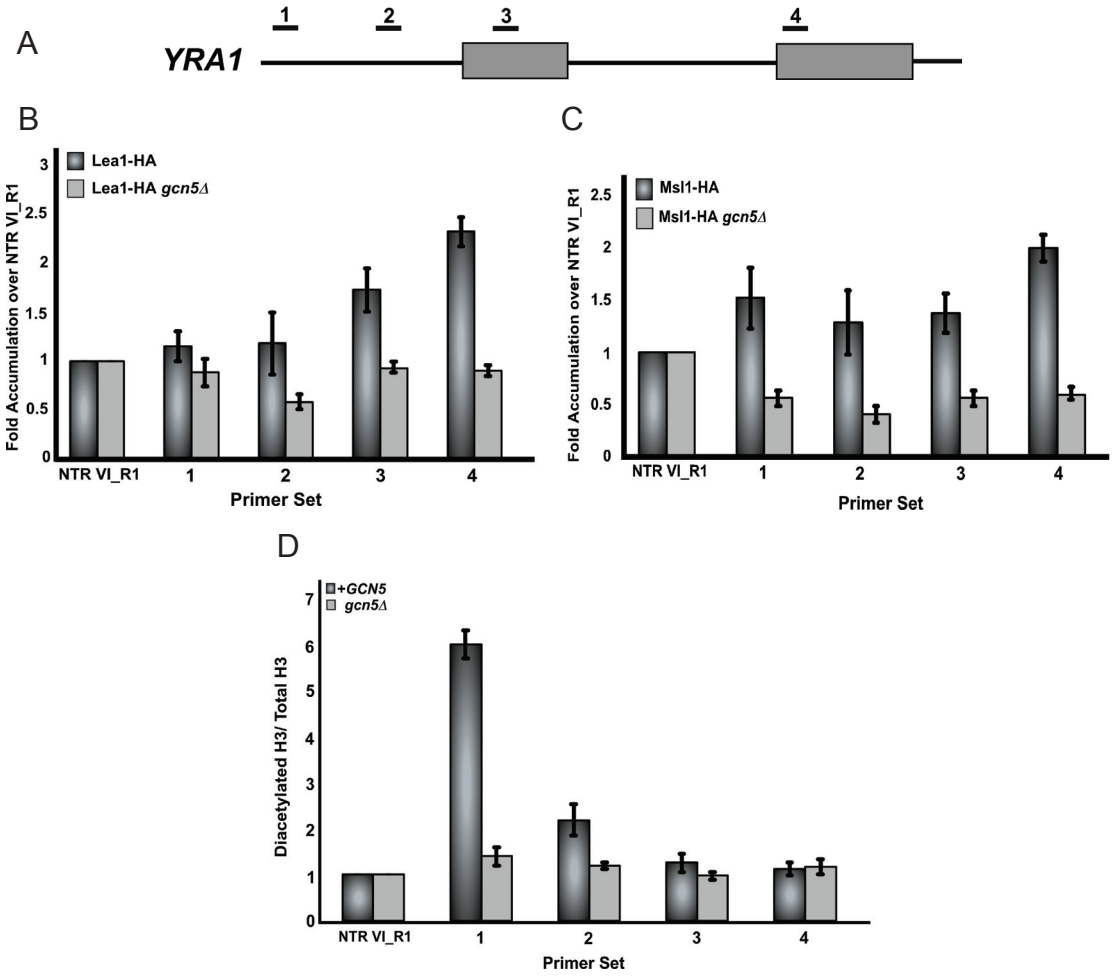

Figure 2.17: Deletion of *GCN5* affects co-transcriptional recruitment of Msl1 and Lea1 to *YRA1* and histone H3 acetylation.

A) Schematic of the intron-containing gene, *YRA1*. Underlined numbers represent the amplicons generated from each primer set used in the study. B) Graph depicting the occupancy of Lea1 at each region of *YRA1* relative to the non-transcribed region, in wild type or *gcn5*Δ cells . Dark grey bars represent Lea1 with wild type *GCN5*, and light grey bars represent Lea1 levels in the *gcn5*Δ strain. C) Bar graph depicting Msl1-HA occupancy within *YRA1* relative to the non-transcribed control. Dark grey bars represent Msl-HA with wild type *GCN5* and light grey bars represent Msl1-HA occupancy in the *gcn5*Δ strain. Data are represented as fold accumulation over the non-transcribed region. D) ChIP analysis of histone H3 K9/14 acetylation in *YRA1* of wild type and *gcn5*Δ strains using an antibody against diacetylated histone H3. Dark grey bars represent wild type and light grey bars represent histone acetylation in a *gcn5*Δ strain. Data are represented as diacetylated histone H3 normalized to the total amount of histone H3 (Total H3). Graphs depict the average of three independent experiments, and error bars represent the standard deviation.

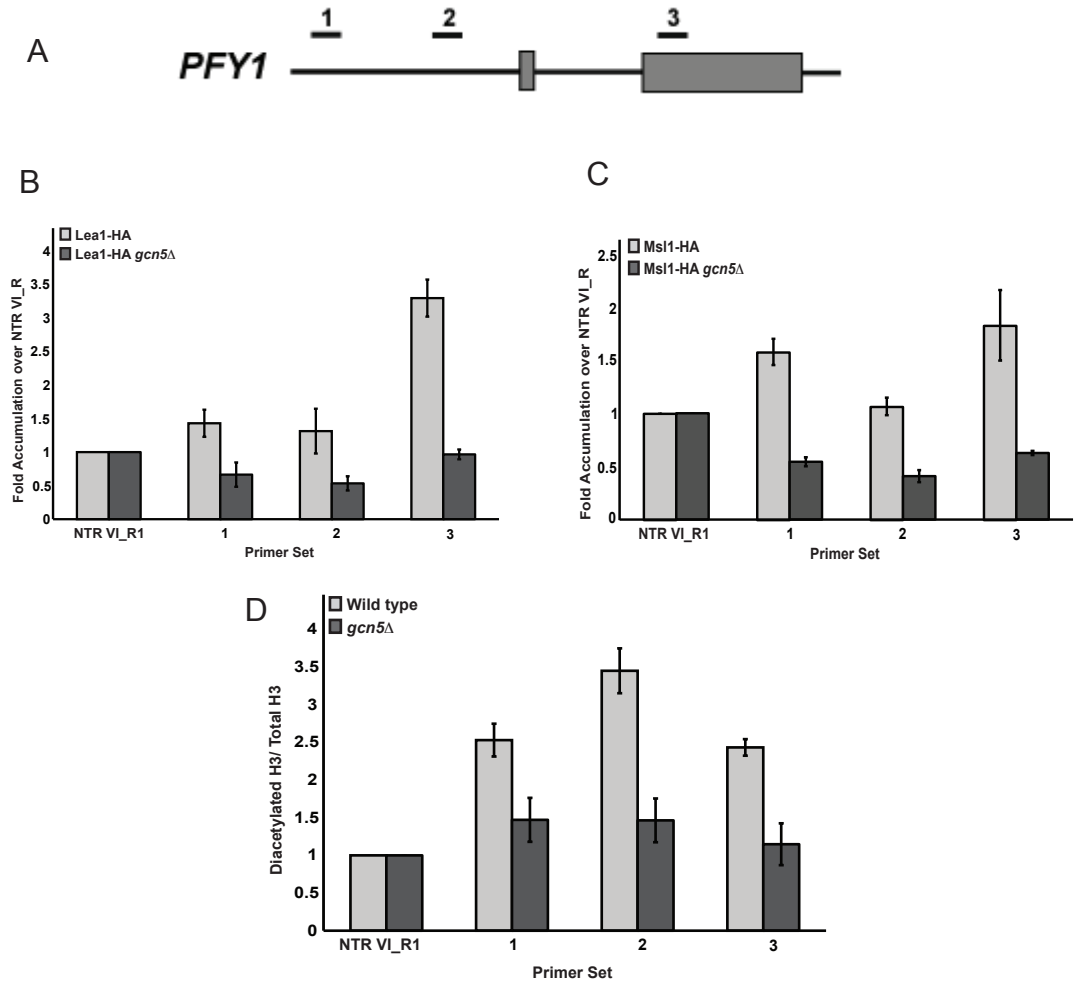

Figure 2.18: Deletion of *GCN5* affects co-transcriptional recruitment of Msl1 and Lea1 to *PFY1* and histone H3 acetylation.

A) Schematic of the intron-containing gene, *PFY1*. Underlined numbers represent the amplicons generated from each primer set used in the study. B) Graph depicting the occupancy of Lea1 at each region of *PFY1* relative to the non-transcribed region, in wild type or *gcn5*Δ cells . Dark grey bars represent Lea1 with wild type *GCN5*, and light grey bars represent Lea1 levels in the *gcn5*Δ strain. C) Bar graph depicting Msl1-HA occupancy within *PFY1* relative to the non-transcribed control. Dark grey bars represent Msl-HA with wild type *GCN5* and light grey bars represent Msl1-HA occupancy in the *gcn5*Δ strain. Data are represented as fold accumulation over the non-transcribed region. D) ChIP analysis of histone H3 K9/14 acetylation in *PFY1* of wild type and *gcn5*Δ strains using an antibody against diacetylated histone H3. Dark grey bars represent wild type and light grey bars represent histone acetylation in a *gcn5*Δ strain. Data are represented as diacetylated histone H3 normalized to the total amount of histone H3 (Total H3). Graphs depict the average of three independent experiments, and error bars represent the standard deviation.

Taken together, these results suggest that Gcn5-dependent co-transcriptional recruitment of Msl1 and Lea1 to the branchpoint is a common feature among intron-containing genes.

Section 2.3: Discussion

Recent work from a number of groups provides evidence of spatial and temporal coordination of transcription and pre-messenger RNA processing. Simultaneously, there has been an emerging understanding of the role of histone modification and the enzymes that catalyze these modifications in regulating gene expression. Here we demonstrate a new function for the histone acetyltransferase Gcn5. In addition to its previously-characterized role in transcriptional activation, Gcn5 can specifically affect co-transcriptional assembly of the spliceosome onto constitutively-spliced genes. Our genetic analysis reveals that Gcn5 has functional interactions with two specific U2 snRNP components Msl1 and Lea1, and these functional interactions depend on Gcn5's HAT activity. Our genetic analysis further provides evidence of the specificity of this interaction and suggests that it most likely occurs within the context of a functional SAGA complex that is targeted to chromatin. These studies demonstrate a novel mechanism whereby a protein complex whose catalytic activity establishes a mark of active transcription also plays a central role in co-transcriptional mRNA processing.

How does Gcn5 affect spliceosome assembly?

In recent years, there has been strong evidence that splicing can occur co-transcriptionally in yeast and in mammals. However, the mechanism by which spliceosome assembly is coordinated with transcription has been difficult to decipher, particularly in yeast. The genetics and ChIP results described above suggest a model in which Gcn5 mediates co-transcriptional spliceosome assembly by affecting histone acetylation. While we have not detected U2 snRNP acetylation, these data do not rule out the possibility that an additional non-histone substrate (or substrates) of Gcn5 can affect co-transcriptional spliceosome assembly, which is something that we continue to explore. It would nonetheless be interesting if Gcn5's acetylation activity is targeted toward a non-histone substrate to abrogate co-transcriptional splicing.

Since previous studies have shown that Gcn5 can affect transcription elongation (Govind et al., 2007), it is possible that Gcn5 effects on transcription elongation could be responsible for its role in co-transcriptional splicing, especially in light of studies that indicate that changes in elongation can influence pre-mRNA splicing (de la Mata et al., 2003, Howe et al., 2003, Lacadie *et al.*, 2006). Nonetheless, several lines of evidence suggest that it is not a Gcn5 effect on elongation per se that underlies its role in co-transcriptional snRNP recruitment. First, *GCN5* deletion does not appear to significantly affect pol II levels throughout *DBP2 or ECM33*. Furthermore, the genetic interactions between *MSL1* or *LEA1* and *GCN5* are not observed with the histone acetyltransferase that acts during elongation, *ELP3*. In light of these findings we

favor a model in which Gcn5-dependent histone acetylation at the promoter facilitates co-transcriptional recruitment of splicing factors to the branchpoint. We think that it is likely that high promoter acetylation facilitates loading of a factor or factors onto elongating RNA polymerases, and these factors then recruit Msl1 and/or Lea1 to the branchpoint.

We cannot rule out that direct interactions between Gcn5 and the U2 snRNP may be important for recruitment, particularly since Gcn5 has been shown to associate both at the promoter and within the body of genes. Although our initial studies do not detect a direct association between Gcn5 and either Msl1 or Lea1, the interactions may be too weak or transient to detect biochemically.

The role of co-transcriptional splicing in mature message formation.

The analysis reported here indicates that deletion of Gcn5 leads to a reproducible increase in unspliced RNA relative to WT cells for both of the genes analyzed. While the amount of unspliced message that accumulates in the absence of Gcn5 is modest on a per gene basis, it is likely that the additive effect across the genome of decreased splicing efficiency when co-transcriptional splicing is abrogated is important. A number of studies of splicing in yeast have found, as we do, that some post-transcriptional splicing can occur even when co-transcriptional splicing is eliminated. Co-transcriptional recognition of splice signals is thought to be a means of increasing the efficiency and perhaps the rate

of splicing. Hence, it is likely that conditions under which optimal splicing is necessary will be particularly sensitive to changes in co-transcriptional splicing, which we are currently exploring. We are also testing whether this Gcn5-dependence for optimal splicing increases under growth conditions in which the cell's transcription is particularly dependent on SAGA, which is reported to be the case under a variety of stress conditions (Huisinga & Pugh, 2004).

Branchpoint recognition is a critical step in coordinating splicing with transcription.

Proper splicing is achieved by sequential recognition of the branchpoint by numerous factors, including the branchpoint binding protein (BBP) and the U2 snRNA (with its associated collection of snRNP-specific proteins). The exchange of BBP for the U2 snRNA is the first ATP-dependent step in splicing, and splice sites are committed to participate in this first ATP-dependent step when spliceosomal rearrangements lock the U2 snRNA into place (Lim & Hertel, 2004). The work described here suggests that branchpoint recognition is a critical step in coordinating splicing with transcription. A recent mammalian study also suggests that branchpoint recognition is closely tied to transcription. This study identified interactions between U2 snRNP components and the H3K4me3 interacting protein Chd1. Chd1 bridges U2 snRNP association with trimethylated histone H3, indicating that U2 snRNP recruitment in mammals is closely tied with transcription and specifically with chromatin "marks" of active transcription (Sims et al., 2007).

Evidence that a transcriptional coactivator that functions at the 5' end of the gene can influence U2 snRNP recruitment is particularly interesting in light of a recent proposal that the majority of second exons in yeast may be too short to support stable recruitment of the U2 snRNP and, as a consequence, most endogenous yeast gene splicing is completed post-transcriptionally. Our results suggest that the activity of Gcn5 facilitates co-transcriptional recruitment of the U2 snRNP to at least a subset of genes. Furthermore, co-transcriptional U2 snRNP recruitment may even involve recruitment of Msl1 before synthesis of the branchpoint since Msl1 appears to have unique interactions with the transcription machinery. Our data suggest that the commitment to splicing is likely made co-transcriptionally, and Gcn5 facilitates U2 snRNP association with the pre-mRNA to allow a fluid transition to a U2 snRNP poised to participate in post-transcriptional splicing catalysis.

Studies of the mammalian counterpart of SAGA suggest that interactions between the complex and the U2 snRNP may be evolutionarily conserved. Martinez *et al.* reported that a U2 snRNP protein copurified with the human STAGA complex, although the functional significance of this interaction was not clear (Martinez, 2001). Our results help to explain the functional link between the chromatin modifying machinery and pre-mRNA splicing and demonstrate that Gcn5, likely within the context of the SAGA complex, has a previously undescribed activity in pre-mRNA splicing.

Portions of this chapter were published as: Gunderson, Felizza Q and Johnson, Tracy L, 2009. Acetylation by the transcriptional coactivator Gcn5 plays a novel role in co-transcriptional spliceosome assembly. PLoS Genetics 5 (10) e1000682.

Chapter 3: A new role for HDACs in co-transcriptional spliceosome assembly and spliceosomal rearrangements

Section 3.1: Introduction

Removal of non-coding sequences from pre-messenger RNA is achieved by the activity of a dynamic ribonucleoprotein complex, the spliceosome. As the spliceosomal snRNPs sequentially recognize specific sequences in the pre-mRNA, the spliceosome undergoes dynamic, ATP-dependent rearrangements of its RNA and protein components. One of the most important advances in the study of RNA processing events such as RNA splicing has been the recognition that much of the splicing in the cell occurs co-transcriptionally, while the RNA polymerase is still actively engaged with the chromatin template. Since RNA splicing is spatially linked to transcription, an obvious prediction is that changes in transcription such as polymerase speed and/or processivity could affect splicing and alternative splicing. In fact in the last several years there has been clear evidence that this is the case (For review (Kornblihtt *et al.*, 2004, Munoz *et al.*, 2010).

The DNA template found in eukaryotic cells is comprised of DNA wrapped around a nucleosome core made up of histones H3, H4, H2A, and H2B. Each of these histones undergoes extensive post-translational modification on their N-terminal tails that affect compaction of DNA and binding of regulatory factors. While it is known that splicing occurs co-transcriptionally in the context of this

template, it is far less well understood how changes in this chromatin template could affect RNA splicing. Recently, a number of studies that cull the available genome wide data show that nucleosomes and specific histone modifications are enriched in exon sequences, suggesting that there may be specific histone "marks" that are associated with splicing signals (Andersson *et al.*, 2009, Choi *et al.*, 2009, Kolasinska-Zwierz et al., 2009, Nahkuri *et al.*, 2009, Schwartz et al., 2009, Spies *et al.*, 2009, Tilgner et al., 2009). The 3-D architecture of the DNA template and nascent RNA transcript provide a mechanism whereby it is likely that the RNA and nucleosomes are in fact in close proximity (Wetterberg *et al.*, 2001). In fact, there have been two studies that show that proteins that bind to methylated histones (both H3K4me3 and H3K36me3) facilitate the recruitment of U snRNPs to the nascent transcript and influence efficiency of splicing and alternative splicing (Sims et al., 2007, Luco et al., 2010). Furthermore, the mammalian SWI/SNF complex involved in chromatin remodeling associates with components of the spliceosome that affect variant exon inclusion (Batsche et al., 2006)

Our own work provided one of the first suggestions of a critical role in yeast for a histone acetyltransferase, the transcriptional coactivator Gcn5, in co-transcriptional recruitment of the U2 snRNP to the pre-mRNA (Gunderson & Johnson, 2009). An initial genetic analysis showed that deletion of *GCN5* or eliminating its catalytic activity, in combination with deletion of genes encoding either of the U2 snRNP proteins Msl1 or Lea1 conferred synthetic-lethality to those cells. Not only did Gcn5 have this effect, but any of the factors in the

SAGA complex that are responsible for targeting Gcn5's activity to nucleosomes or maintaining the structural integrity of the complex had the same effect. While there was no evidence of Gcn5-dependent acetylation of U2 snRNP proteins, Gcn5 dependent acetylation in the 5'region of several intron-containing genes was observed. These same genes required Gcn5 for co-transcriptional recruitment of the U2 snRNP and, not surprisingly given the stepwise nature of recruitment, all steps downstream of U2 snRNP association.

Post-translational modification of histones, especially acetylation, and spliceosome assembly are not only spatially and temporally linked, but they are both highly dynamic processes. For example, in addition to histone acetylation, histone *de*acetylation is critical for proper gene expression. Histone acetylation dynamics has been shown to be important for cellular function. Comprehensive genome-wide interaction data reveal striking interactions between HATs and HDACs. This analysis confirmed that hyperacetylation (by HDAC deletion) and hypoacetylation (by removal of HAT activity) can be equally deleterious for the cell (Lin et al., 2008b), which supports previous studies that suggest that a delicate balance of acetylation and deacetylation is crucial for proper cellular function (Vogelauer et al., 2000). Recent studies also demonstrate that both acetylation and deacetylation occur within the coding region of genes and that rapid removal of acetyl groups from histones within the coding region is achieved by the activities of multiple HDACs (Ginsburg *et al.*, 2009, Govind et al., 2007). While they are less well understood, all of the histone modifications identified so

far appear to be reversible, although the timing of the addition and removal of histone marks is far from clear.

Meanwhile, as histones are being modified, and the polymerase traverses the chromatin template to synthesize the RNA, the spliceosomal snRNPs associate with the pre-mRNA in another highly dynamic set of interactions. Work from several labs have demonstrated that the stepwise exchange of factors during co-transcriptional spliceosome assembly can be measured by chromatin IP (ChIP) (Kotovic et al., 2003, Lacadie & Rosbash, 2005, Gornemann et al., 2005). The 5' splice site is recognized by the U1 snRNP. Then the U2 snRNP associates with the branchpoint (a step that we have shown to occur co-transcriptionally in a manner dependent upon the catalytic activity of Gcn5) (Gunderson & Johnson, 2009). ATP-dependent rearrangements in the spliceosome facilitate release of some U2 snRNP interactions and the addition of the U4/U6•U5 triple-snRNP. More rearrangements that involve strengthening of some interactions and weakening of others (with concomitant release of some factors) leads to the formation of the catalytic center and the catalysis of the two transesterification steps.

Our initial observation that Gcn5 was required for co-transcriptional U2 snRNP recruitment and the steps downstream of U2 snRNP association, strongly suggested that histone acetylation has an important impact on co-transcriptional spliceosome assembly. We were intrigued by the possibility that we could not only confirm that acetylation at specific histone residues was important for recruitment of U2 snRNP, but that histone *de*acetylation might provide important

cues for snRNP association with the nascent transcript and perhaps might also support spliceosomal rearrangements.

Here we show that, like deletion of *GCN5*, mutation or deletion of histone H3 lysine residues that are targeted by Gcn5 leads to synthetic lethality when combined with *LEA1* or *MSL1* deletion. When Gcn5 association with intron-containing genes is examined, we observe Gcn5 throughout the gene. Gcn5-dependent acetylation seems most pronounced at the promoter, that is, until acetylation is analyzed in the absence of multiple HDACs. HDAC deletion reveals the presence of strong acetylation throughout the body of the gene, acetylation that was masked by the activity of the HDACs whose removal of acetyl groups from histone H3 masks the presence of histone marks. Interestingly, at least in one case, we observe an overlap between histone H3 levels near the intron/exon2 boundary, where we also observe a peak in Lea1/Msl1. Interestingly, when the HDACs are removed and these histone marks are hyperstabilized, we observe a striking inability for the U2 snRNP interactions with the branchpoint to be exchanged for the necessary downstream snRNPs, indicating that histone acetylation dynamics is coupled with spliceosome dynamics. These data lead to a model in which acetyl marks within the gene lead to recruitment of splicing factors--likely via the activity of a protein that transiently interacts with acetylated histones. Moreover, rapid removal of these marks is necessary to weaken specific snRNP interactions with the nascent transcript such that they can be exchanged for subsequent snRNPs, in a stepwise manner. Finally, we show that these functional interactions between histone H3 and

HDACs and the snRNPs are essential for cell viability and proper spliced message production.

Section 3.2: Results

Mutation of histone H3 residues targeted by Gcn5 confers synthetic lethality when combined with *LEA1* and *MSL1* mutant cells.

I previously demonstrated that deletion of the gene encoding Gcn5 or eliminating its catalytic activity led to a severe synthetic growth defect when combined with deletion of genes encoding either *LEA1* or *MSL1*. Furthermore, Gcn5 catalytic activity was required for their co-transcriptional recruitment to intron-containing genes. I have shown that intron-containing genes bound to histone H3 were acetylated in a Gcn5-dependent manner (Gunderson & Johnson, 2009).

To determine whether acetyation of histone residues were important for co-transcriptional spliceosome assembly, I decided to examine co-transcriptional recruitment of Lea1-HA and Msl1-HA in strains in which endogenous histone H3 and histone H4 were deleted and expressed from CEN plasmids (Wang et al., 1998). In working with these strains, I discovered that these strains did not behave like wild type and their histone H3 expression pattern differed from that of the chromosome expressed histone H3. This result made it difficult to determine the effect of histone mutations in co-transcriptional splicing.

Therefore, to address if acetylation of histone residues were importance for co-transcriptional splicing, we turned to a commercially available yeast histone point mutant collection (Dai *et al.*, 2008). This collection contains histone point mutations that have been integrated into the chromosome. To further elucidate whether acetylation of specific N-terminal residues was important for these functional interactions, we analyzed growth in strains in which deletion of *LEA1* or *MSL1* was combined with mutation of key residues in histone H3 that are targets of Gcn5: H3K9A, H3K14A, or a short N-terminal tail deletion that includes both K9 and K14, Δ9-16 (Dai et al., 2008). At all temperatures tested, a deletion of *LEA1* in combination with the histone point mutant *H3K9A* had little effect on growth. While, mutation of histone *H3K14A* resulted in a synthetic growth defect (Figure 3.1 A). The truncation of histone H3 that eliminates residues 9 to 16 in combination with deletion of *LEA1* resulted in a severe synthetic growth phenotype (Figure 3.1 A). Additionally, we examined whether the N-terminal truncation produced truncated histones by immunoblotting extracts prepared from Δ9-16 cells and probed for histone H3 and acetylated histone H3 K9/14. As expected, the truncation produced histones that were smaller in molecular weight and were not detectable using acetylated histone H3 K9/14 specific antibody (Figure 3.2).

Viability of cells deleted of *MSL1* in combination with a histone H3 point mutations or truncation was also analyzed. Truncation of histone H3 in combination with deletion of *MSL1* also resulted in a synthetic growth phenotype (Figure 3.1 B). In fact, as with *LEA1* deletion at 37^{o}C severe growth defects are

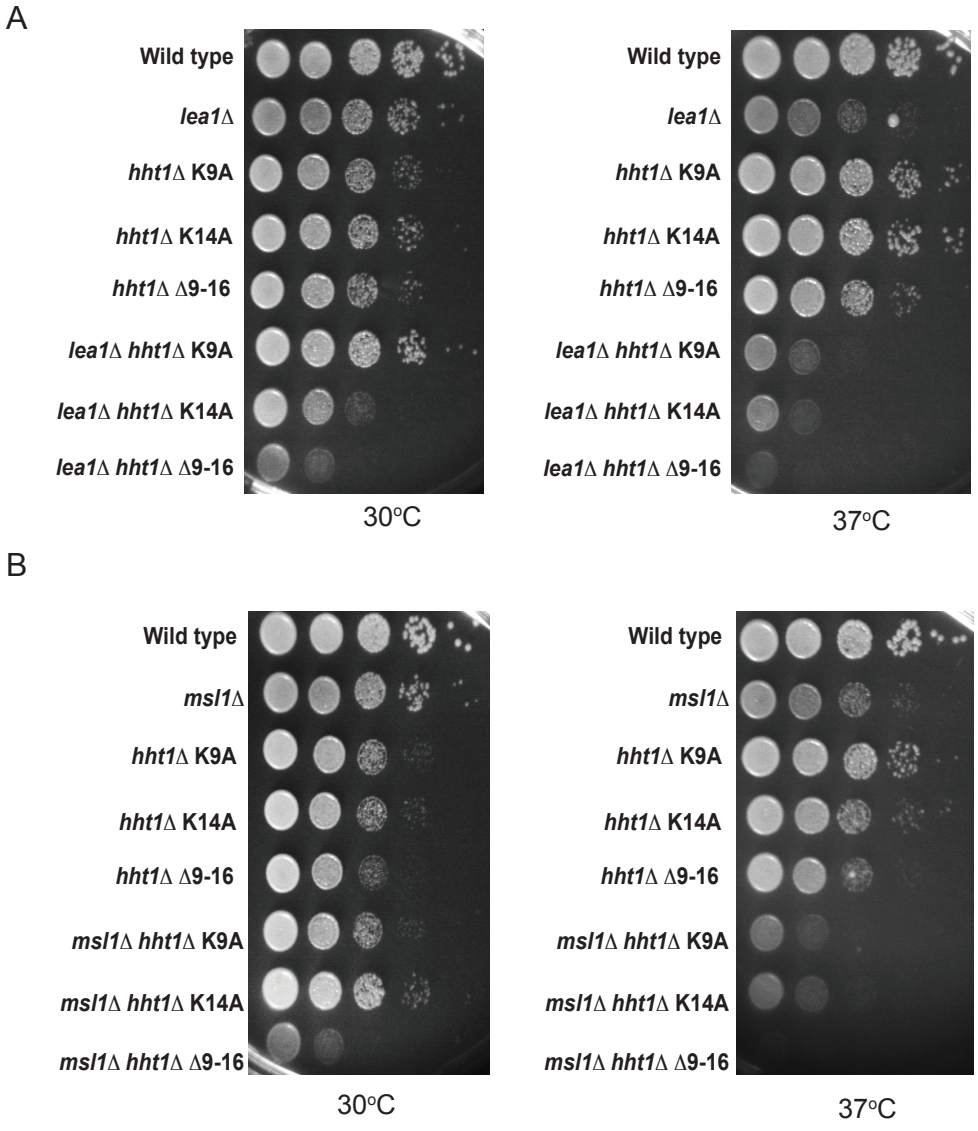

Figure 3.1: Deletion of the genes encoding the U2 snRNP components, *LEA1* and *MSL1* exhibit genetic interactions with histone H3 N-terminal tail residues.
A) Dilution series of the double mutant *lea1*Δ and histone H3 (*hht1*) point mutants or truncation. Cells were grown at 30°C in YPD medium until the desired $O.D._{600}$ was obtained. Cells were spotted on to YPD plates as a ten-fold serial dilution and grown at 30°C or 37°C for 2 days. B) Dilution series of the double mutant *msl1*Δ and histone H3 (*hht1*) point mutants or truncation. Cells were treated as described in panel A.

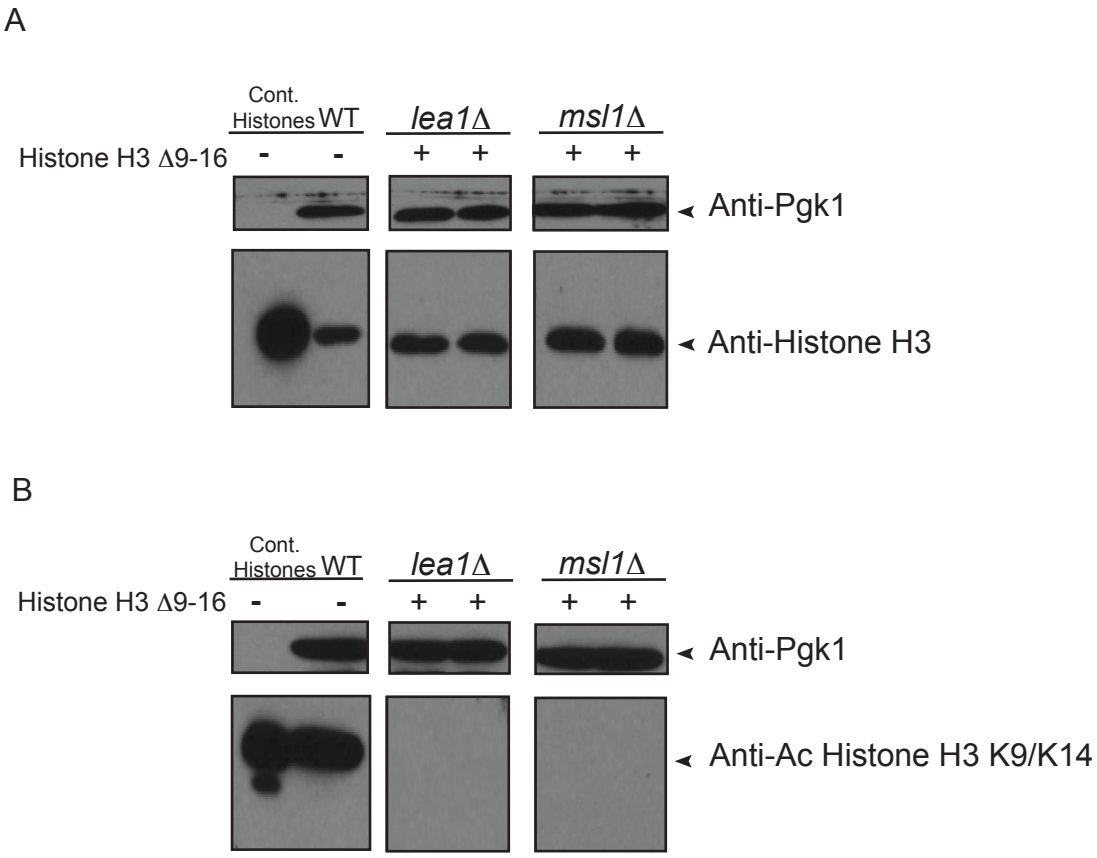

Figure 3.2: Protein expression analysis of histone H3 truncation mutant used in this study.

A) Protein immunoblot of strains harboring histone H3 N-terminal tail truncation (Δ9-16) and presence or absence of *MSL1* or *LEA1*. Cells were grown in YPD media to the same OD_{600} (between 0.6 and 0.8), and whole-cell extracts were prepared from equivalent cell numbers (see supplemental Materials and Methods). Two different isolates from each strain was tested. As a control, acid soluable histones purified from HeLa cells were loaded (Millipore). Proteins were resolved on a 15% SDS-PAGE and probed with Anti-Histone H3 CT PAN (Upstate/Millipore) or Anti-Pgk1 (Invitrogen) as a loading control. B) Protein immunoblot of acetylated histone H3 in truncation mutant in the presence and absence of *MSL1* or *LEA1*. Lysates were treated as in panel A except using the following antibodies: Anti-Acteylated histone H3 K9/14 (Upstate/Millipore) and Anti-Pgk1 (Invitrogen) as a loading control.

also observed with *msl1Δ* histone H3 *K9A*, *msl1Δ* histone H3 *K14A,* and most dramatically *msl1Δ* H3 Δ9-16. These results suggest that acetylation of the N-terminal tail of histone H3 has a functional interaction with *LEA1* and *MSL1.*

It is interesting that the synthetic growth defects observed with the double mutants of either *LEA1* or *MSL1* and a catalytic mutant of *GCN5* are more severe at all temperatures than the histone point mutants. Hence, we cannot rule out the possibility that acetylation of residues in addition to 9 and 14 contribute to Gcn5's activity in co-transcriptional splicing. Nonetheless, these results along with the severe synthetic growth defect observed with *lea1Δ* histone H3 *Δ9-16* and *K14A* provide strong evidence that the functional interactions between *GCN5* catalytic activity and *MSL1/LEA1* are due to Gcn5's role in acetylating histone substrates.

Since we detect a functional interaction between *LEA1/MSL1* and mutations in histone H3, this lead to the prediction that splicing would be affected by mutation of specific lysine residues in histone H3. To address this, we examined if truncation of the N-terminal tail of histone H3 would affect accumulation of *DBP2* and *ECM33* pre-mRNA.

Previously, we have shown that a deletion of *GCN5* results in an increase in *DBP2* and *ECM33* unspliced pre-mRNA, (Gunderson & Johnson, 2009). Hence we examined splicing of *DBP2* and *ECM33* in the histone H3 truncation mutant by quantitative RT-PCR to determine the ratio of unspliced pre-mRNA to total RNA. We observed that the histone H3 truncation mutant reproducibly exhibits a 2 to 2.5-fold increase in intron accumulation compared to wild type

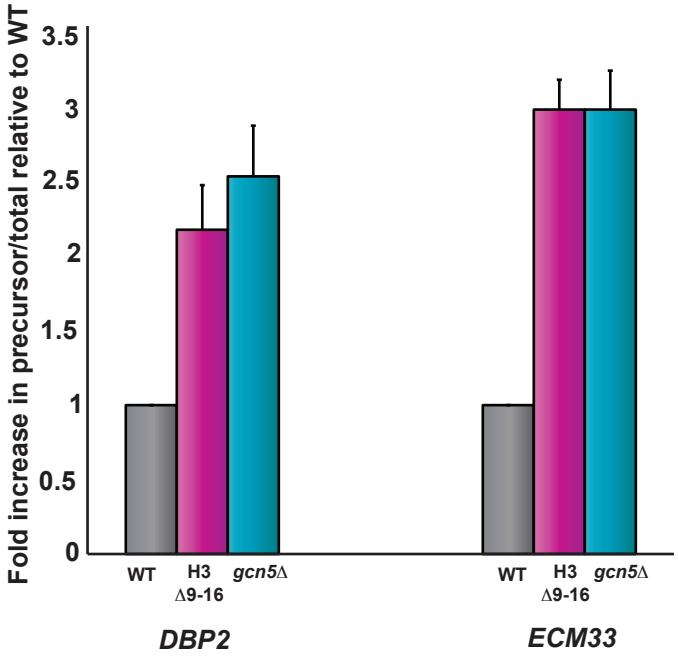

Figure 3.3: Truncation of Histone H3 N-terminal tail alters the splicing of *DBP2* and *ECM33* transcripts.

Quantitative RT-PCR of *DBP2* and *ECM33* in the histone H3 truncation mutant histone H3 Δ9-16 versus wild type. A) Graph represents the fold increase in precursor *DBP2* or *ECM33* relative to mature message relative to wild type in histone H3 Δ9-16 strain. Data are represented as a fold increase in the ratio of precursor (unspliced)/total *DBP2* or *ECM33* message relative to wild type. Graph represents three independent experiments and error bars represent standard error of the mean.

(Figure 3.3). This increase in intron accumulation is comparable to a deletion of *GCN5* (2.5 to 3-fold increase) for both intron-containing genes, *DBP2* and *ECM33* (Figure 3.3).

Although, the intron accumulation observed for the histone H3 truncation mutant is moderate when compared to deletion of core components of the spliceosome, such as the splicing factors, *LEA1/MSL1* (Figure 3.14). This result is consistent with what we previously reported with a *GCN5* deletion (Gunderson & Johnson, 2009). These data suggest that maximal production of these spliced messages is tied to proper histone modification and that splicing within the context of chromatin (co-transcriptional splicing) contributes to efficient message production. Taken together, these data suggest that splicing of *DBP2* and *ECM33* are sensitive to truncation of histone H3 N-terminal tails and further strengthens the argument that Gcn5 catalytic activity targeted towards histones plays an important role in co-transcriptional splicing. Subsequent experiments (Appendix 1) will define conditions under which Gcn5 catalytic activity towards histones is required for maximal splicing.

Gcn5 associates throughout intron-containing genes and Gcn5-dependent histone H3 acetylation occurs within the body of intron-containing genes.

Gcn5 is recruited to actively transcribed genes and catalyzes histone acetylation and TBP binding at the promoter (reviewed in (Hampsey, 1997b, MacDonald & Howe, 2009, Timmers & Tora, 2005). More recently, it has been shown that Gcn5 can also be found associated within the body of actively transcribed genes and can affect histone acetylation downstream of the promoter

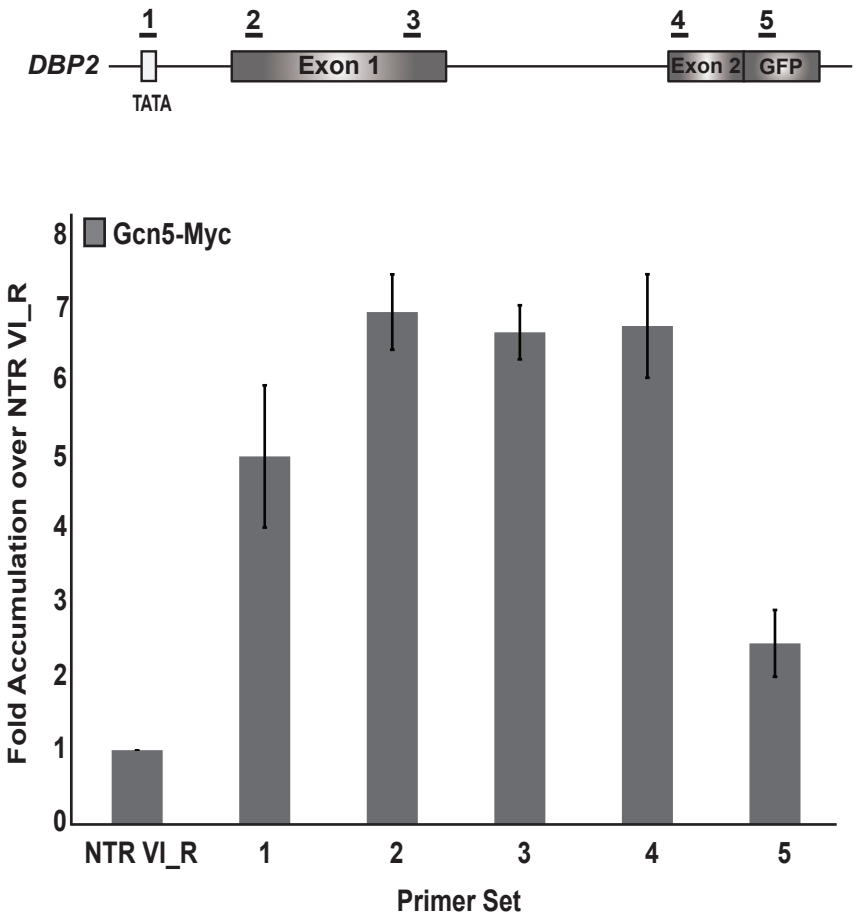

Figure 3.4: Gcn5 is actively recruited to the intron-containing gene *DBP2*.
A) Schematic of the intron-containing gene *DBP2*. Underlined numbers represent the amplicons for each primer set used in this study. B) Graph depicting the recruitment of Gcn5-13xMyc to *DBP2* relative to the non-transcribed region. Graph depicts the average of three independent experiments, +/-1 standard deviation.

(Ginsburg *et al.*, 2009, Govind et al., 2007). In order to evaluate the role of Gcn5-dependent acetylation on splicing of intron-containing genes, we first examined Gcn5 occupancy within our model intron-containing genes, *DBP2.* We observed Gcn5 both in the promoter region and throughout the coding region *DBP2* (Figure 3.4), consistent with our observation of Gcn5-dependent acetylation of this intron-containing gene (Gunderson & Johnson, 2009).

Our previous studies demonstrated a peak in histone acetylation in the promoter region of the intron-containing genes that we analyzed. We considered the possibility that some acetylation marks that are placed by Gcn5 within these genes are removed by histone deacetylases (HDACs), which could mask the true extent of histone acetylation that occurs in the body of the gene. In fact, studies have demonstrated that significant histone acetylation in the coding region can only be detected in the absence of HDACs. Hence, we next wanted to address whether histone deacetylation or acetylation *dynamics* might be masking acetylation in the coding region that might be important for co-transcriptional spliceosome assembly.

To address this possibility, we used ChIP to examine the histone H3 diacetylation profile of *DBP2* and *ECM33* in cells deleted for multiple HDACs. *HOS3 HOS2* deletion has previously been shown to increase histone H3 acetylation in the coding region (Ginsburg et al., 2009, Govind et al., 2007). Furthermore, Hos3 and Hos2 target the same histones as Gcn5 (Carmen *et al.*, 1999, Wang et al., 2002). As previously reported, a single deletion of either HDAC does not significantly affect histone H3 diacetylation at the promoter or in

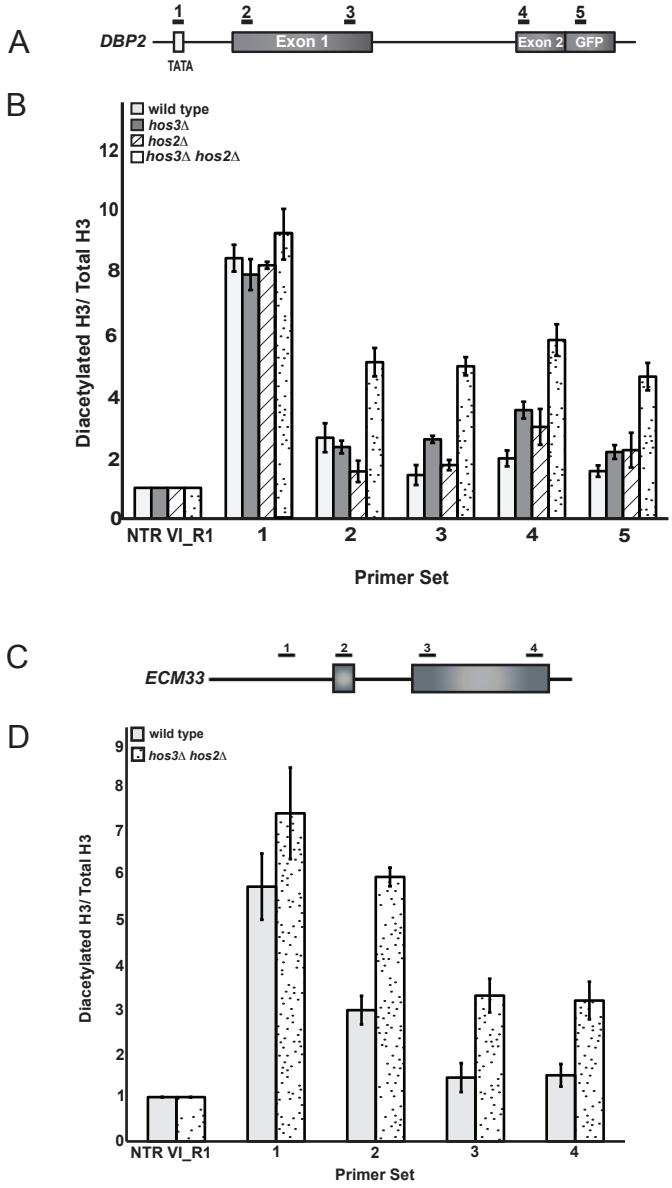

Figure 3.5: Gcn5-dependent histone acetylation in the coding region of *DBP2* and *ECM33* is masked by the dynamics of histone deacetylation.
A) Schematic of the intron-containing gene *DBP2*. Underlined numbers represent the amplicons for each primer set used in this study. B) ChIP analysis of histone H3 K9/14 acetylation of *DBP2* in wild type and histone deacetylase mutants using an antibody that recognizes acetylated histones. Data are represented as diacetylated histone H3 normalized to the total amount of histone H3 (Total H3). C) Schematic of the intron-containing gene, *ECM33.* Underlined numbers represent the amplicons for each primer set used in this study. D) Chromatin IP analysis of diacetylation of histone H3 in wild type and *HOS2 HOS3* double mutant. Light grey bars represent wild type and hashed bars represent the HDAC double mutant. Data is represented as diacetylated H3 normalized to the total amount of histone H3. Graphs represent the average of three independent experiments, +/- 1 standard deviation.

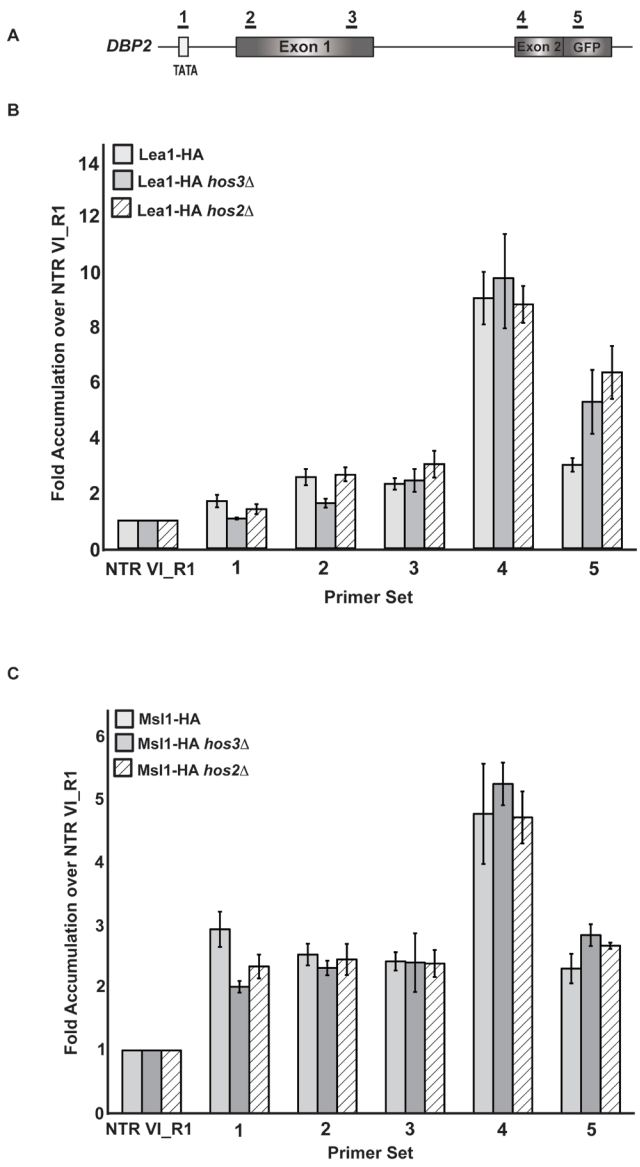

Figure 3.6: Deletion of either HDAC *HOS2* or *HOS3* alone does not affect co-transcriptional U2 snRNP recruitment.

A) Schematic of the intron-containing gene *DBP2.* Underlined numbers represent the amplicons for each primer set used in this study. B) Graph depicting the occupancy of Lea1-HA at each region of *DBP2* in the presence or absence of *HOS2* or *HOS3* relative to the non-transcribed control. C) Graphs showing the occupancy of Msl1-HA at each region of *DBP2* in the presence and absence of *HOS2* or *HOS3* relative to the non-transcribed control. Graphs represent the average of three independent experiments, +/-1 standard deviation.

the coding region (Govind et al., 2007, Gunderson & Johnson, 2009). However, deletion of both *HOS3* and *HOS2* leads to an increase in histone H3 acetylation throughout both *DBP2* and *ECM33* (Figure 3.5 B). We consistently observe, a second peak in enrichment of acetylated H3 in *DBP2* at primer set 4, the primer set corresponding to the branchpoint region of the intron where we also detect co-transcriptional recruitment of Lea1 and Msl1 (Gornemann et al., 2005, Gunderson & Johnson, 2009). For *ECM33* histone H3 acetylation increases within the body of the gene about three-fold (Figure 3.5 D). The overall trend for *EMC33* is different from *DBP2* in that there is a gradual decrease in acetylation from the 5' end to the 3' end, indicating that there are gene specific effects of *HOS3 HOS2* double deletion in the body of intron-containing genes. Nonetheless, these data show that there is acetylation within the body of genes containing splicing signals, and raises the possibility that the rapid deacetylation mediated by the HDACs' effects on co-transcriptional spliceosome assembly. Which is what we addressed next.

Histone deacetylase activity alters co-transcriptional recruitment of Lea1 and Msl1 and alters spliceosomal rearrangements.

Co-transcriptional spliceosome assembly has been shown to occur in a stepwise manner. When co-transcriptional spliceosome assembly and spliceosomal rearrangements are perturbed, such when the cap-binding complex (CBC) is deleted, there is an observable lag in the disengagement of snRNPs with pre-mRNA, and factors that are recruited downstream of the lag show

severely diminished association with the pre-mRNA (Gornemann et al., 2005, Kotovic et al., 2003, Lacadie & Rosbash, 2005, Tardiff & Rosbash, 2006). Since deletion of HDACs leads to a dramatic increase in histone acetylation in the coding region, we decided to re-examine the co-transcriptional recruitment of Lea1 and Msl1 to *DBP2* in the absence of both *HOS3* and *HOS2* by ChIP. While single deletions of either *HOS3* or *HOS2* had little effect on co-transcriptional recruitment of Lea1 (Figure 3.6), in the *hos3Δ hos2Δ* cells, there is an increase in the peak signal at primer set 4, and strikingly, the typically rapid decrease in signal using primers downstream of primer set 4 is not observed (Figure 3.7). Instead there is a lag in U2 association that is typical of a defect in snRNP rearrangements (Gornemann et al., 2005). Importantly, total protein levels of Lea1 and Msl1 are unchanged (Figure 3.7 D).

We next examined Msl1 recruitment to *DBP2*. Similar to Lea1, we observe a slight increase in signal at primer set 4 and a decrease in U2 snRNP dissociation in the double HDAC mutant. (Figure 3.7 C). To rule out the possibility that this lag in the dissociation of the U2 snRNP from the pre-mRNA is a gene specific effect, we examined the co-transcriptional recruitment of Lea1 and Msl1 in the HDAC double deletion background to *ECM33*. Double deletion of *HOS3* and *HOS2* lead to an overall increase in association of Lea1 and Msl1 to the *ECM33* branchpoint as indicated by enrichment at primer set 3 (Figure 3.8). As with *DBP2* there is a lag in the dissociation of the U2 snRNP as indicated by an increase in enrichment of both Lea1 and Msl1 at primer sets downstream of the branchpoint. Taken together, these results suggest that the activity of multiple

HDACs working together to remove acetyl groups from histone H3 is critical to spliceosomal rearrangements involving the U2 snRNP.

We have shown that the functional relationship between Gcn5-dependent histone acetylation on U2 snRNP recruitment can be revealed by analysis of synthetic genetic interactions. Hence, we predicted that the HDAC double mutants would also show genetic interactions when combined with deletion of *MSL1* and *LEA1*. Our observations suggest that the HDACs contribute to the dynamics of spliceosome assembly such that their deletion prevents U2 snRNP release. Hence, we predicted that conditions under which normally transient interactions are hyperstabilized or destabilized (such as lowered temperature or elevated temperature, respectively) would result in a growth phenotype in the triple mutants *lea1Δ hos3Δ hos2Δ* and *msl1Δ hos3Δ hos2Δ*. While we previously observed no change in viability when the single HDAC deletions were combined with a deletion of *MSL1*or *LEA1* (Gunderson & Johnson, 2009) strains deleted for either *LEA1* or *MSL1* and *HOS3* and *HOS2* exhibited a severe synthetic growth defect when grown at 16^{o}C, 25^{o}C and 37^{o}C (Figure 3.9). Growth defects at low temperatures often reflect defects in interactions within multiprotein complexes such as the ribosome, for which this phenotype was first exploited (Guthrie *et al.*, 1969, Hampsey, 1997a). Growth defects at elevated temperatures suggest complex destabilization (Hampsey, 1997a). These results support a model in which HDACs and *MSL1/LEA1* collaborate to affect a common function, namely proper spliceosome dynamics. We considered the possibility that just as the inappropriate hyperstabilization of the U2 snRNP proteins is revealed in the

HDAC double mutants, we would also observe hyperstabilization of other spliceosomal proteins in the mutant background.

Histone deacetylation is necessary for recruitment of snRNPs downstream of U2.

Co-transcriptional spliceosome assembly has been shown to occur in a step-wise manner (Gornemann et al., 2005, Lacadie & Rosbash, 2005). Based on the defects in U2 snRNP release and the cold sensitivity and temperature sensitivity observed in the triple mutants, we hypothesized that HDAC deletion would adversely affect steps downstream of U2 rearrangements. Once again the CBC studies provide an example of this effect. Deletion of the cap-binding complex (CBC), a complex involved in the exchange of factors during splicing (O'Mullane & Eperon, 1998), led to a persistence of the U1 snRNP as measured by chromatin IP and prevented proper recruitment of the downstream U snRNP's (Gornemann et al., 2005). To determine if the HDACs had a similar effect, we examined the co-transcriptional recruitment of the U5 snRNP (represented by Snu114), presumably in the context of the triple snRNP (Gornemann et al., 2005), in the presence and absence of the HDACs Hos3 and Hos2. ChIP of Snu114 in wild type cells shows that the U5 snRNP is enriched downstream of the 3' splice site, a result that is consistent with previous observations (Gornemann et al., 2005, Gunderson & Johnson, 2009). However, double deletion of both the *HOS3* and *HOS2* genes led to a nearly 50% decrease at its peak (represented by primer set 5) in the association of U5 snRNP (Figure 3.10

B) to *DBP2* pre-mRNA. Similarly, when we examined recruitment of Snu114 to *ECM33* in the absence of *HOS3* and *HOS2* we observed a dramatic decrease in the co-transcriptional recruitment of the U5 snRNP (Figure 3.10 D).

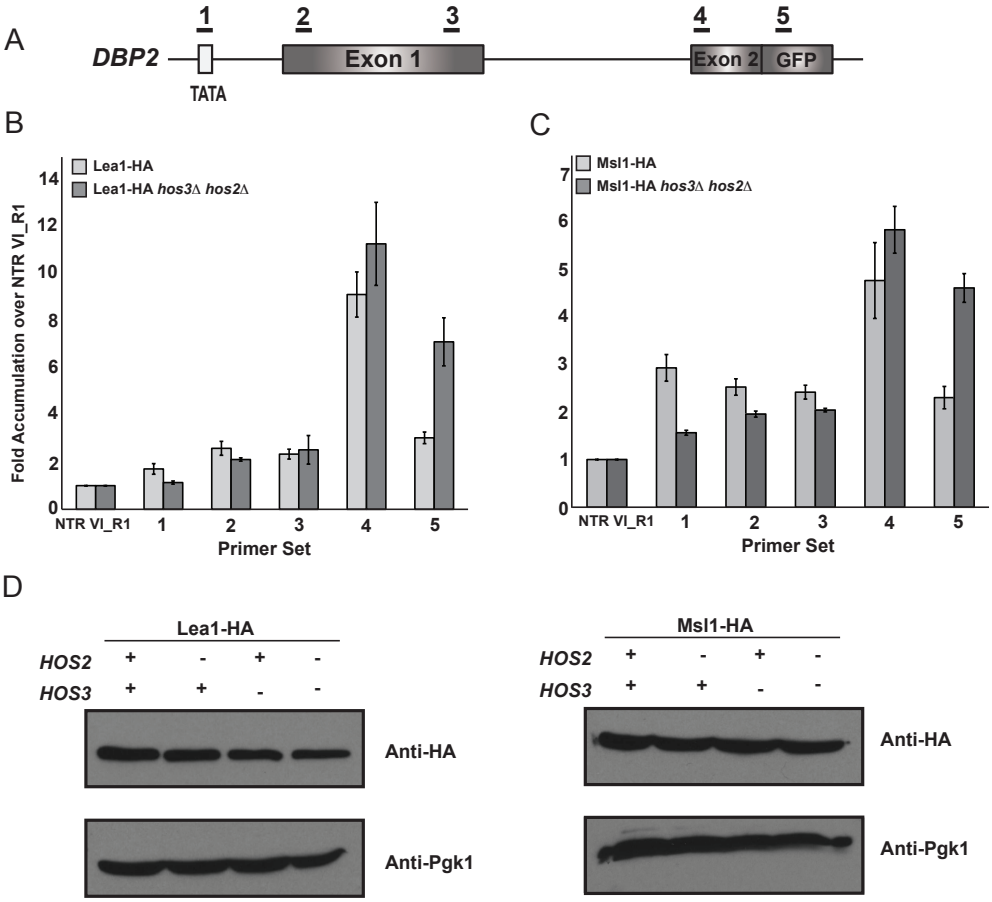

Figure 3.7: Hyperacetylation of histone H3 in the coding region of *DBP2* alters co-transcriptional recruitment of Msl1/Lea1.

A) Schematic of the intron-containing gene *DBP2*. Underlined numbers represent the amplicons for each primer set used in this study. B) Graph depicting the occupancy of Lea1-HA at each region of *DBP2* in the presence or absence of multiple histone deactylases (HDACs) relative to the non-transcribed control. Light grey bar depicts the occupancy of Lea1 in the presence of HDACs. Dark grey bars represent Lea1-HA occupancy in the absence of HDACs. C) Graphs showing the occupancy of Msl1-HA at each region of *DBP2* in the presence and absence of HDACs relative to the non-transcribed control. Grey bar depicts the occupancy of Msl1 in the presence of HDACs. Dark grey bars represent Msl1-HA occupancy in the absence of HDACs. Graphs represent the average of three independent experiments, +/-1 standard deviation. D) Protein Immunoblot of strains used for ChIP assays. Wild type and hos3D hos2D cultures were grown in YPD liquid medium and whole cell extracts were prepared (see Material and Methods) and probed with anti-HA 12CA5 (Roche), shown in the top panel. Extracts were also probed with anti-PGK1 (Invitrogen) as a loading control (bottom panel).

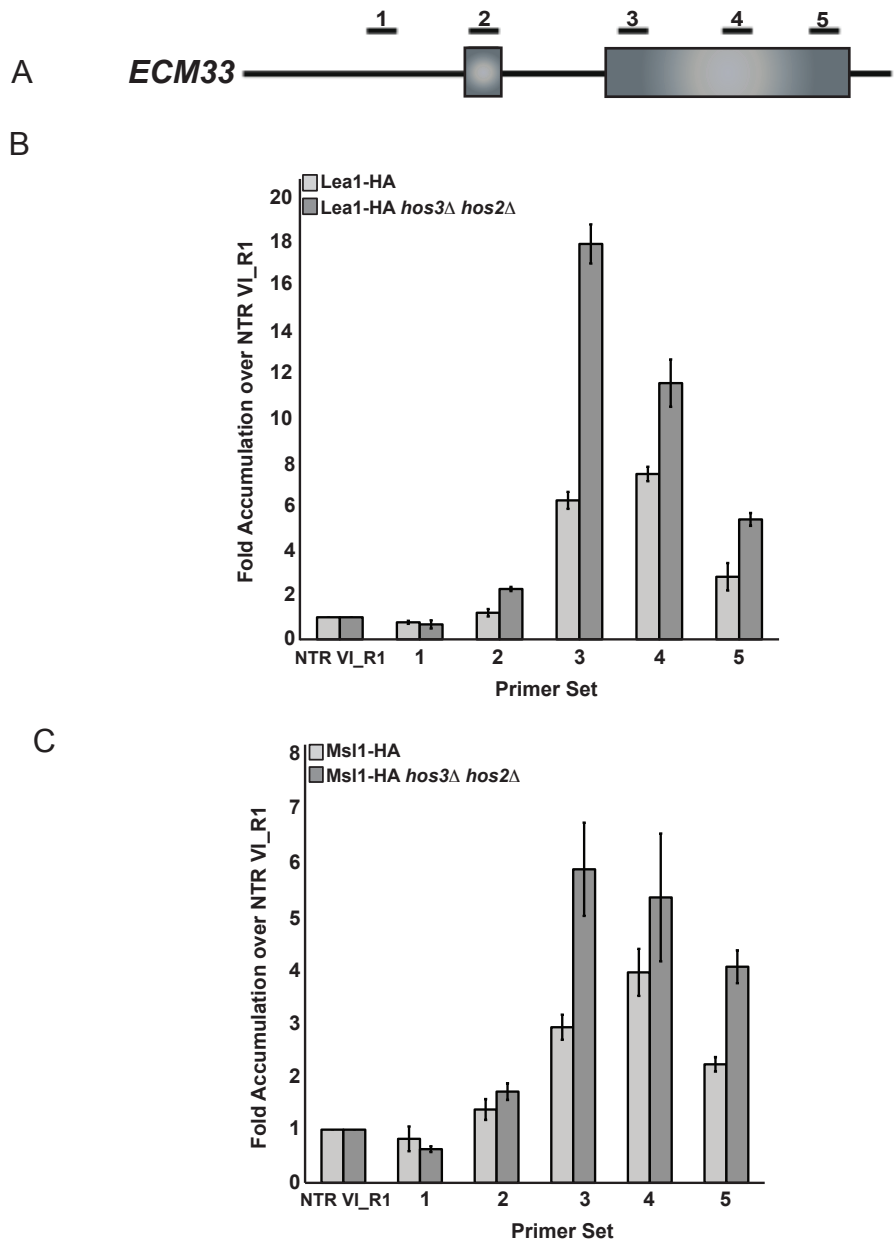

Figure 3.8: Hyperacetylation of histone H3 in the coding region of *ECM33* alters co-transcriptional recruitment of Msl1/Lea1.
A) Schematic of the intron-containing gene *ECM33.* Underlined numbers represent the amplicons for each primer set used in this study. B) Graph depicting the occupancy of Lea1-HA at each region of *ECM33* in the presence or absence of multiple histone deactylases (HDACs) relative to the non-transcribed control. Light grey bar depicts the occupancy of Lea1 in the presence of HDACs. Dark grey bars represent Lea1-HA occupancy in the absence of HDACs. C) Graphs showing the occupancy of Msl1-HA at each region of *ECM33* in the presence and absence of HDACs relative to the non-transcribed control. Grey bar depicts the occupancy of Msl1 in the presence of HDACs. Dark grey bars represent Msl1-HA occupancy in the absence of HDACs. Graphs represent the average of three independent experiments, +/-1 standard deviation.

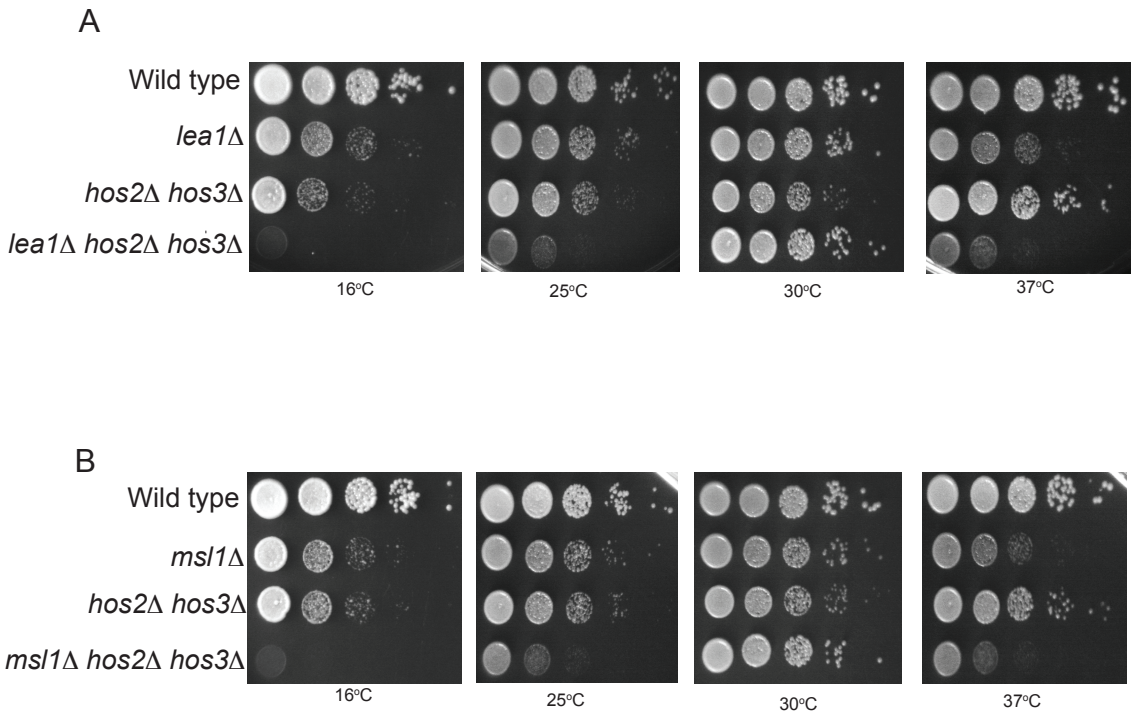

Figure 3.9: The triple mutants, *LEA1 HOS2 HOS3* and *MSL1 HOS2 HOS3* exhibit cold and temperature sensitivity.

A) Dilution series of the triple mutant, *LEA1 HOS2 HOS3*. Cells were grown at 30°C in YPD liquid medium until the desired $O.D._{600}$ was obtained. Cells were spotted onto YPD plates as a ten-fold serial dilution. Plates were incubated for 2 days at 30°C and 37°C and three days at 25°C and 5 days at 16°C. B) Dilution series of the triple mutants, *MSL1 HOS2 HOS3* cells were treated as described for panel A.

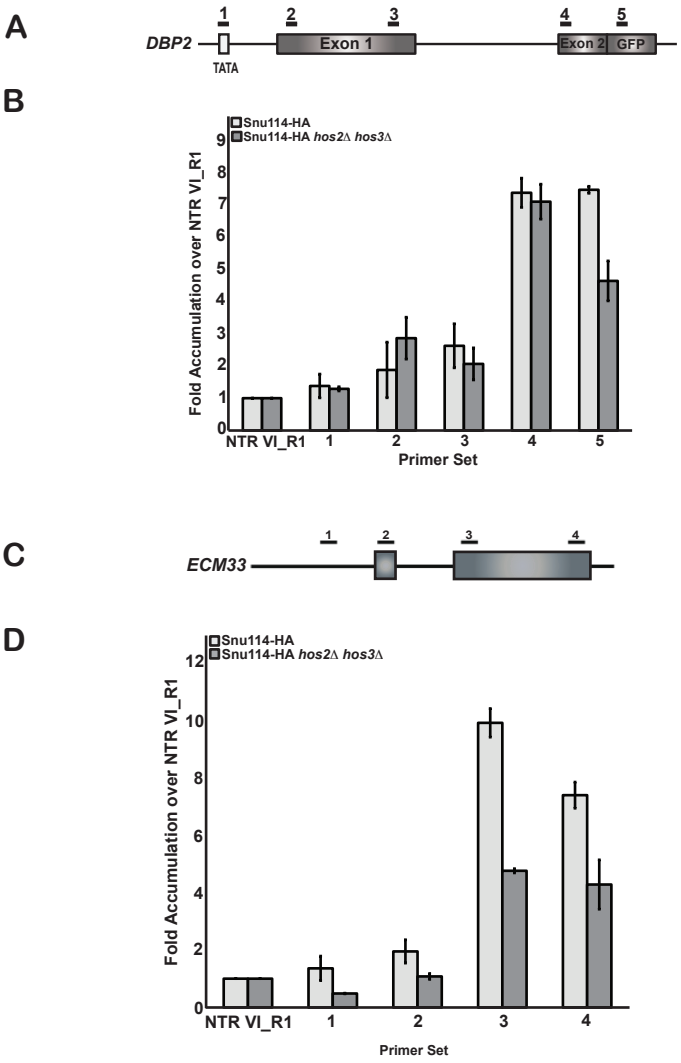

Figure 3.10: Deletion of *HOS2* and *HOS3* affects co-transcriptional recruitment of U5 snRNP.

A) Schematic of the intron-containing gene *DBP2.* Underlined numbers represent the amplicons for each primer set used in this study. B) Bar graph depicting the co-transcriptional recruitment of U5 snRNP (Sun114-HA) to *DBP2* in the presence and absence of *HOS2 HOS3.* Light grey bars represent the occupancy of Snu114-HA in a wild type background and the dark grey bars represent Snu114-HA recruitment in the *HOS2 HOS3* double deletion. Occupancy is measured as fold accumulation over the non-transcribed control. C) Schematic of the intron-containing gene *ECM33.* Underlined numbers represent the amplicons generated by each primer set used in this study. D) Bar graph depicting the co-transcriptional recruitment of U5 snRNP (Sun114-HA) to *ECM33* in the presence and absence of *HOS2 HOS3.* Light grey bars represent the occupancy of Snu114-HA in a wild type background and the dark grey bars represent Snu114-HA recruitment in the *HOS2 HOS3* double deletion. Occupancy is measured as fold accumulation over the non-transcribed control. Graphs represent the average of at least three independent experiments, and error bars represent the standard deviation.

We next examined the effect of *HOS3* and *HOS2* double deletion on the recruitment of a factor downstream of U5 snRNP recruitment, Prp19. Prp19 is a component of the nineteen complex and is required for the stable association of the U5 and U6 snRNAs with the spliceosome after dissociation of U4 (Chan *et al.*, 2003). As with the U5 snRNP recruitment, we detected a decrease in the recruitment of Prp19 to *DBP2* and *ECM33* in the absence of both *HOS3* and *HOS2* (Figure 3.12 B and D, respectively). To exclude the possibility that these results are due to a decrease in protein expression of Snu114 and Prp19 in the absence of the HDACs, western blot analysis was performed, and this analysis did not reveal significant changes in the levels of expression of these proteins (Figure 3.12). These results indicate that, while deletion of multiple HDACs increases the affinity of the U2 snRNP for the branchpoint, this negatively impacts the U2 snRNP and alters the subsequent steps of splicing.

To determine if RNA polymerase II transcription was altered by deletion of the two HDACs, we next examined RNAPII recruitment to *DBP2* and *ECM33* by ChIP in the *hos3*Δ *hos2*Δ strains. We found that double deletion of *HOS3* and *HOS2* had minimal effects on RNAPII occupancy of *DBP2* (Figure 6A). If anything, there is a slight increase in Pol II association to this gene. We observed a similar trend with *ECM33* (Figure 6B). While we cannot rule out the possibility that these small effects influence the different trends observed for U2 and downstream snRNPs, it seems unlikely that this accounts for the strong effects caused by HDAC deletion that we observe. These results suggest the changes we observe in the co-transcriptional recruitment profile of the triple snRNP and

Prp19 are not primarily due to defective transcription elongation; rather changes in the dynamics of histone acetylation, specifically, influence snRNP rearrangements.

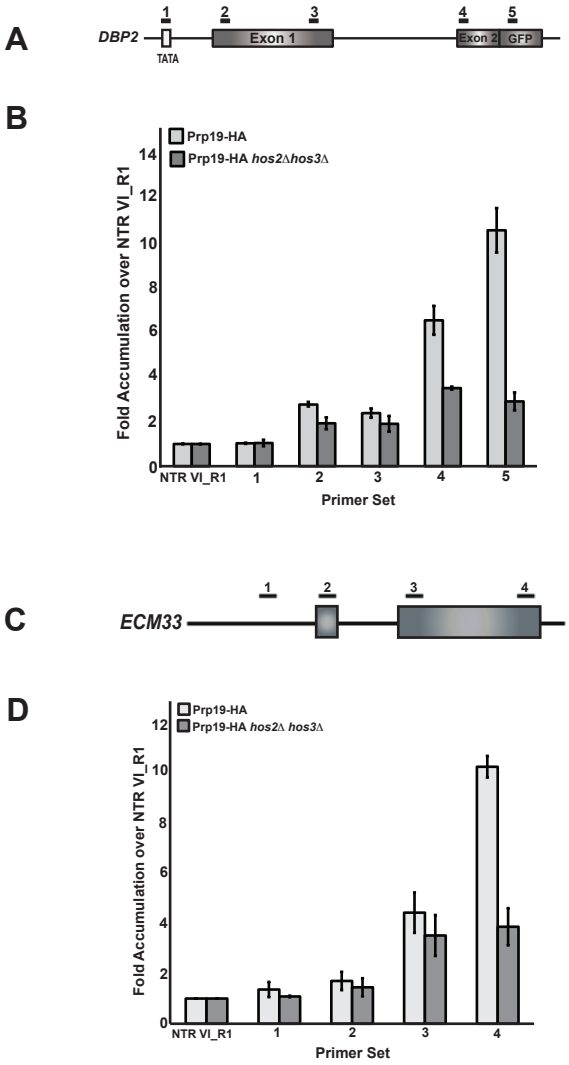

Figure 3.11: Deletion of *HOS2* and *HOS3* affects the co-transcriptional recruitment of Prp19.

A) Schematic of the intron-containing gene *DBP2.* Underlined numbers represent the amplicons for each primer set used in this study. B) Bar graph represents the recruitment of Prp19-HA to *DBP2* in the presence and absence of *HOS2 HOS3.* Light grey bars represent wild type and dark grey bars represent the *HOS2 HOS3* double mutant. C) Schematic of the intron-containing gene *ECM33.* Underlined numbers represent the amplicons generated by each primer set used in this study. D) Bar graph represents the recruitment of Prp19-HA to *ECM33* in the presence and absence of *HOS2 HOS3.* Light grey bars represent wild type and dark grey bars represent the *HOS2 HOS3* double mutant. Graphs represent the average of at least three independent experiments, and error bars represent the standard deviation.

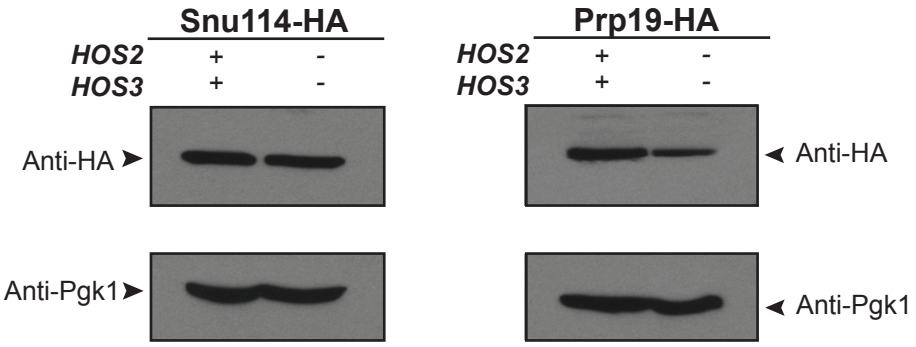

Figure 3.12: Deletion of both *HOS3* and *HOS2* does not alter protein levels of spliceosomal proteins used in ChIP assays.
Protein immunoblot of U5 snRNP component, Snu114-HA and NineTeen Complex component, Prp19-HA in the presence and absence of *HOS3 HOS2.* Strains were grown in YPD liquid medium and whole cell extracts were prepared (see Material and Methods) and probed with anti-HA 12CA5 (Roche), shown in the top panel. Extracts were also probed with anti-PGK1 (Invitrogen) as a loading control (bottom panel).

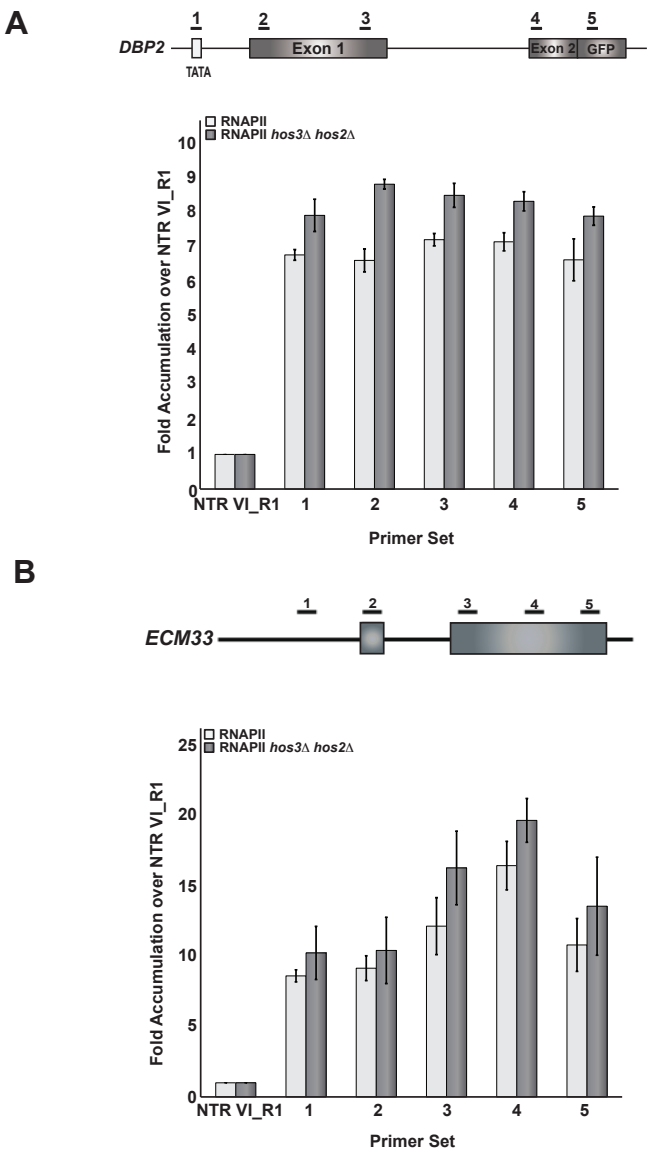

Figure 3.13: Deletion of *HOS3* and *HOS2* does not significantly alter recruitment of RNAPII to intron-containing genes.
A) Graph represents recruitment of RNAPII across the intron-containing gene, *DBP2* in the presence and absence of *HOS3* and *HOS2*. Light grey bars represent wild type and dark grey bars represent *HOS3 HOS2* double deletion. Data is normalized to a non-transcribed control. B) Recruitment of RNAPII to the intron-containing gene *ECM33* in the presence and absence of HDACs *HOS3* and *HOS2*. Light grey bars represent RNAPII recruitment for wild type and dark grey bars represent recruitment in the *HOS3 HOS2* double deletion. Data is normalized to a non-transcribed control. Graphs represent the average of three-independent experiments, +/- 1 standard deviation.

We previously reported that a deletion of the histone acetyltransferase *GCN5* led to an increase in unspliced *DBP2* and *EMC33* transcripts relative to wild type (Gunderson & Johnson, 2009). Since we detected an alteration in the dynamics of spliceosome assembly by the deletion of the HDACs *HOS3* and *HOS2* we wanted to examine how this affects splicing of these messages. Quantitative RT-PCR was performed to examine the amount of unspliced (precursor) *DBP2* and *EMC33* transcript in the HDAC double deletion strain. Double deletion of *HOS3* and *HOS2* resulted in an approximate two-fold increase in unspliced *DBP2* and *EMC33* transcript relative to wild type (Figure 3.14 A). While the overall splicing defect is less than that observed with bona fide splicing factors, Msl1 or Lea1 are deleted – presumably because both co-transcriptional and post-transcriptional splicing are affected by these mutations (Figure 3.14 B), we find that as with a *gcn5Δ*, altering the dynamics of co-transcriptional spliceosome assembly through HDAC deletion leads to defective splicing.

These data lead to a model in which Gcn5-mediated histone acetylation is required for co-transcriptional recruitment of the U2 snRNP. Histone deacetylation on the other hand, is required for normal loss of U2 snRNP and the subsequent association of snRNPs acting downstream of U2.

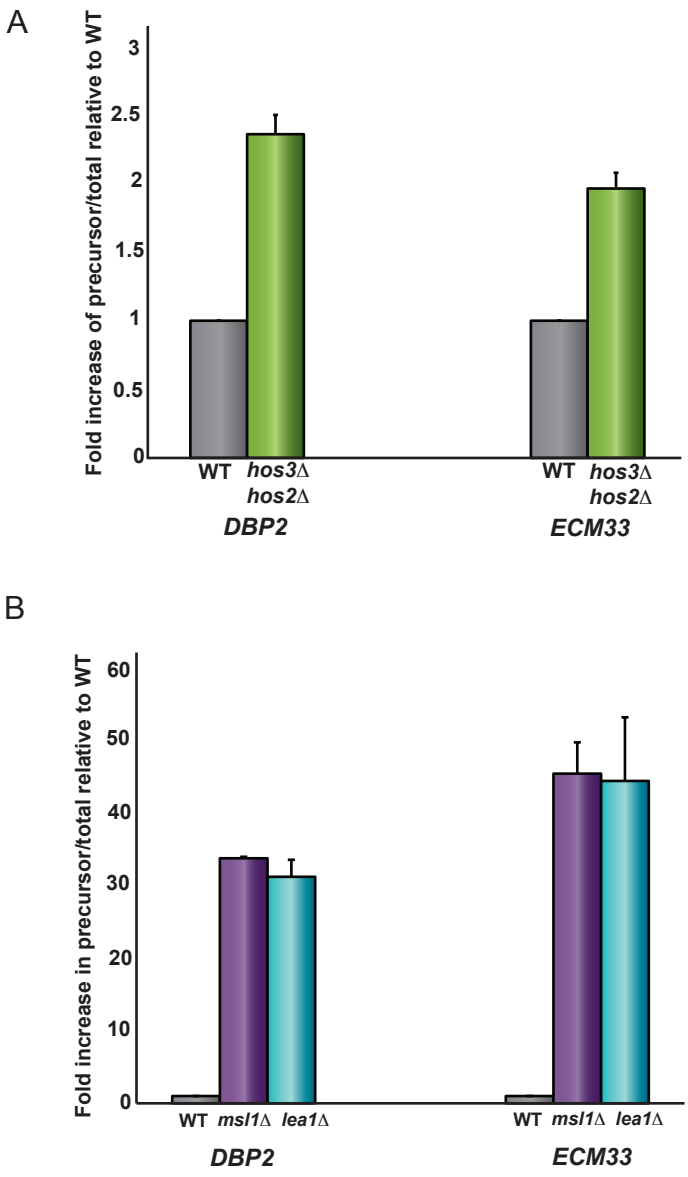

Figure 3.14: Deletion of *HOS3* and *HOS2* alters the splicing of *DBP2* and *ECM33* transcripts.
Qauntitative RT-PCR of *DBP2* and *ECM33* in the absence of *HOS3 HOS2, MSL1* or *LEA1*. A) Graph represents the fold increase in precursor *DBP2* or *ECM33* relative to mature message relative in wild type in *HOS3 HOS2* double deletion strains. Data is represented as a fold increase in the ratio of precursor/ (unspliced) total *DBP2* or *ECM33* message relative to wild type. B) Same as in panel A with the exception of *MSL1* and *LEA1* deleted cells. Error bars represent standard error of the mean.

Section 3.3: Discussion

Splicing and transcription are both highly dynamic processes that have been shown to be spatial and temporally coordinated. Transcription occurs within the context of a chromatin template, which the polymerase navigates with the assistance of accessory factors that modify the chromatin. Nonetheless, the effects of these modifications on splicing have been poorly understood. Previously, we demonstrated that the Gcn5 HAT activity was critical for co-transcriptional U2 snRNP association with the branchpoint (Gunderson & Johnson, 2009). Here, we provide evidence that histone acetylation and deacetylation affect co-transcriptional splicing by facilitating the dynamic rearrangements of the spliceosome co-transcriptionally. Not only does Gcn5 show strong functional interactions with specific U2 snRNP components (*MSL1/LEA1*) (Gunderson & Johnson, 2009), but similar interactions are observed when the histone residues targeted by Gcn5 are mutated or deleted (Figure 3.1). When we examined splicing of intron-containing genes in these histone mutants we found that truncation of the N-terminal tail of histone H3, which removes residues 9-16, results in an accumulation of unspliced *DBP2* and *ECM33* pre-mRNA to levels similar to a deletion of *GCN5* (Figure 3.3), This result suggests that either deletion of *GCN5* or absence of the key residues on the N-terminal tail of histone H3 that Gcn5 targets are important for co-transcriptional splicing. Although we cannot rule out the possibility that other histone substrates targeted by Gcn5 also affect co-transcriptional spliceosome assembly, these

results strongly suggest that acetylation of at least histone H3 at these residues is necessary for splicing. Additionally, we found that double deletion of the histone deacetylases, *HOS3* and *HOS2* leads to an increase in histone acetylation in the region of intron-containing genes containing splicing signals, and that this increase in histone acetylation alters the ordered exchange in spliceosomal snRNPs and hampers proper stepwise co-transcriptional assembly of the spliceosome on the pre-mRNA (Figures 3.7, 3.8, 3.10, and 3.11). As a consequence, in the absence of the HDACs, splicing defects are observed, and cells become increasingly dependent on a fully functional spliceosome for viability (Figure 3.9). These data provide some of the first evidence in yeast that dynamic modification of histones contribute to the dynamics of spliceosome assembly.

Dynamic histone acetylation in intron-containing genes mirrors dynamic spliceosome assembly.

In situ analysis of co-transcriptionally assembled spliceosomes illustrate that nascent RNPs are found along the chromatin axis. And although there is an extensive exchange of splicing complexes within the nascent transcript, they do not appear to be associated with the polymerase itself (Wetterberg et al, 2001). Our data suggest that the chromatin may provide signals for exchange of factors that assemble on pre-mRNA co-transcriptionally. These studies confirm that, like spliceosome assembly, histone acetylation within the coding region of intron-containing genes is very dynamic. In fact, only by deleting multiple histone

deacetylases (HDACs) can the patterns of histone acetylation be revealed (Ginsburg et al, 2009; Govind et al, 2007). We deleted the HDACs Hos3 and Hos2 and observed an increase in histone H3 acetylation in the coding regions of both intron-containing genes tested, *DBP2* and *ECM33* (Figure 3.5). These results suggest that since Gcn5 is located throughout intron-containing genes (Figure 3.4) and is able to acetylate histones in the coding region, it helps to establish acetylation that is important for co-transcriptional spliceosome assembly. Work that is currently under way examines the genome wide pattern of histone acetylation within intron-containing genes to determine if acetylation is particularly enriched in this class of genes and, if so, where.

We have also determined that although Msl1 and Lea1 are recruited to the branchpoint in the *hos3Δ hos2Δ* double mutant, persistent acetylation prevented proper U2 snRNP rearrangement and destabilization as indicated by persistence in the signal (Figure 3.7 and 3.8). Since the spliceosome assembles onto the pre-mRNA in a stepwise manner, recruitment of factors downstream of the U2 snRNP were analyzed to reveal a decrease in their recruitment (Figures 3.10 and 3.11). Notably, when U2 snRNP recruitment is eliminated (as when *GCN5* is deleted), no recruitment of downstream factors is observed, whereas here the level of U2 persistence roughly correlates with the decrease in association by downstream factors. This is consistent with there being a tight relationship between U2 association and the association of downstream factors. Although we cannot rule out the possibility that HDACs could affect the recruitment of downstream factors independently of their effect on U2, these results strongly

suggest that an increase in histone acetylation due to the lack of HDACs results in the alteration of the dynamic rearrangements of the spliceosome. This raises the question of how exactly acetylated histones contribute to snRNP association with the pre-mRNA.

A number of reports indicate that the elongation properties of the polymerase can influence co-transcriptional splice site recognition in both yeast and mammals (reviewed in Kornblihtt, 2006). In light of these studies, it is possible that changes in RNA polymerase II processivity that occur in the absence of the genes encoding Hos3 and Hos2 may alter co-transcriptional spliceosome assembly. Indeed for both *DBP2* and *ECM33*, we detect an increase in polymerase throughout the body of the genes, which may be an indication of a change in polymerase processivity as it encounters acetylated histones. However, the changes in polymerase occupancy that occur when Hos3 and Hos2 are deleted are mild relative to the changes that we observe in Lea1/Msl1, Snu114, and Prp19 recruitment. This suggests another mechanism by which histone acetylation alters recruitment of the snRNPs besides changes in the polymerase processivity. Studies of mammalian, co-transcriptional splicing suggest that histone modifications, such as methylation, create binding sites for factors that facilitate spliceosome assembly and alternative splicing. It is possible that acetyl marks likewise create such binding sites and that some protein (or proteins) binds to acetylated histone H3 tails to facilitate recruitment of the spliceosome to the nearby RNA.

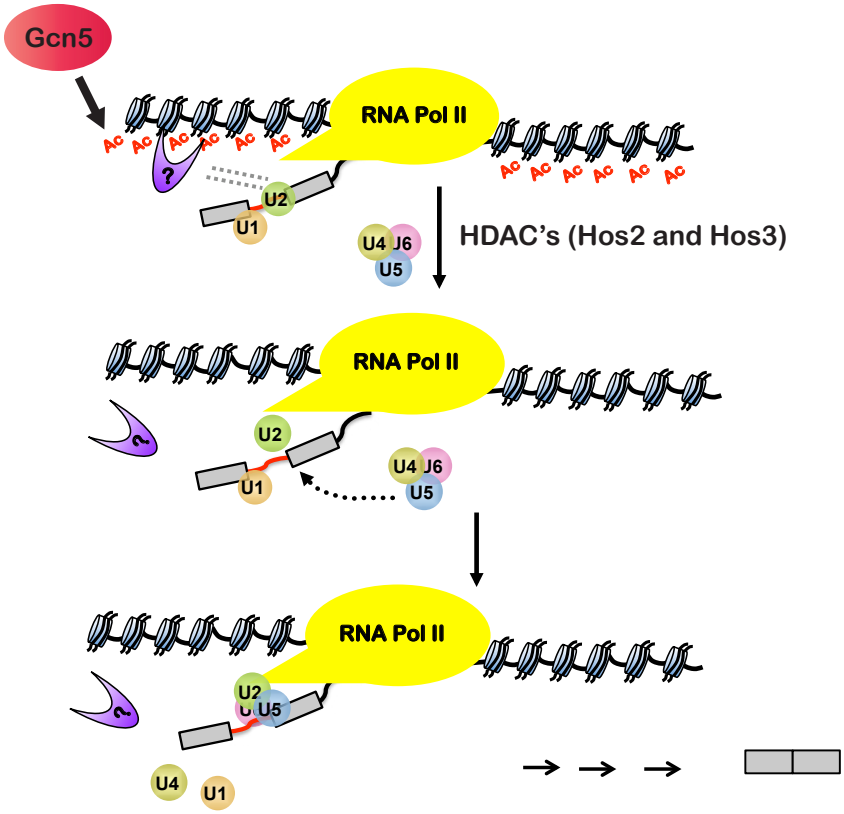

Figure 3.15: Histone acetylation and *de*acetylation play a role in co-transcriptional splicing.

Model summarizing the findings of this study. Gcn5-dependent histone acetylation creates binding sites for an unknown factor that is able to interact with U2snRNP proteins which in turn recruits the U2snRNP co-transcriptionally. Upon recruitment of the U2 snRNP to the intron branchpoint, Hos3 and Hos2 deacetylate histones. This allows for the proper release of the U2 snRNP and allows for assembly of the spliceosome. Deletion of HDACs, thus increases histone acetylation and in turn, hyperstabilizes once transient interaction with the unknown factor resulting in altered spliceosome assembly.

Since neither Msl1 nor Lea1 contains a bromodomain we are exploring a variety of other candidates that may carry out this function. In such a model, this unknown factor interacts with both histones and U2 snRNP proteins to allow for co-transcriptional spliceosome assembly. Since histone acetylation is dynamic, deacetylation allows for the proper release of the U2 snRNP and allows the subsequent rearrangements to occur (Figure 3.15). Hence, when HDACs are deleted, this results in persistent histone acetylation such that the unknown protein associated with U2 also persists, stabilizing once transient interactions, delaying U2 snRNP release and inhibiting the recruitment of downstream snRNPs (Figure 3.15). Interestingly, mammalian studies have shown that histone H3K4me3 provides binding sites for a factor, Chd1, which associates with snRNPs and facilitates their recruitment (Sims et al, 2007). More recent studies have also shown that alternative splicing can be regulated by splicing factors that are recruited to introns by proteins that bind to H3K36me3 histones (Luco et al, 2010). Both of these studies indicate a precedent for factors that "bridge" histone marks and the spliceosome. Since histone methylation appears to be a relatively stable mark, it seems unlikely that protein binding to methylation marks could facilitate spliceosome dynamics (and our preliminary analysis shows no evidence of such a role for yeast Chd1). However, dynamic acetylation could play such a role, which is consistent with our finding that acetylation and deacetylation are essential for proper co-transcriptional spliceosome assembly such that factors are not only recruited to the pre-mRNA by acetylation, but are also released in response to deacetylation. Since spliceosomal rearrangements

are ATP dependent, we predict that there are important interactions between the histone modifying machinery and the ATP-dependent RNPases that are central to the rearrangements described here; it will be interesting to identify and characterize these interactions.

Portions of this chapter have been submitted for publication as: Gunderson, FQ and Johnson, TL. Histone acetylation dynamics plays a critical role in co-transcriptional spliceosome assembly and spliceosome rearrangements. EMBO J.

Chapter 4: Identification of a novel role for Msl1 and Lea1 in transcription

Section 4.1: Introduction

Transcription and pre-mRNA splicing have been studied as biochemically distinct reactions. Evidence from this study and others have shown that pre-mRNA splicing can occur while the RNA polymerase is actively engaging with the DNA template in yeast and higher eukaryotes. From the data presented here, we have found that a transcription factor, Gcn5, can affect co-transcriptional spliceosome assembly and subsequent splicing. Our evidence strengthens the hypothesis that transcription, and more specifically, the state of chromatin is functionally coupled with pre-mRNA splicing. While there have been many studies demonstrating how transcription can affect splicing, there is little evidence of the reciprocal relationship, namely, how splicing can affect transcription.

In mammals, there have been reports that suggest that splicing factors can affect transcription. A study that explored how splicing factors can affect transcription showed that several spliceosomal snRNPs had interactions with the transcription elongation factor, TAT-SF1 and this interaction stimulated RNA polymerase II elongation (Fong, 2001). Additionally, the human splicing factor, SKIP was shown to have a crucial role in Tat-dependent transcription (Bres *et al.*, 2005). Recently, with the advent of Chromatin IP and tiling arrays, it was revealed that the human splicing factor, SC35 could affect transcription

elongation (Lin *et al.*, 2008a). When cells were depleted of SC35 and the location of RNA polymerase II was examined by tiling array, RNA polymerase II accumulated in the body of intron-containing genes.

Whereas the studies above examined the affect of splicing factors on transcriptional elongation, it is also known that splicing factors can affect transcription initiation. One of the first studies to suggest a role for splicing factors in transcription initiation showed that U1 snRNA had a specific association with the general transcription factor, TFIIH (Kwek *et al.*, 2002). TFIIH is directly implicated in transcription initiation (Hampsey, 1998, Yudkovsky *et al.*, 2000, Feaver *et al.*, 1994, Orphanides *et al.*, 1996). These studies showed that when U1 snRNA associated with TFIIH there was an increase in RNA pol II transcription initiation. This increase is due to the exposure of a promoter proximal 5' splice site via a TFIIH-U1 interaction that allows Pol II to advance into elongation with high efficiency. This study suggests that the association of the U1 snRNA with the 5' splice site could stimulate recruitment of transcription initiation factors, including TFIIH to enhance preinitiation complex assembly (Damgaard *et al.*, 2008). Consistent with this, it has been shown that the presence of a 5' splice site within a gene could stimulate its transcription (Hampsey, 1998, Yudkovsky et al., 2000, Feaver et al., 1994, Orphanides et al., 1996).

All of the studies thus far that have examined how splicing factors can directly affect transcription have been in mammals. To date, there are no known published data showing splicing factors in yeast that can affect transcription. However, work in preparation for submission (Hossain et al., in review) shows

that the yeast cap binding complex (CBC), which plays a critical role in pre-mRNA splicing helps to establish proper RNAPII CTD phosphorylation and histone modification through out the genome. At this point it is unclear whether the CBC has multiple distinct functions or if its co-transcriptionally recruited to intron-containing genes influences transcription. However, this provides some of the first evidence of a role for a splicing factor in transcription in yeast.

Our previous data examining the co-transcriptional recruitment of Msl1 and Lea1 to the intron-containing gene, *DBP2* consistently showed enrichment of Msl1 to the promoter region, independent of splicing signals (Gunderson & Johnson, 2009). We therefore decided to examine whether the splicing factors, Msl1 and Lea1 had any affect on transcription. The data presented here show that, whereas Lea1 recruitment at the brapnchpoint is dependent on Msl1, Msl1 association near the promoter occurs independent of Lea1, and without Msl1 recruitment, promoter acetylation in decreased, suggesting a splicing-independent role for Msl1 in transcription. Deletion of either, Msl1 or Lea1 leads to an increase in acetylation near the branchpoint. In light of our finding of an important role for histone deactylation in spliceosome assembly, we propose a model whereby Msl1 and Lea1 facilitate HDAC recruitment to help drive co-transcriptional spliceosomal rearrangements.

Section 4.2: Results

Recruitment of Msl1 to the promoter of *DBP2* occurs independently from its binding partner Lea1.

We were intrigued by the early co-transcriptional recruitment of Msl1 to *DBP2;* therefore we wanted to determine if the early recruitment of Msl1 was dependent on *LEA1*. For proper spliceosome assembly to occur and subsequently splicing, both Msl1 and Lea1 must be bound to the U2 snRNA for the proper addition of the U2 snRNP to the spliceosome (Caspary & Seraphin, 1998). Therefore, we hypothesized that since both factors are required to be in a complex for splicing to occur, co-transcriptional recruitment of Msl1 would be dependent on Lea1 and vice versa, i.e. Lea1 recruitment would be dependent on Msl1. To test this, we examined the co-transcriptional recruitment of Msl1 to *DBP2* in the absence of *LEA1* by ChIP and found that the early recruitment of Msl1 to the promoter of *DBP2* was not dependent on the presence of Lea1. However, co-transcriptional recruitment to the intron branchpoint was abolished in the absence of *LEA1* (Figure 4.1 B). We also tested Lea1 recruitment in the absence of *MSL1* by ChIP and found that *MSL1* was required for the co-transcriptional recruitment of Lea1 to the intron branchpoint (Figure 4.1 C). These results suggest that although both proteins are required for recruitment of the complex to the branchpoint, Msl1 is recruited to the promoter of *DBP2* independently of Lea1. Importantly, our previous data shows that this recruitment to the promoter is Gcn5 independent. Specifically, we don not believe that Msl1

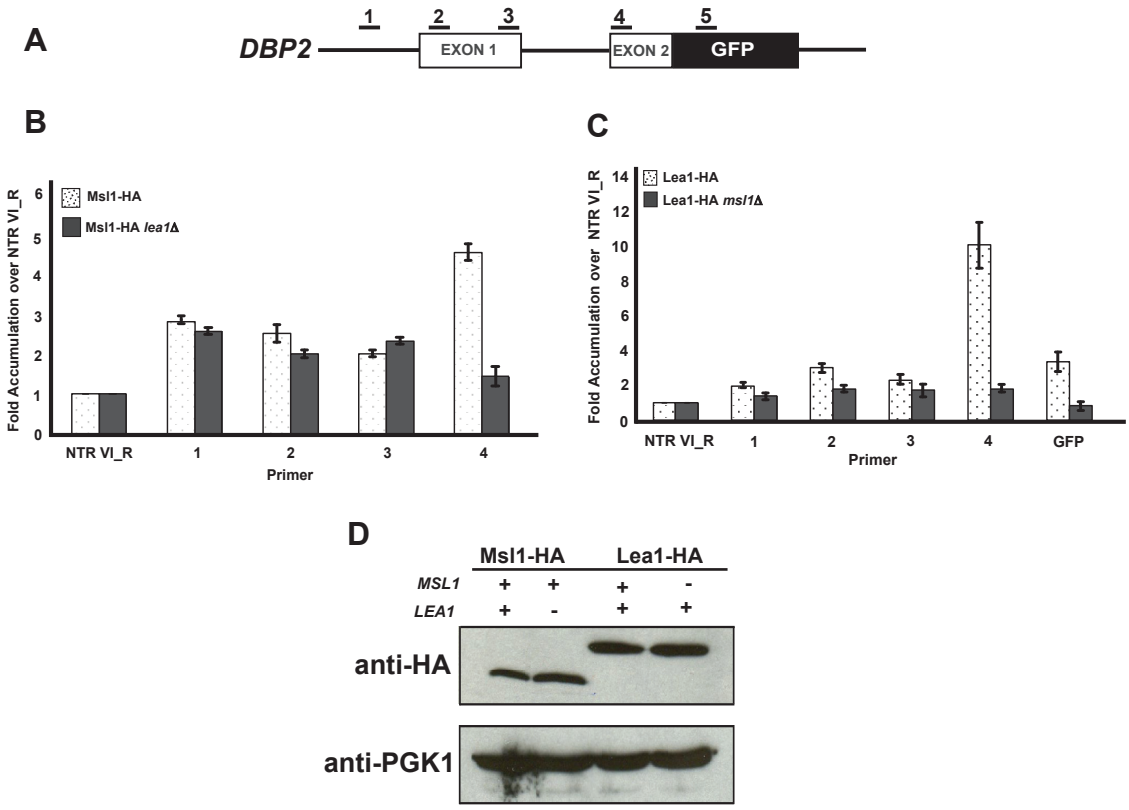

Figure 4.1: Msl1 is recruited co-transcriptionally to the promoter of *DBP2* independently of splicing signals.

A) Schematic of the intron-containing gene, *DBP2*. Underlined numbers represent amplicons generated from each primer set used in the study. B) Graph depicting the occupancy of Msl1 at each region of *DBP2* relative to the non-transcribed region, in wild type or *lea1*Δ. Light grey bars represent Msl1 with wild type *LEA1* and dark grey bars represent Msl1 levels in the *lea1*Δ strain. C) Graph depicting the occupancy of Lea1 in wild type and *msl1*Δ. Light grey bars represent Lea1 with wild type *MSL1* and dark grey bars represent Lea1 recruitment in *msl1*Δ strain. All graphs depict the average of at least three independent experiments, and error bars represent the standard deviation. D) Protein Immunoblot of strains used for ChIP assays. Wild type and *mls1*Δ or *lea1*Δ cultures were grown in YPD liquid medium and whole cell extracts were prepared (see Material and Methods) and probed with anti-HA 12CA5 (Roche), shown in the top panel. Extracts were also probed with anti-PGK (Invitrogen) as a loading control (bottom panel).

association in the promoter region is dependent on acetylation of histones. One possible explanation for these results is that Msl1 or Lea1 protein levels decrease when the other factor is missing. However, we observe that no change in protein levels of Lea1 when *MSL1* is deleted or vice versa. Therefore the decrease in recruitment at the intron branchpoint is not due to a decrease in protein levels (Figure 4.1 D). The results obtained from these experiments also correlate with what has been previously shown, namely that although each protein is stable in extracts derived from strains deleted of its partner, Msl1 and Lea1 are required for stable binding to U2 snRNA (Caspary & Seraphin, 1998).

Deletion of *MSL1* leads to a decrease in histone H3 diacetylation of the intron-containing gene, *DBP2.*

Our discovery of branchpoint independent association of Msl1 at the promoter raises the possibility that the U2 snRNP protein Msl1 might influence transcriptional events at the promoter. We examined histone H3 acetylation in the absence of the U2 snRNP proteins, Msl1 and Lea1 by ChIP using an antibody against histone H3 acetylated on lysine 9/14, and found that deletion of *MSL1* reduced the level of histone acetylation at the promoter; however, deletion of *LEA1* did not (Figure 4.2). Interestingly, although deletion of *LEA1* did not alter the amount of histone acetylation at the promoter, both Lea1 and Msl1 seem to influence H3 acetylation in downstream regions in *DBP2.* Surprisingly, instead of

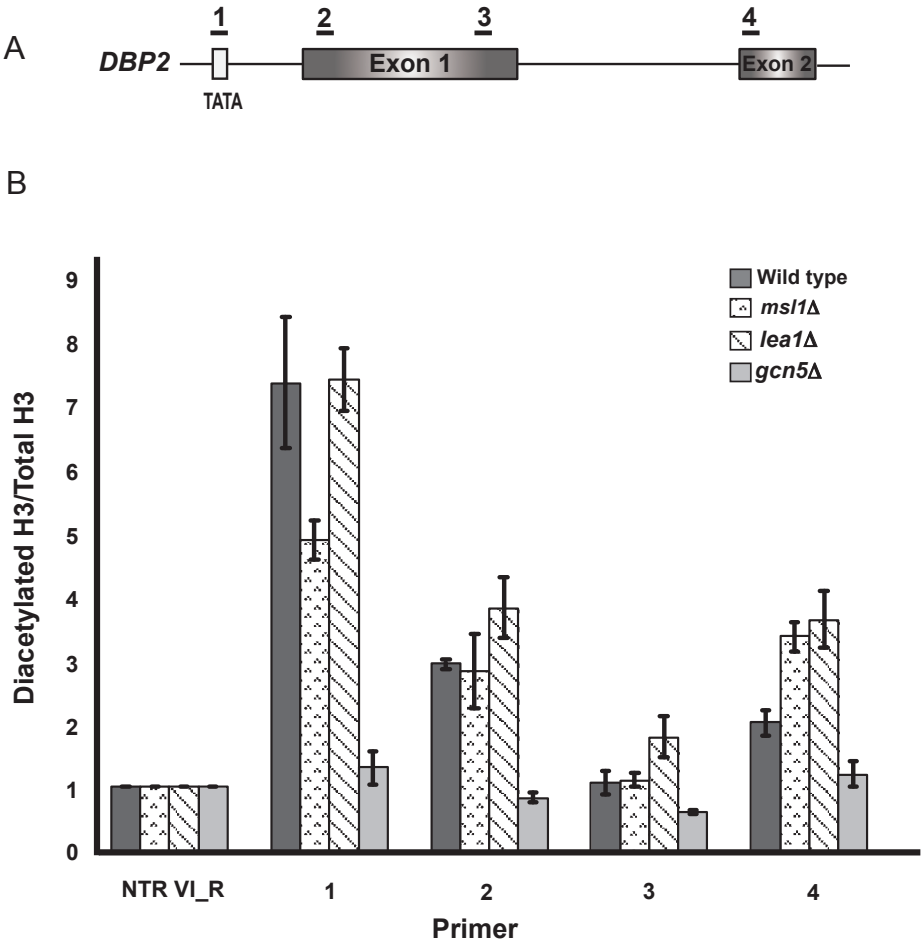

Figure 4.2: Deletion of *MSL1* affects diacetylation of *DBP2* –bound histones.
ChIP analysis of histone H3 K9/14 acetylation within *DBP2* in wild type, *msl1*Δ, *lea1*Δ and *gcn5*Δ strains using an antibody directed against diacetylated histone H3 (Upstate). Data are represented as diacetylated histone H3 normalized to the total amount of histone H3 (Total H3). All graphs depict the average of at least three independent experiments, and error bars represent the standard deviation.

a decrease in acetylation in these regions, H3 acetylation increases in the coding region of *DBP2* (Figure 4.2, primer set 4). From these results, we hypothesize that splicing factors either recruit HDACs to the body of intron-containing genes or modulates HDAC activity at intron-containing genes.

Deletion of *MSL1* alters recruitment of RNA polymerase II to sites of transcription initiation.

It is known that acetylation of histone tails changes the compaction of chromatin to expose DNA sequences that the RNA polymerase II recognizes and binds to initiation transcription. Since we observed a decrease in histone H3 acetylation at the promoter of *DBP2* in the absence of *MSL1,* we chose to examine the recruitment of RNAP polymerase II to intron-containing genes in the absence of the splicing factors, *MSL1* and *LEA1.*

To examine recruitment of the RNA polymerase II to the intron-containing gene *DBP2,* we used ChIP with an antibody that recognizes both the phosphorylated and unphosphorylated form of the RNAPII (8WG16, Covance). When we examined recruitment of RNAPII in the absence of *MSL1* we detected a decrease in the amount of RNAPII at the promoter when compared to wild type cells (Figure 4.3 B). However, we did not detect a decrease in the amount of RNAPII in the coding region. We also examined recruitment of RNAPII in the absence of *LEA1* and we do not detect a change in the recruitment profile of RNAPII when compared to wild type (Figure 4.3 C). These results suggest that deletion of *MSL1,* specifically, affects recruitment of RNAPII to the promoter.

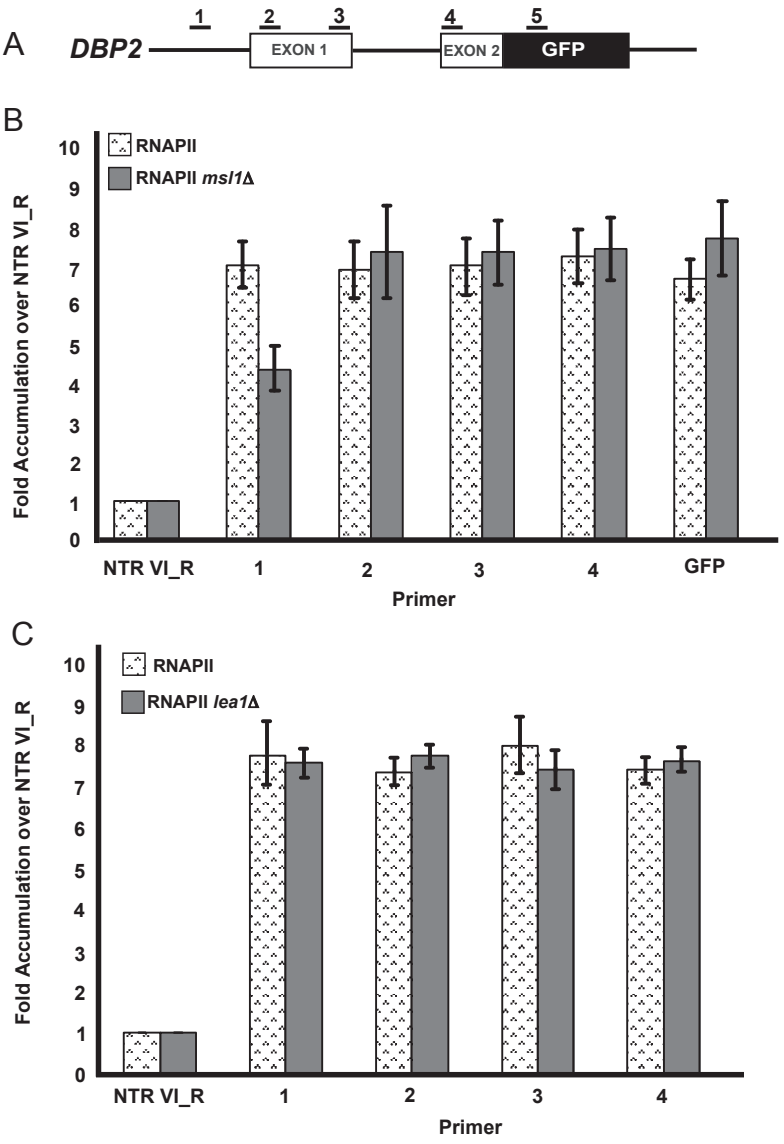

Figure 4.3: Deletion of *MSL1* affects recruitment of RNAPII to the promoter of the intron-containing gene, *DBP2.*

A) Schematic of the intron-containing gene, *DBP2*. Underlined numbers represent amplicons generated from each primer set used in the study. B) Bar graph depicting RNA pol II occupancy within *DBP2* relative to the non-transcribed control. Pattern bars represent RNAP II occupancy in the wild type strain and dark grey bars represent RNAP II occupancy in the *msl1*Δ strain. C) Graph depicting the occupancy of RNAPII within *DBP2* relative to the non-transcribed region. Pattern bars represent RNAP II occupancy in the wild type strain and dark grey bars represent RNAP II occupancy in the *leal1*Δ strain. All graphs depict the average of at least three independent experiments, and error bars represent the standard deviation.

The results presented here, suggest a U2 snRNP-independent, co-transcriptional recruitment of Msl1 to the promoter of the intron-containing gene *DBP2*. Furthermore, and deletion of *MSL1* (and not *LEA1*) leads to a decrease in histone H3 diacetylation at the promoter and subsequent decrease in RNAPII enrichment at the promoter. Finally, although the effect on transcription is not clear, our data suggests that the Msl1/Lea1 heterodimer may either facilitate histone H3 deactylation in downstream regions of genes, or protect these regions from acetylation. These results lead to the hypothesis that U2 snRNP may affect histone modification and transcription in order to coordinate transcription and splicing.

Section 4.3: Discussion

In this chapter, we examined whether splicing factors could affect transcription in yeast. We show that Msl1 is recruited independently of its splicing binding partner, Lea1, to the promoter of *DBP2*. Additionally, deletion of *MSL1* decreases histone H3 acetylation and RNAPII occupancy at the promoter. Since Msl2 associates in a region of the chromatin devoid of RNA splicing signals, Msl1 may have a more general effect on transcription. These results are the first evidence in yeast, that a splicing factor can directly affect the state of chromatin and, in turn, affect transcription.

We were surprised to observe that Msl1 and Lea1, presumably in a complex, can affect histone acetylation downstream of the promoter in the opposite manner to the effects mediated through Msl1. Deletion of either *MSL1*

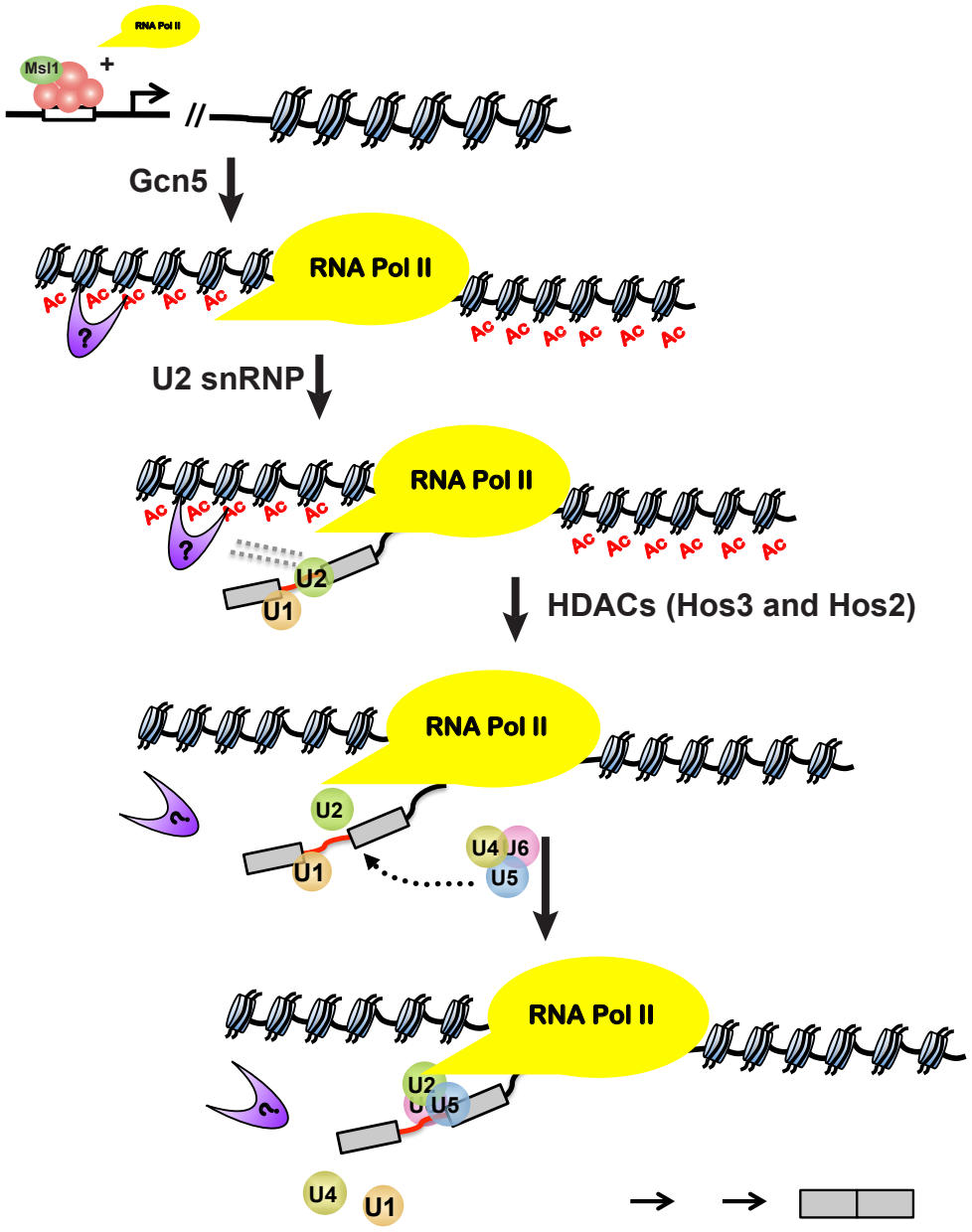

Figure 4.4: Presence of U2 snRNP either recruits or alters HDAC activity to modulate co-transcriptional splicing.
Msl1 is recruited to the promoter in a Gcn5-independent manner and may physical interactions with transcription initiation factors to recruit the RNAPII. Since, Msl1 is present at the promoter this allows for recruitment of Gcn5 to acetylate histones. Histone acetylation in turn recruits an adapter protein that in turn, recruits the U2 snRNP. Once the U2 snRNP is associated, the presence of the U2 snRNP can recruit HDACs to deacetylate histones for proper spliceosomal rearrangements and subsequent splicing.

or *LEA1* led to an increase in acetylation. These results suggest that the presence of the U2 snRNP may help recruit HDACs to the body of intron-containing genes to allow for histone deacetylation that is necessary for the rearrangements that occur during spliceosome assembly (Figure 4.4). To test this hypothesis, we will need to examine histone H3 acetylation in the body of other intron-containing genes, to establish that it is not a gene specific effect. Additionally, we will examine whether Msl1 or Lea1 directly recruit Hos2, Hos3, or Gcn5 to the body of intron-containing genes. To do this, we will examine the recruitment of Hos2, Hos3, and Gcn5 in the absence of either *MSL1* or *LEA1* by chromatin IP. If we observe an affect in recruitment of these factors in the absence of either *MSL1* or *LEA1* this leads to the possibility that Msl1 and Lea1 actively recruit these factors to intron-containing genes. To test this hypothesis, we will examine physical interactions between HDACs and Msl1/Lea1. Results from this study would suggest that the U2 snRNP proteins, Msl1 and Lea1 physically recruit HDACs to intro-containing genes.

Since we did not observe a change in Pol II occupancy, the role of Msl1/Lea1 in histone acetylation may be primarily to affect splicing. As such, Msl1/Lea1 affects on acetylation may be specific to intron-containing genes. To test this hypothesis, a genome-wide analysis of the recruitment of Msl1 and Lea1 will provide evidence as to whether these factors are recruited to primarily intron-containing genes or not.

The results presented here are provocative and could lead to a variety of different research directions. For example, it will be important to determine how

Msl1 is recruited to these upstream regions. Specifically, it will be important to determine if Msl1 recruitment to the promoter is (1) RNA dependent and (2) U2 snRNP dependent. This can be analyzed by carrying out ChIP to assess Msl1 occupancy in the presence of RNase and by using complementary oligos to specifically degrade U2 snRNA. It is also possible that Msl1 associates with the polymerase or some other protein that binds at the promoter. Large-scale genetic interactions studies have described genetic and physical interactions between *MSL1* and factors that are involved in transcription initiation (Fromont-Racine et al., 1997, Sanders et al., 2002). Such as Tra1 and Taf4. Future experiments will involve targeted analysis of these interactions and their Lea1 dependence. It will also be important to determine how Msl1 affects histone acetylation by examining Gcn5 recruitment in the absence of *MSL1*. Msl1 may be recruited early in order to facilitate snRNP recruitment downstream regions if the gene contains an intron. The early recruitment of Msl1 to the promoter of intron-containing genes might provide the appropriate signals to recruit the splicing machinery to splice intron-containing genes co-transcriptionally and, suggests a role for Msl1 outside of splicing.

Chapter 5: Summary of data and future directions

Section 5.1: Summary of data

The mechanistic details of pre-mRNA splicing and transcription have been characterized from *in vitro* biochemical analysis. However, recent evidence, including the data presented here, indicate that these processes are spatially and temporally coordinated; pre-mRNA splicing can occur while the RNA polymerase is still actively engaged with the DNA template. The template DNA that the polymerase navigates is packaged into the highly ordered chromatin structure, and the protein components of chromatin undergo a variety of post-translational modifications that change its conformation and allow transcription to occur. Studies examining the coordination of transcription and pre-mRNA splicing have focused on the effects of changes in transcription elongation on alternative splice site choice called the “kinetic coupling model” (Kornblihtt et al., 2004). However, the role of specific histone marks in co-transcriptional, constitutive splicing has been poorly understood despite scattered reports in the literature that suggested a functional link between chromatin and splicing (reviewed in Allemand *et al.*, 2008, Schwartz et al., 2009). To elucidate the role of chromatin in co-transcriptional splicing, I set out to identify functional interactions between non-essential splicing factors and chromatin-associated factors in the budding yeast, *Sacchromyces cerevisiae* using a screen for synthetic lethality.

I discovered that the gene encoding the histone acetyltransferase *GCN5* had a functional interaction with the genes encoding the two U2 snRNP components, Msl1 and Lea1. Deletion of *GCN5* or mutation of its catalytic domain in combination with a deletion of *MSL1* or *LEA1* led to a synthetic lethal phenotype (Figure 2.1). Further characterization of this interaction revealed that Gcn5 was critical for co-transcriptional recruitment of Msl1/Lea1. Deletion of Gcn5 or a loss of function mutation in its catalytic domain abrogated co-transcriptional recruitment of the U2 snRNP (Figures 2.7 and 2.9). Meanwhile, recruitment of the RNA polyermase II was unaffected.

Since spliceosome assembly occurs in a stepwise manner, I demonstrated that deletion of the gene encoding Gcn5 not only abrogates recruitment of the U2 snRNP but also recruitment of downstream snRNPs, suggesting that recruitment of the U2 snRNP is a critical step in co-transcriptional spliceosome assembly (Figures 2.15 and 2.16). A critical question that I have also addressed is what target of Gcn'5 catalytic activity is responsible for the observed effects on splicing.

Here I provide evidence that Gcn5's *histone* acetyltransferase activity is important for co-transcriptional recruitment of the U2 snRNP. Although I find no evidence that Gcn5 directly acetylates a splicing factor, I do show that Gcn5 acetylates histone tails within intron-containing genes. Furthermore, deletion or mutation of histone H3 residues that are known targets of Gcn5's catalytic activity show similar genetic interactions and splicing defects as deletion of *GCN5* (Figure 3.1). Notably, either H3K14 or K9 alone show as strong of an interaction

as Δ9-16, suggesting that acetylation of one residue can compensate for the lack of acetylation of the other. This raises several questions about histone acetylation and co-transcriptional spliceosome assembly: 1) Where along intron-contaning genes does acetylation occur, and is this important? 2) How much acetylation is important?

Our initial examination of histone H3 diacetylation of intron-containing genes revealed an enrichment of histone acetylation at the promoter region and very little in the body of the gene (Figure 2.13). This result was intriguing since the effects on spliceosome assembly were observed in the middle and near the 3' end of the intron. Recent literature has shown that acetylation of histone tails is a very dynamic progress (reviewed in MacDonald & Howe, 2009). The removal of acetyl groups from histone N-terminal tails is catalyzed by multiple, redundant histone deacetylases (HDACs) and occurs very rapidly. Because this is such a dynamic process, it suggests that the rapid turnover of this mark could mask acetylation in the body of the gene that can only be revealed by deletion of mutiple HDAC's. When I deleted the HDACs *HOS3* and *HOS2*, I found a significant increase in histone acetylation in the body of the intron-containing genes used in these studies (Figure 3.5). Interestingly, the precise peaks in histone H3 acetylation in the body were gene specific. The peak was always in the region of U2 snRNP recruitment, but in one case it precisely overlaps with the U2 peak. Work examining genome-wide histone acetylation patterns in the absence of mutiple HDACs will be immensely informative for establishing the generality of the patterns I observe. I predict that intron-containing genes may

have a specific pattern of acetylation in the body of the gene that is important for co-transcriptional spliceosome assembly.

To further elucidate the role of histone acetylation in co-transcriptional splicing, I examined the co-transcriptional recruitment of the U2 snRNP proteins, Lea1 and Msl1 to intron-containing genes in strains deleted of both *HOS3* and *HOS2*. Deletion of the HDACs results in a persistence of these factors on the pre-mRNA and leads to a decrease in the recruitment of the downstream snRNP's (Figures 3.7, 3.8, 3.10, and 3.11). These results led to our current model, which histone acetylation recruits an "adaptor" protein that interacts with the U2 snRNP and that HDACs are recruited to deacetylate histones in the body of the gene and allows for proper release of the U2 snRNP and allows subsequent rearrangements to occur (Figure 3.15).

Deletion of *GCN5,* mutation of histone tails, and deletion of multiple HDACs all result in a splicing defect. Deletion of *HOS3* and *HOS2* results in a splicing defect that was slightly less pronounced, likely because in the double deletion of *HOS3* and *HOS2*, co-transcriptional recruitment is not completely abrogated like a deletion of *GCN5.* Taken together these results suggest that co-transcriptional spliceosome assembly is sensitive to changes in histone acetylation.

However, the splicing defect is not as dramatic as deletion of a bona fide splicing factor. This result suggests that post-transcriptional splicing can still occur. It is likely that the additive effect of disrupting co-transcriptional splicing across the genome has important implications for optimal cellular function,

particularly under conditions in which optimal splicing of particular genes is required for cell viability. This hypothesis is currently being tested in experiments described in the next section.

Here, we provide evidence to show that histone acetylation plays a role in splicing by altering the dynamic rearrangements of the spliceosome co-transcriptionally. This is the first indication in yeast as to a mechanism by which chromatin can affect splicing.

Because of the close spatial and temporal proximity of histone acetylation and deactylation, I chose to address the long-standing question of whether splicing factors could influence transcription by looking at Msl1/Lea1 effect on histone acetylation and RNA polymerase II occupancy. In this study I show that the U2 snRNP component, Msl1 can be recruited to the promoter region of intron-containing genes independently of its splicing binding partner, Lea1 (Figure 4.1). Additionally, deletion of the gene encoding *MSL1* results in a decrease in histone H3 acetylation in the promoter and a decrease in the recruitment of the RNAPII to the site of transcription initiation of intron-containing genes (Figure 4.2 and 4.3, respectively).

Interestingly, deletion of either Msl1 or Lea1 results in an increase in histone H3 acetylation in the body of intron-containing genes (Figure 4.2). These results suggest that the U2 snRNP may directly recruit HDACs to the body of intron-containing genes to deaceylate histone tails promoting the necessary rearrangements for spliceosome assembly (Figure 4.4).

Section 5.2: Future Directions

At the beginning of these studies, little was known about the role of chromatin in pre-mRNA processing events. These studies shed light on the importance of chromatin in co-transcriptional splicing. Very recently, there have been studies of nucleosome occupancy and histone modifications that correlate with intron-exon junctions (Andersson et al., 2009, Choi et al., 2009, Kolasinska-Zwierz et al., 2009, Nahkuri et al., 2009, Schwartz et al., 2009, Spies et al., 2009, Tilgner et al., 2009). Furthermore, it has been shown in mammals that histone modifications can influence alternative splicing (Luco et al., 2010). Our studies provide the first evidence of a role for histone modification in co-transcriptional splicing. In yeast in which genetic and biochemical analysis is more tractable. Nonetheless, all these findings strongly support a role for chromatin in co-transcriptional splicing and have opened the door to try to understand the mechanism by which chromatin can affect splicing on a genome-wide level. Furthermore, our studies raise the importance of co-transcriptional splicing, particularly when rapid, efficient, and regulated splicing is required by the cell.

Identification of histone binding proteins that may recruit the U2 snRNP.

In the model presented in chapter 3, we propose that Gcn5-dependent histone acetylation may provide binding sites for an adaptor protein that recruits the U2 snRNP co-transcriptionally. Mammalian studies have shown that histone methylation provides binding sites for the factor, Chd1, which associates with

snRNP's and facilitates their recruitment (Sims et al., 2007). Therefore, the next question to address is to identify the "adapter" protein. One possible candidate is Swi1. Swi1 is a component of the chromatin remodeling complex SWI/SNF. Mammalian SWI/SNF complex has been show to play role in alternative splicing (Batsche et al., 2006). Swi1 contains a bromodomain that can bind to acetylated histone tails and has been shown to have a functional interaction with the U2 snRNP (Fromont-Racine et al., 1997). Therefore, making Swi1 an ideal candidate. To test this one can use ChIP to detect if SWI/SNF recruitment to intron-containing genes is dependent on Gcn5. Then, U2 snRNP recruitment to intron-containing genes can be analyzed in the presence of *SWI1* mutants that have lost the ability to bind to acetylated histones due to a deletion of the bromodomain (Prochasson *et al.*, 2003). This will indicate that the ability of Swi1 to bind to acetylated histones facilitates U2 snRNP recruitment to intron-containing genes. Additionally, one could examine if the recruitment of the U2 snRNP coincides with the recruitment of Swi1 by using *SWI1* mutants that cannot bind acetylated histones (Prochasson et al., 2003) by ChIP-DiChIP.

Elucidating a role for the U2 snRNP in transcription.

In light of the splicing-independent Msl1 recruitment to the promoter region of a gene, we predict that it may play a role in the recruitment of transcription factors involved in initiation. In fact, reports in the literature have indicated that Msl1 has physical and genetic interactions with factors that have been implicated in transcription initiation including Tra1, Taf4 and Ssl2 (Fromont-

Racine et al., 1997, Sanders et al., 2002). First, recruitment of these factors can be examined in the absence of *MSL1*. Furthermore, to see if Msl1 and these factors interact co-transcriptionally, we can test by ChIP-DiChIP the recruitment of Msl1 and Tra1, Taf4 and Ssl2 to *DBP2* and other intron-containing genes. These experiments will reveal whether the splicing factor, Msl1 is positioned at the promoter in a complex with the transcription initiation machinery. It is also possible that the transcription initiation factors are required for the stable association of Msl1 near the promoter. Using Tra1, Taf4, and Ssl2 mutants, we can analyze these factors' effects on Msl1 association. The positioning of Msl1 early in transcription might be a signal for the proper recruitment of the U2 snRNP to the intron-containing genes.

An exciting possibility that is raised from the splicing-independent recruitment of Msl1 to the promoter region is the possibility of Msl1 being recruited to intronless genes. To address this, examination of the recruitment of Msl1 on a whole-genome scale using ChIP-chip could be done. Briefly, ChIP-chip uses the same principles as conventional ChIP. However, instead of examining recruitment to individual genes by qPCR, ChIP-chip can examine whole genome recruitment by microarray. If its found that Msl1 is associated with not only intron-containing genes but also intronless genes, this would suggest that Msl1 is a multi-functional protein that may play a more general role in transcription. Its presence at the promoter could facilitate spliceosome assembly, if the gene contains an intron. If Msl1 associates only with intron-containing genes, this

would suggest that Msl1 recruitment at the promoter “marks” that the gene needs to be spliced.

It will also be interesting to examine Msl1 effects on transcription more closely. Msl1’s effect on transcription might reveal itself through changes in RNAPII occupancy or changes in RNAPII CTD phosphorylation. A deletion of *MSL1* could lead to changes in transcription factor recruitment and concomitant changes to the physical attributes of the carboxyl-terminal domain (CTD) of the RNAPII. Msl1 could also affect transcription by effecting changes in RNAPII pausing on the transcript. These are mechanisms that can be analyzed by ChIP and or nuclear run-on assays. Data from these assays would be one of the first indications of a splicing factor affecting transcription initiation in yeast.

Why do cells require co-transcriptional splicing?

In these studies, we used the intron-containing genes, DBP2 and ECM33 as model genes that allowed for good resolution of spliceosome assembly by ChIP. Using these genes I was able to detect spliceosome assembly and disruption of spliceosome assembly in the HAT mutants. I have shown that I can detect a reproducible increase in unspliced *DBP2* and *ECM33* transcripts when strains are deleted of *GCN5*, the double mutant H*OS3 HOS2* and in the histone H3 truncation mutant. Like others, I observed that these genes are also post-transcriptionally spliced. It is likely that specific genes are particularly sensitive to Gcn5-dependent co-transcriptional splicing. Using splicing sensitive microarrays we predict that these genes can be revealed. Initial experiments have been

performed and need to be validated. It is also possible that co-transcriptional splicing is particularly important under specific environmental conditions. To test this, genome-wide splicing can be examined under different conditions to reveal genes whose splicing is dependent on Gcn5. From a genome wide analysis of RNA expression, it was found that SAGA dependent genes are specifically induced under stress conditions (Huisinga & Pugh, 2004). Additionally, it has been shown that under stress conditions, splicing becomes crucial for viability (Pleiss *et al.*, 2007). This raises the possibility that stress conditions, will reveal particularly important co-transcriptional splicing events that are dependent on Gcn5. The *gcn5Δ, hos3Δ hos2Δ* double deletion, and histone H3 truncation mutant strains can be grown under several stress conditions, and splicing profile can be examined using splicing microarray. Under osmotic stress conditions the SAGA complex is required for cell survival (Zapater *et al.*, 2007). Furthermore, strains deleted of *MSL1* have been shown to be sensitive to osmotic stress (Goossens *et al.*, 2002). Results from these experiments would suggest the importance of co-transcriptional splicing in adaptation to an environmental stress.

An additional method to examine the importance of co-transcriptional splicing in response to stress is through the use of the microfluidic platform in which one can examine gene expression under dynamically changing conditions. I have done pilot experiments examining splicing of *DBP2* under caffeine stress and those experiments are detailed in Appendix 1.

The intricate relationship between transcription and splicing reveals an intriguing level of complexity underlying eukaryotic gene expression. We have discovered a novel function for the Gcn5 histone acetyltransferase, in co-transcriptional spliceosome assembly. Deciphering the relationship between transcription and splicing will provide a mechanistic understanding of the coordination of these two processes will help us better understand how the overall gene expression program of the cell is regulated.

Chapter 6: Materials and Methods

Yeast Strains, Media, and DNA Constructs

All *S. cerevisiae* strains used in this study are listed in Table 6.1. Strains described in Table 6.1 are in the BY4743 strain background, with the exception of Lea1-HA and Msl1-HA strains used for ChIP assays, provided by Karla Neugebauer. All strains were propagated according to standard procedures in either rich media (YPD) or appropriate selective media. Plasmid shuffling was performed on 5- fluoroorotic acid (5-FOA) plates. Plasmids used in this study are listed in Table 6.2.

Strains harboring histone H3 point mutations and/or truncation were obtained from Open Biosystems as described by (Dai et al., 2008). The *hos3*Δ deletion strain was created by using the "marker swap" method (Voth *et al.*, 2003).. Briefly, plasmid containing the CLONAT resistance gene with flanking region homology region to KanMx4 was digested with EcoRI and the linear fragment corresponding to CLONAT resistance gene with flanking KanMX4 homology was introduced into a *HOS3::KanMX4* strain by LiOAc transformation. CLONAT resistant and KanMX4 sensitive colonies were examined by genomic PCR to confirm the genotype.

Gcn5-13XMyc, was constructed using a PCR based method for tagging chromosomal genes by yeast transformation (Longtine *et al.*, 1998). The pFA6a-13Myc-His3MX6 plasmid was used as a template, and transformants were selected on synthetic complete medium lacking histidine (SC-His medium). His^+ colonies were analyzed by colony PCR to verify the presence of the tag in the

gene of interest and by Western analysis to verify expression of the tagged protein.

Standard methods for mating, sporulation, transformations, and tetrad analysis were used as described in *Methods in Yeast Genetics: A Cold Spring Harbor Laboratory Course Manual* (Burke *et al.*, 2000). The genotype of each viable spore was confirmed by PCR.

Viability Assay/ Dilution Series

For growth analysis described in chapter 2, strains containing a wild type copy of *GCN5* on a centromeric pRS316 (*URA3)* plasmid were selected for plasmid loss on 5-FOA. Strains were then grown overnight in YPD media at 30^{o}C. Cells were diluted to an O.D.$_{600}$ of 0.1 in 10 ml of YPD, and incubated at 30^{o} until all strains reached an O.D.$_{600}$ of 0.35. A ten-fold serial dilution of each strain was spotted onto YPD plates and incubated 3-5 days at 30^{o}.

For growth analysis described in chapter 2 and 3, strains were then grown overnight in YPD media at 30^{o}C. Cells were diluted to an O.D.600 of 0.1 in 10ml of YPD, and incubated at 30^{o} until all strains reached an O.D.600 of 0.5. A ten-fold serial dilution of each strain was spotted onto YPD plates, and incubated 3 days at 30^{o}.

Yeast Whole Cell Extract / Western Blot Analysis

Cells were grown to an O.D.$_{600}$ of 1.0 and lysed using FA-1 Lysis buffer (50 mM HEPES-KOH pH 7.5, 140 mM NaCl, 1 mM EDTA pH 8.0, 1% Triton-X,

0.1% Deoxycholate, plus protease inhibitors) and 0.5 mm glass beads with 5 minutes of vortexing at 4°C. The supernatant was cleared by centrifugation and protein concentration was determined by Bradford Assay (Bio-Rad). 50 μg of total protein was fractionated by SDS-PAGE electrophoresis and transferred to a nitrocellulose membrane for immunoblotting with 1:2000 dilution of anti-PGK1 (Molecular Probes) and 1:1000 dilution of anti-HA 12CA5 (Roche), followed by chemiluminescent detection (Pierce).

Chromatin Immunoprecipitation (ChIP)

Cells were grown in YPD to an $O.D._{600}$ 0.5-0.7 and then crosslinked for 15 minutes with formaldehyde to a final concentration of 1%. Cells were disrupted with glass beads (0.5 mm) for 40 minutes at 4°C and lysates were cleared by centrifugation. To shear chromatin, lysates were sonicated for a total of six minutes at 30% intensity (15 seconds on, 15 seconds off, and on ice). After sonication, samples were precleared with CL4B Sepharose beads (Sigma). The precleared samples were then used for immunoprecipitation with either 12CA5 (Roche) antibody against the HA epitope or 8WG16 (Covance) antibody against RNA pol II. After immunoprecipitation, samples were washed and incubated overnight at 65° to reverse crosslinking, followed by incubation with Proteinase K (Sigma). DNA was purified using a PCR product purification kit (Qiagen) and analyzed by real-time PCR. Input DNA was diluted 1:20 and 1 μl of this was used in a 25 μl reaction volume. For ChIP DNA, samples were diluted 1:5 and 1 μl of this was used in a 25μl reaction volume. Reactions consisted of 12.5 μl SYBR

GREEN Master Mix (Applied Biosystems) and 0.5 μM Primers. Real time PCR was performed using an ABI7700 (Applied Biosystems). All samples were run in triplicate for each independent experiment.

For quantification, standard curves were generated for each primer set, and DNA concentration for each INPUT and ChIP sample was calculated. ChIP values were divided by the INPUT, and these values were divided by the non-transcribed control and expressed as fold accumulation over the non-transcribed control. Reported values are averages of at least three independent experiments, and error bars represent the standard deviation.

For histone H3 acetylation ChIP, the ChIP protocol described above was used except samples were sonicated for seven minutes at 30% intensity (15 seconds on, 15 seconds, off, and on ice). Samples were used for immunoprecipitation with either anti-acetylated histone H3 (Upstate 06-599) or anti-histone H3 (AbCam ab1791) overnight at 4^{o}C.

For quantification, standard curves were generated for each primer set. DNA concentration for each INPUT and ChIP sample was calculated using these standard curves and normalized to the non-transcribed control VI_R1. The normalized IP values calculated for acetylated H3 were divided by the normalized IP values calculated for total H3. These values are expressed as diacetylated H3 over total Histone H3. Reported values are averages of three independent experiments, and error bars represent the standard deviation.

The data in figures 2.7, 2.11, and 2.15 were generated by standard PCR analysis, ethidium bromide staining, and quantification. The reaction volume was

50 μl, with 0.75 μl of template for INPUT, and 5 μl of template for ChIP DNA. Primers were used at a final concentration of 1 μM. PCR products were analyzed on a 1.75% agarose gel. Results were quantified using ImageQuant software (Molecular Dynamics). Primer sequences are listed in Tables 6.3 and 6.4.

Quantitative RT-PCR

Total cellular RNA was extracted by hot phenol-chloroform extraction. Prior to cDNA synthesis, total RNA was treated with DNase I (Promega) according to the manufacturer's protocol. cDNA was synthesized from 1 μg of DNase-treated RNA in a 20 μl reaction mixture containing 1X First Strand Buffer, 2 mM each dNTP, 10 mM DTT, 2U RNasin (Promega), 1 μM gene-specific primer, and 200U of SuperScript II (Invitrogen). Quantitative PCR was performed using an ABI Prism 7700 Sequence Detector. Primer sequences are listed in Table S5. cDNA was diluted 1:20 and 1 μl of this was used in a 25 μl reaction volume. Reactions consist of 12.5 μl SYBR GREEN Master Mix (Applied Biosystems) and 0.5 μM Primers. All samples were run in triplicate for each independent experiment. Primers were designed to amplify unspliced (precursor) message using an intron-specific primer and total message amplification using primers specific to exon 2. Primer sequences are listed in Table 6.5.

For quantification, standard curves were generated for each primer set, and to calculate ratio of precursor to total RNA, amount of unspliced (precursor) transcript was divided by the total amount of transcript (both spliced and unspliced).

Immunoprecipitation

Cultures (100 ml) were grown to an $O.D._{600}$ of 1.0, centrifuged and washed with 1X TBS. Pellets were then resuspended in 400 μl of Lysis buffer (50mM HEPES-KOH pH 7.5, 140mM NaCl, 1mM EDTA pH 8.0, 1% Triton-X, 0.1% Deoxycholate, 0.1M DTT, 40U/ml RNasin (Promega), 1 μg/ml Leupeptin, 1μg/ml Pepstatin A, 0.2mM Benzamidine) and lyzed for 12 minutes at 4 ^{o}C with 0.5mm glass beads. Lysates were centrifuged for 10 minutes. Protein concentration was determined using Bradford Assay (Bio-Rad). Equal concentrations of lysates were precleared with CL4B Sepharose beads for 2 hours at 4 ^{o}C. For immunoprecipitation with the HA tag, precleared lysates were incubated with 0.4 mg/ml of anti-HA (Roche) for 3 hours at 4^{o}C. Gamma-bind G sepharose (GE healthcare) were added to lysate-antibody mixture and incubated for an addiotnal hour at 4^{o}C After incaubation, complexes we washed with lysis buffer and resuspended and boiled in 2X SDS- loading buffer.

For immunoprecipitation of TAP-tagged strains, precleared lysates were added to pre-equilbrated IgG Sepharose beads (Amersham Biosciences) for 2.5 hours at 4 ^{o}C. Following incubation with IgG beads, bound complexes were washed with lysis buffer and resuspended and boiled in 2X SDS- loading buffer.

In a parallel experiment, following incubation with IgG beads, bound complexes were washed with lysis buffer and resuspended in 200 μl of sterile RNase free water and incubated with TEV protease (Invitrogen) for 2 hours at 16^{o}C to cleave the complexes from the beads. Beads were resuspended and boiled in 2X-SDS loading buffer.

For western blot analysis, 5μl of INPUT and 12μl of IP were separated by SDS-PAGE electrophoresis and transferred to a nitrocellulose membrane for immunoblotting with 1:1000 dilution of anti-Acetyl K-103 (Cell Signaling) followed by chemiluminescent detection (Pierce).

U2 snRNA Immunoprecipitation

Cultures (100 ml) were grown to an O.D.$_{600}$ of 1.0, centrifuged and washed with 1X TBS. Pellets were then resuspended in 400 μl of Lysis buffer (50mM HEPES-KOH pH 7.5, 140mM NaCl, 1mM EDTA pH 8.0, 1% Triton-X, 0.1% Deoxycholate, 0.1M DTT, 40U/ml RNasin (Promega), 1 μg/ml Leupeptin, 1μg/ml Pepstatin A, 0.2mM Benzamidine) and lyzed for 12 minutes at 4 ^{o}C with 0.5mm glass beads. Lysates were centrifuged for 10 minutes. Protein concentration was determined using Bradford Assay (Bio-Rad). Equal concentrations of lysates were precleared with CL4B Sepharose beads for 2 hours at 4 ^{o}C. This precleared lysate was added to pre-equilbrated IgG Sepharose beads (Amersham Biosciences) for 2.5 hours at 4 ^{o}C. Following incubation with IgG beads, bound complexes were washed with lysis buffer and resuspended in 200 μl of sterile RNase free water and. 100μl was used for

western blot analysis and the remaining sample was treated with TEV protease (Invitrogen) to cleave the complexes from the beads and followed by treatment with 1mg/ml Proteinase K (Invitrogen). RNA was extracted using TRIzol (Invitrogen).

Primer Extension

RNA was resuspended in Annealing Mix (50mM Tris pH 8.0, 200mM KCl, 40U/ml RNasin (Promega), radiolabeled U2 snRNA, U6 snRNA, or U3 snoRNA-specific oligo and incubated for 10 minutes at 65 ^{o}C. To this mix, AMV reverse transcriptase (Promega) was added and incubated for one hour at 37 ^{o}C. cDNA was ethanol precipitated and resuspended in formamide loading buffer and heated for 5 minutes at 95 ^{o}C and separated on a 6% Urea denaturing gel. Gel was dried and exposed to phospohimager cassette overnight and scanned using Typhoon phosphorimager (Amersham Biosciences).

Table 6.1: List of strains used in these studies

Name	Parent	Relevant Phenotype	Reference
TJY1701	BY4743	*MATα his3Δ1 leu2Δ0 lys2Δ0 ura3Δ0*	Open Biosystems
TJY0386	BY4741	*gcn5Δ::KanMX4*	Open Biosystems
TJY0396	BY4742	*msl1Δ::KanMX4*	Open Biosystems
TJY0462	BY4742	*lea1Δ::KanMX4*	Open Biosystems
TJY0408	BY4742	*cus1Δ::KanMX4 [URA3 CUS1]*	Open Biosystems
TJY0547	BY4742	*cus1Δ::KanMX4 [LEU2 CUS 1-54]*	Open Biosystems
TJY2042	BY4741	*spt3Δ::KanMX4*	Open Biosystems
TJY2043	BY4741	*spt7Δ::KanMX4*	Open Biosystems
TJY2044	BY4741	*spt8Δ::KanMX4*	Open Biosystems
TJY0499	BY4741	*sas3Δ::KanMX4*	Open Biosystems
TJY0500	BY4741	*ubp8Δ::KanMX4*	Open Biosystems
TJY0504	BY4741	*ada2Δ::KanMX4*	Open Biosystems
TJY2045	BY4741	*ada3Δ::KanMX4*	Open Biosystems
TJY0443	BY4741	*elp3Δ::KanMX4*	Open Biosystems
TJY0001	LG1	*LEA1-HA$_3$:TRP1 DBP2-GFP:KanMX4*	(Gornemann et al., 2005)
TJY0476	LG1	*MSL1-HA$_3$::TRP1*	(Gornemann et al., 2005)
TJY0447	BY4743	*gcn5Δ::KanMX4 msl1Δ::KanMX4*	This study
TJY0469	BY4743	*gcn5Δ::KanMX4 lea1Δ::KanMX4*	This study
TJY0441	BY4743	*gcn5Δ::KanMX4 mud2Δ::KanMX4*	This study
TJY0457	BY4743	*gcn5Δ::KanMX4 cus2Δ::KanMX4*	This study

Table 6.1: List of strains used in these studies, Continued

Name	Parent	Relevant Phenotype	Reference
TJY0543	BY4743	*gcn5Δ::KanMX4 cus1Δ::KanMX4 [LEU2 CUS1-54]*	This study
TJY0528	BY4743	*ada2Δ::KanMX4 msl1Δ::KanMX4*	This study
TJY0527	BY4743	*ada2Δ::KanMX4 lea1Δ::KanMX4*	This study
TJY0540	BY4743	*ada3Δ::KanMX4 msl1Δ::KanMX4*	This study
TJY0541	BY4743	*ada3Δ::KanMX4 leal1Δ::KanMX4*	This study
TJY0531	BY4743	*spt3Δ::KanMX4 msl1Δ::KanMX4*	This study
TJY0532	BY4743	*spt3Δ::KanMX4 lea1Δ::KanMX4*	This study
TJY0544	BY4743	*spt8Δ::KanMX4 msl1Δ::KanMX4*	This study
TJY0533	BY4743	*spt8Δ::KanMX4 lea1Δ::KanMX4*	This study
TJY0534	BY4743	*spt7Δ::KanMX4 msl1Δ::KanMX4*	This study
TJY0535	BY4743	*spt7Δ::KanMX4 lea1Δ::KanMX4*	This study
TJY0529	BY4743	*sas3Δ::KanMX4 msl1Δ::KanMX4*	This study
TJY0530	BY4743	*sas3Δ::KanMX4 lea1Δ::KanMX4*	This study
TJY0423	BY4743	*elp3Δ::KanMX4 msl1Δ::KanMX4*	This study
TJY0468	BY4743	*elp3Δ::KanMX4 lea1Δ::KanMX4*	This study
TJY0548	BY4743	*LEA1-HA$_3$:TRP1 DBP2-GFP:KanMX4 gcn5Δ::KanMX4*	This study
TJY0549	LG1	*MSL1-HA$_3$:TRP1 gcn5Δ::KanMX4*	This study
TJY0566	LG1	*PRP42-HA$_3$:HIS3*	(Gornemann et al., 2005)
TJY0567	LG1	*PRP42-HA$_3$:HIS3 gcn5Δ::KanMX4*	This study
TJY0575	LG1	*SNU114-HA$_3$:TRP1 DBP2-GFP:KanMX4 gcn5Δ::KanMX4*	This study

Table 6.1: List of strains used in these studies, Continued

Name	Parent	Relevant Phenotype	Reference
TJY1706	BY4742	*mud2Δ::KanMX4*	Open Biosystems
TJY0124	BY4742	*cus2Δ::KanMX4*	Open Biosystems
TJY2856	BY4743	*ubp8Δ::KanMX4 msl1Δ::KanMX4*	This study
TJY2852	BY4743	*ubp8Δ::KanMX4 lea1Δ::KanMX4*	This study
TJY0475	LG1	*SNU114-HA$_3$:TRP1 DBP2-GFP:KanMX4*	(Gornemann et al., 2005)
TJY2365	BY4743	*sgf11Δ::KanMX4 lea1Δ::KanMX4*	This study
TJY2366	BY4743	*sgf11Δ::KanMX4 msl1Δ::KanMX4*	This study
TJY2669	BY4743	*MSL1-HA$_3$:TRP1 DBP2-GFP:KanMX4*	This study
TJY2685	BY4743	*MSL1-HA$_3$:TRP1 DBP2-GFP:KanMX4 gcn5Δ::KanMX4*	This study
TJY0562	BY4743	*rpd3Δ::KanMx4 lea1Δ::KanMx4*	This study
TJY0563	BY4743	*rpd3Δ::KanMx4 msl1Δ::KanMx4*	This study
TJY3225	BY4743	*hos2Δ::KanMx4 msl1Δ::KanMx4*	This study
TJY3227	BY4743	*hos2Δ::KanMx4 lea1Δ::KanMx4*	This study
TJY3220	BY4743	*hos3Δ::KanMx4 msl1Δ::KanMx4*	This study
TJY3222	BY4743	*hos3Δ::KanMx4 lea1Δ::KanMx4*	This study
TJY0558	BY4743	*rpd3Δ::KanMx4*	This study
TJY3141	BY4743	*hos2Δ::KanMx4*	This study
TJY3144	BY4743	*hos3Δ::KanMx4*	This study

Table 6.1: List of strains used in these studies, Continued

Name	Parent	Relevant Phenotype	Reference
TJY4318	S288C	*MATa his3Δ200 leu2Δ0 lys2Δ0 trp1Δ63 ura3Δ0 met15Δ0 can1::MFA1pr-HIS3 hht1-hhf1::NatMX4 hht2-hhf2::[H3 K9A]*-URA3*	(Dai, et al., 2008)
TJY4319	S288C	*MATa his3Δ200 leu2Δ0 lys2Δ0 trp1Δ63 ura3Δ0 met15Δ0 can1::MFA1pr-HIS3 hht1-hhf1::NatMX4 hht2-hhf2::[H3 K14A]*-URA3*	(Dai, et al., 2008)
TJY4321	S288C	*MATa his3Δ200 leu2Δ0 lys2Δ0 trp1Δ63 ura3Δ0 met15Δ0 can1::MFA1pr-HIS3 hht1-hhf1::NatMX4 hht2-hhf2::[H3 Δ9-16]*-URA3*	(Dai, et al., 2008)
TJY4339	S288C	*isogenic to TJY4318 except msl1Δ::KanMX4*	This work
TJY4341	S288C	*isogenic to TJY4319 except msl1Δ::KanMX4*	This work
TJY4343	S288C	*isogenic to TJY4321 except msl1Δ::KanMX4*	This work
TJY4334	S288C	*isogenic to TJY4318 except lea1Δ::KanMX4*	This work
TJY4335	S288C	*isogenic to TJY4319 except lea1Δ::KanMX4*	This work
TJY4337	S288C	*isogenic to TJY4321 except lea1Δ::KanMX4*	This work
TJY3522	BY4743	*GCN5-13XMyc:HIS3*	This work
TJY3401	BY4742	*hos2Δ::KanMX4*	This work
TJY4315	BY4742	*hos3Δ::NatMX4*	This work
TJY4312	BY4742	*hos2Δ::KanMX4 hos3Δ::NatMX4*	This work
TJY4325	LG1	*LEA1-HA$_3$:TRP1 DBP2-GFP:KanMX4 hos2Δ::KanMX4 hos3Δ::NatMX4*	This work
TJY4327	LG1	*MSL1-HA$_3$:TRP1 DBP2-GFP:KanMX4 hos2Δ::KanMX4 hos3Δ::NatMX4*	This work
TJY4430	BY4743	*msl1Δ::KanMX4 hos2Δ::KanMX4 hos3Δ::NatMX4*	This work
TJY4431	BY4743	*lea1Δ::KanMX4 hos2Δ::KanMX4 hos3Δ::NatMX4*	This work
TJY0474	LG1	*PRP19-HA$_3$:TRP1 DBP2-GFP:KanMX4*	This work

Table 6.1: List of strains used in these studies, Continued

Name	Parent	Relevant Phenotype	Reference
TJY4434	LG1	*SNU114-HA$_3$:TRP1 DBP2-GFP:KanMX4 hos2Δ::KanMX4 hos3Δ::NatMX4*	This work
TJY4435	LG1	*PRP19-HA$_3$:TRP1 DBP2-GFP:KanMX4 hos2Δ::KanMX4 hos3Δ::NatMX4*	This work
TJY0491	BY4741	*LEA1-TAP:HIS3*	Open Biosystems
TJY0493	BY4741	*LEA1-TAP:HIS3 gcn5Δ::KanMX4*	This work
TJY0490	BY4741	*MSL1-TAP:HIS3*	Open Biosystems
TJY0492	BY4741	*MSL1-TAP:HIS3 gcn5Δ::KanMX4*	This work
TJY2050	LG1	*LEA1-HA$_3$:TRP1*	This work
TJY2617	LG1	*LEA1-HA$_3$:TRP1 DBP2-GFP:KanMX4 msl1Δ::KanMX4*	This work
TJY2501	LG1	*MSL1-HA$_3$:TRP1 lea1Δ::KanMX4*	This work
TJY0545	LG1	*LEA1-HA$_3$:TRP1 DBP2-GFP:KanMX4 gcn5Δ::KanMX4 + [LEU2 GCN5]*	This work
TJY0546	LG1	*MSL1-HA$_3$::TRP1 gcn5Δ::KanMX4 + [LEU2 GCN5]*	This work
TJY3202	S288C	*LEA1-HA$_3$:TRP1 DBP2-GFP:NatMX H3::LEU2 H4::HIS3 +[Ycp50-copy II]*	This work
TJY0565	S288C	*WZ43 H3::LEU2 H4::HIS3+ [Ycp50-copy II]*	Zhang et al., 1998
TJY4307	LG1	*LEA1-HA$_3$:TRP1 DBP2-GFP:KanMX4 hos2Δ::KanMX4*	This work
TJY3753	LG1	*LEA1-HA$_3$:TRP1 DBP2-GFP:KanMX4 hos3Δ::NatMX4*	This work
TJY4309	LG1	*MSL1-HA$_3$:TRP1 DBP2-GFP:KanMX4 hos2Δ::KanMX4*	This work
TJY3755	LG1	*MSL1-HA$_3$:TRP1 DBP2-GFP:KanMX4 hos3Δ::NatMX4*	This work

Table 6.2: List of plasmids used in this study.

Plasmid Number	Plasmid Description	Plasmid backbone	Reference
pLP1641	**GCN5**	pRS 316	L. Pillus
pLP1520	**GCN5 KQL/AAA**	pRS 414	(Wang et al., 1998)
pLP1521	**GCN5 LKN/AAA**	pRS 414	(Wang et al., 1998)
pFG001	**GCN5**	pRS 414	This study
pLP1523	***GCN5***	pRS 315	L. Pillus
pFG003	**GCN5 KQL/AAA**	pRS 316	This study
pFG004	**GCN5 LKN/AAA**	pRS 316	This study
	CUS1	pRS 316	(Wells et al., 1996)
	CUS1-54	pRS 315	(Wells et al., 1996)
pLP1630	**KanMX to NatMX marker swap**		A. Tong, Boone lab Univ. of Toronto
Ycp50-copy II	**HHT2-HHF2**	pRS316	(Zhang et al.,1998)

Table 6.3: Sequences of primers used for ChIP.

Primer Name	Sequence
DBP2 –379 F	5’-CACGCTAGTATAGATACAGC-3’
DBP2 –91 R	5’-TATTTGAGCGTAGGACAGTC-3’
DBP2 104 F	5’-ACAGACCACAAGGCGGTAAC-3’
DBP2 346 R	5’-CGAAAGTGGTGATTGGCTTT-3’
DBP2 900 F	5’-TTGATGTGGTCTGCCACTTG-3’
DBP2 1078 R	5’-CGTTGTCTTGAGAGGCTGTTTC-3’
DBP2 1409 F	5’-TGACAACCATGATAGTACAGAAGAGAG-3’
DBP2 1558 R	5’-TTTCCGATACTCCCCATCG-3’
DBP2 1877 F	5’-ATGCCGTCATCCTTCTTGAC-3’
DBP2 1970 R	5’-TCGAACTTGGGATGCAACAG-3’
DBP2 2392 F	5’-TTCACCGAA CAA AAC AAA GG-3’
DBP2 2612 R	5’-CCACCATCTCTCTGCCTGTT- 3’
NTR VI_R F	5’-CAGGCAGTCCTTTCTATTTC-3’
NTR VI_R R	5’-GCTTGTTAACTCTCCGACAG-3’

Table 6.4: Sequences of primers used for *DBP2, ECM33, YRA1* ChIP.

Primer Name	Sequence
DBP2 –379RT F	GGCGTATTCCGTATTGAATGAT
DBP2 –91RT R	GTATAAGTTATTTGAGCGTAGGACAGTC
DBP2 104RT F	TCGGTGGTCGTTCCAATTAC
DBP2 346RT R	ATCTCACTGTCCGATCTGTCG
DBP2 900RT F	TTGATGTGGTCTGCCACTTG
DBP2 1078RT R	CGTTGTCTTGAGAGGCTGTTTC
DBP2 2392RT F	GTGGCTATGGCCGTAGAGG
DBP2 2612RT R	TAGTTTGAACGACCTCTGTTACCC
GFP 104RT F	CTGTCAGTGGAGAGGGTGAAG
GFP 346RT R	CTGGGTATCTTGAAAAGCATTG
ECM33 -296F	AATTTTCGGTAGCGTGCTTG
ECM33 -213R	TGCAAGAGAGGTCCGTTGAT
ECM33 +8F	ATTCAAGAACGCTTTGACTGCT
ECM33 +127R	TCGAGATTTGTGAGGAAAGAGG
ECM33 +454F	TCCGCTGCTTTGGCTAGTAT
ECM33 +560R	CACCGGTGATTTTCTTGATAGAG
ECM33 +1075F	TGGTGGTGCCATTGAAGTTAC
ECM33 + 1163R	GAGTCGAAGTTAGCACCACCTC
ECM33 +1296F	GCTGCTGTTGGCGTTGCTTACTAT
ECM33 +1421R	AGTGATGAACCAACCGTCTCA
PFY1 -504F	GAAGAGGAGGCTGCGTTTG
PFY-420R	CGAGAGGCGTTCTCTTCATC
PFY1 -316F	TCATCGAGGACGACGAAGAC
PFY1 -230R	CACTCCATTTCTTTGCGATTG
PFY1 282F	GCTGTTTGGGCTACTTCTGG
PFY1 365R	AACCAGCTGGATTGTCGAAG
YRA1 -494F	GGATTTCCCCGAACAGCTA
YRA1 -416R	ATTGCGCCCACAAGTTTCTA
YRA1 -242F	GTTGTTTTTCCACGGCTTTC
YRA1 -155R	AAAGCGAACGGAAGAAGTGA
YRA1 63F	TAGAGCCCGTGTCGGTGGTAC
YRA1 171R	CGTTTGGAGGTGCCCTAGTA
YRA1 338F	ACGAAAGGGGCCAATCTACT
YRA1 451R	ATCTTGATCTGCCTCCATCG
NTR VI_RRT F	CTAGTTGCACTAGGCGCAAAA
NTR VI_ RRT R	ACGCTTGCACTTGAAAAAGC

Table 6.5: *DBP2* and *ECM33* primers used for quantitative RT-PCR.

Primer Name	**Sequence**
DBP2 EI_2.2F	TGAGACAATGTTAGTCCA
DBP2 EI_2.2R	AGTACCAGTACCTGCTCTACC
DBP2 Exon2_2F	CGTTATCAACTACGATATGCCAGG
ECM33 I260F	TCTCGTTGAGATGGTTTTGG
ECM33 E2_515R	CACCGGTGATGGTCAAGTTAC
ECM33 E2_435F	CTGCCACTGCTACTGCTCAA

Appendix 1: Significance of co-transcriptional splicing for cell adaptation to environmental stress

Section A1.1: Introduction

In our studies of co-transcriptional splicing, *DBP2* and *ECM33* were used because they are particularly amenable to ChIP analysis. While we detect a reproducible increase in unspliced *DBP2* and *ECM33* in a *GCN5* deletion strain, we observe, as others have, that these genes are also post-transcriptionally spliced making it difficult to assess the full importance of Gcn5-mediated co-transcriptional splicing (Gornemann et al., 2005, Lacadie & Rosbash, 2005). It is also possible that cells become more dependent on co-transcriptional splicing under stress conditions in which rapid, efficient splice site recognition becomes more critical. Importantly, recent studies of genome-wide splicing have shown that under stress conditions, splicing becomes crucial for viability (Pleiss et al., 2007) and under the same stress conditions, SAGA becomes particularly important for gene expression (Huisinga & Pugh, 2004). Because of these, we suspect that we would detect important changes in cellular function when co-transcriptional splicing is abrogated under stress conditions. Therefore, we predict that stress conditions might reveal a particular dependence on Gcn5 for optimal co-transcriptional splicing.

To test this, we have undertaken experiments to look at: 1) The importance of introns in a cell's ability to response to changes. 2) The

importance of Gcn5-dependent co-transcriptional splicing of intron-containing genes under stress conditions. To do this, we have initiated collaboration with Jeff Hasty in Bioengineering to use a microfluidic platform to study Gcn5-dependent splicing in single cells under different environmental conditions.

In the last several years the use of microfludics has allowed for the study of gene expression in single cells that are grown in a dynamic environment (Bennett & Hasty, 2009, Bennett *et al.*, 2008). The microfluidic platform allows one to test how cells respond and grow in a microenvironment that mimics what the cell encounters when grown in culture. This platform allows for the manipulation and control of very small liquid volumes that can be periodically introduced to the cells as gradients. This microchemostat contains a peristaltic pump and micromechanical valves to add media, remove waste and, recover cells (Groisman *et al.*, 2005). To follow a protein of interest, genes are chromosomally tagged with a fluorescent tag and fluorescence intensity is monitored over time. The advantage of microfluidics over flow cytometry is that it allows for a more controlled environment and cells do not have to be fixed to visualize fluorescent signals. Additionally, flow cytometry measures an end-point and results in snapshots of gene expression patterns in individual cells (Longo & Hasty, 2006). Microfluidics on the other hand, allows for single-cell fluorescence data over many cellular generations (Cookson *et al.*, 2005).

Section A1.2: Results

Optimization studies to determine if introns affect the cell's ability to respond to environmental stress.

To test whether the presence of an intron is important for the cell's response to an environmental stress, *S. cerevisiae* were grown under several stress conditions, starting first with osmotic stress to examine Gcn5-dependent expression in single cells using microfluidics. Osmotic stress was chosen because there is evidence that under osmotic stress conditions, SAGA because particularly important for the expression of genes that respond to stress (Zapater et al., 2007). The experimental rationale was that we might observe differences in gene expression of an intron-containing gene (e.g. *DBP2-GFP)* in the presence and in the absence of the intron under environmental stress conditions. First, as proof of principle, we examined expression of the protein encoded by *DBP2:GFP* to determine what happens to Dbp2-GFP fluorescence intensity over time in response to an environmental stress.

Cells were exposed to caffeine for a three-hour pulse and then allowed to recover in non-stress media for 3 hours. Caffeine, which destabilizes the cell wall, was chosen because deletion of several components of the SAGA complex result in increased caffeine sensitivity (Hampsey, 1997a, Larschan & Winston, 2005, Sterner et al., 1999, Sterner *et al.*, 2002b). This cycle was repeated for a span of 24 hours. Fluorescence intensity of Dbp2-GFP was measured for the entire length of time. In order to measure GFP fluorescence in the presence of caffeine, a rhodamine dye was added to the stress media that allowed for the

tracking of the caffeine pulses over time. Fluorescence intensity for an individual cells were calculated using NIH ImageJ and plotted against the fluorescence of the caffeine pulse (Figure A1.1). When cells are exposed to a caffeine pulse, expression of Dbp2-GFP decreases and expression increases when caffeine is removed from the media. From these results we concluded that Dbp2-GFP fluorescence was affected by the addition of caffeine.

However, the time allotted in non-stress media was not sufficient to recover fluorescence to levels before stress. With this in mind, we decided to optimize the duration of the stress pulse and recovery after pulse. These experiments served the purpose of demonstrating that Dbp2-GFP was not so stable as to preclude observation of fluctuations.

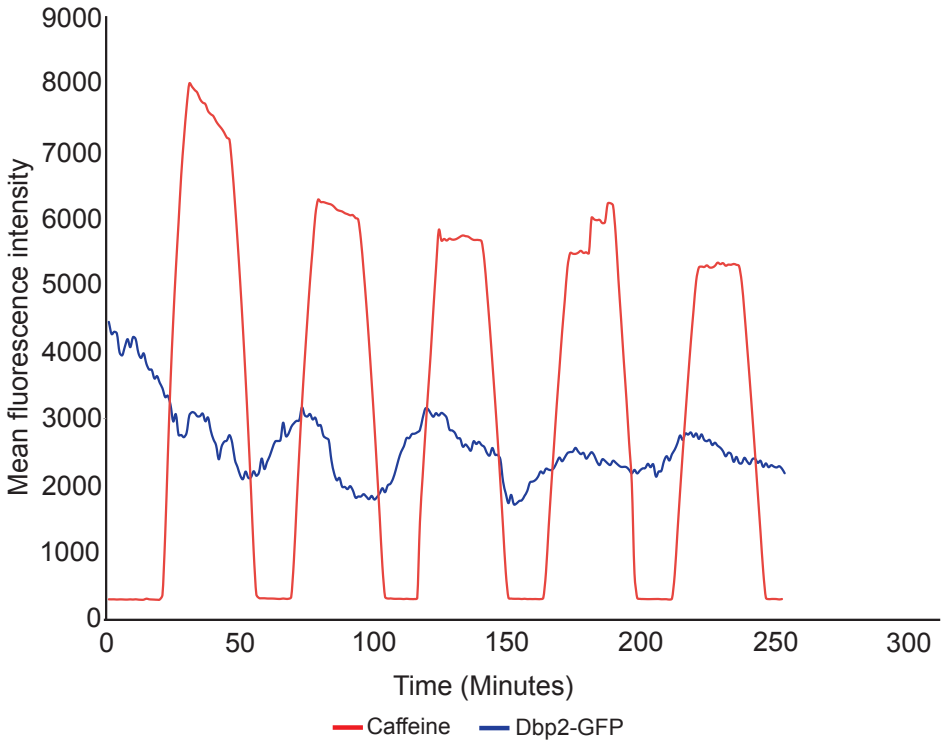

Figure A1.1: Dbp2-GFP fluorescence changes over time when cells were treated with 9mM caffeine.

Microfluidic analysis of Dbp2-GFP fluorescence over a 300 minute time period. Images were captured every five minutes and images were analyzed with Image J software. Refer to appendix section 1.4, material and methods for more details. Red line represents the pulses of caffeine containing medium. Blue line represents Dbp2-GFP fluorescence.

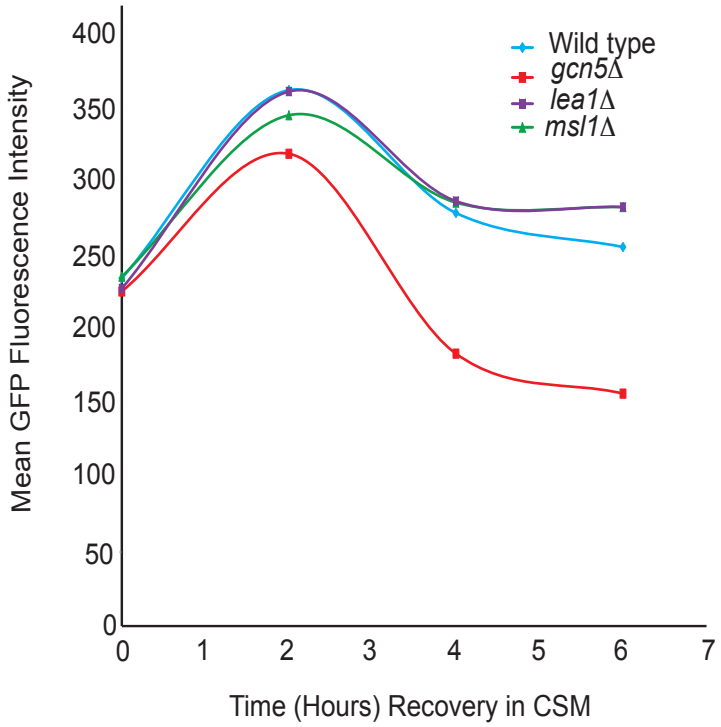

Figure A1.2: Recovery of GFP expression occurs two hours post stress exposure. Flow cytometry analysis of Dbp2-GFP expression post stress exposure in synthetic complete medium. A) Analysis of Dbp2-GFP expression in wild type, *gcn5*Δ, *msl1*Δ and *lea1*Δ after exposure to 9mM Caffeine medium and a 6 hour recovery in synthetic complete medium by flow cytometry. Samples were collected at every two-hour time point during recovery. Data are represented as mean GFP fluorescence over time. Data has been gated.

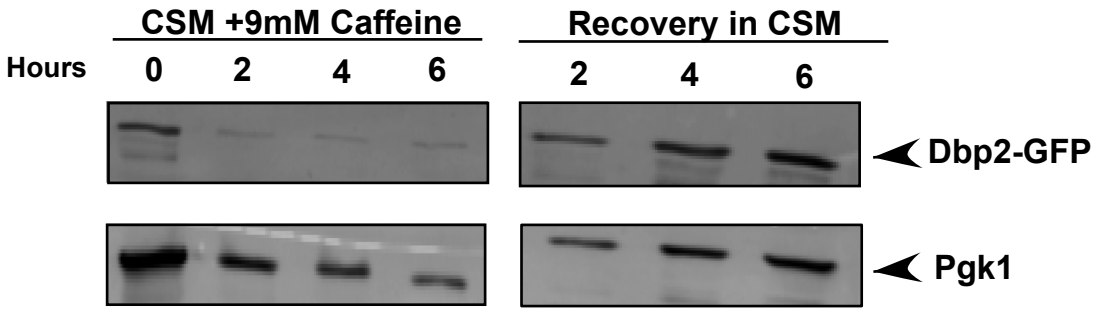

Figure A1.3: Dbp2-GFP fluorescence is recovered after two hours of growth in CSM medium following stress.

Western blot analysis of Dbp2-GFP expression after eight hours of growth in 9mM Caffeine containing medium and recovery in non-stress medium for six hours. Samples were collected every two hours and prepared as described in materials and methods. Samples were separated by SDS-PAGE and probed with the following antibodies; anti-GFP (Roche) and anti-Pgk1 (Invitrogen) as a loading control.

To optimize the stress pulse, a time course was performed in which cells were grown in the presence of caffeine, and samples were collected every two hours for western blot analysis and FACS analysis. This allowed us to determine the expression of Dbp2 and fluorescence intensity over an eight-hour time course (Figure A1.2). In order to measure the cells recovery, the stress media was washed out (after eight-hour exposure) and replaced with non-stress media. Then samples were taken every two hours for an eight-hour time course. These samples were also subjected to western blot analysis and FACS analysis to determine the amount of GFP expression and fluorescence intensity, respectively (Figure A1.3). We observed that after a 8-hour exposure to caffeine, Dbp2 expression decreased as detected by both FACS and western blot analysis. When cells were in the absence of stress, increased expression of Dbp2 could be detected after two hours (Figures A1.2 and A1.3, respectively). From these optimization studies, we determined that after two hours in stress media the expression of Dbp2-GFP went down and after a two-hour recovery in non-stress media, Dbp2-GFP fluorescence was back to pre-stress levels.

With this information in hand, we will next analyze GFP expression in a strain in which Dbp2-GFP has been deleted of its intron. We will be eager to see if the profile of response to changes in environmental conditions in the absence of the intron. In particular, we will be able to measure both the amplitude and period of the response. Preliminary attempts to delete the intron using the delitto perfectto method (Storici *et al.*, 2001) have been unsuccessful. The advantage of using this method will allow us to remove the intron using oligonucleotides with

out a use of a selectable marker. Oligo design, transformation of the oligos, are just a few of the steps that need troubleshooting to get this system up and running.

Section A1.3: Future studies: Analysis of a role for co-transcriptional splicing in cellular response to environmental changes

Although were we able to detect an increase in unspliced *DBP2* and *ECM33* messages, these genes can also be post-transcriptionally spliced. Others have shown that some yeast messages are post-transcriptionally spliced (Tardiff *et al.*, 2006). This raises the question as to whether co-transcriptional splicing might be important for a rapid response to changing conditions.

Since we know that deletion of *GCN5* abrogates co-transcriptional spliceosome assembly, we can analyze the cells' response to changing environmental conditions when *GCN5* is deleted (loss of co-transcriptional splicing). Gcn5 has been characterized to play a critical role in transcription. If deletion of *GCN5* led to a change in the cells' ability to response to stress, we would like to distinguish if this effect is due to Gcn5's role in other gene expression events (e.g. transcription) or splicing. To address this, we will examine Dbp2-GFP expression in the presence and in the absence of its intron. Results from these experiments will give us a clue as to why co-transcriptional splicing is necessary for environmental stress response.

For these preliminary studies, we used Dbp2-GFP because this gene was used for our ChIP studies, and it already had a GFP tag. Thus, we realize that this may not be the ideal gene to use for these studies. Therefore, we will examine splicing in the presence and absence of stress by microarray. Using the method, we will be able to identify intron-containing genes that respond to stress. Once these genes are identified, the intron will be deleted and then examine the cells' response to stress. Additionally, we will also examine expression in the absence of *GCN5* and in the presence and absence of the intron. If changes in the ability of the cell to response to environmental stress under any of these conditions are detected, we can confirm this effect on co-transcriptional splicing by ChIP.

Using these strains will allow us to determine how the cell responds to environmental stress when splicing has been compromised. If we detect a difference in the way cells respond to environmental stress due to changes in co-transcriptional splicing, this would be the first evidence for the importance of co-transcriptional splicing in yeast.

Section A1.4: Materials and Methods

Microfluidics

Cells containing *DBP2:GFP* were grown in synthetic complete (SC) medium overnight at 30^{o}C. The following day, cells were subcultured into 5ml fresh SC medium and grown at 30^{o}C until an O.D.600 of 0.3-0.5 was obtained. Cells were then mounted onto a microfluidic chip that allowed for a dynamic-controlled mixing environment. Images were taken every 5 minutes for a 24-hour time period. Caffeine medium contained sulphorhodamine 101 (Sigma) to ensure correct waveform generation. An upstream fluidic switch controlled the input of the medium into the chamber by mixing the flows on stress and non-stress media (Bennett et al., 2008). The mixing ratio of the two media was software-controlled that produced time-varying waveforms consistently (Bennett et al., 2008).

The resulting images were quantified using ImageJ (NIH) for fluorescence intensity over time and pulse of stress medium.

Stress Time Course and Flow Cytometry

Cells were grown overnight in synthetic complete medium at 30^{o}C. The following day, cells were subcultured into SC medium with 9mM caffeine or 1.2M NaCl. Cells were grown for 6 hours at 30^{o}C and 2-hour time points (1ml) were collected for flow cytometry analysis and protein immunoblot. After six hours in stress conditions, the stress-containing medium was washed out twice with 20ml of dH_20. Then, cell pellets were resuspended in SC medium and grown for

another 6 hours at 30^{o}C and 2-hour time points (1ml) were taken for flow cytometry analysis and protein immunoblot.

For flow cytometry, time point samples were spun down for for 30 seconds at 13K rpm. Supernatant was discarded and cell pellet was resuspended in 1X PBS and GFP expression was measured using FACS Calibur (BD). Data were analyzed using FlowJo (Tree Star) software and data is represented as GFP mean intensity over time.

For protein immunoblot, samples were treated as described in (Hossain *et al.*, 2009). Proteins were separated on a 10% SDS-PAGE and probed for GFP using anti-GFP (Roche) and anti-Pgk1 (Invitrogen) as a loading control.

References

Allemand, E., E. Batsche & C. Muchardt, (2008) Splicing, transcription, and chromatin: a menage a trois. *Curr Opin Genet Dev* **18**: 145-151.

Andersson, R., S. Enroth, A. Rada-Iglesias, C. Wadelius & J. Komorowski, (2009) Nucleosomes are well positioned in exons and carry characteristic histone modifications. *Genome Res* **19**: 1732-1741.

Ares, M., Jr., (1986) U2 RNA from yeast is unexpectedly large and contains homology to vertebrate U4, U5, and U6 small nuclear RNAs. *Cell* **47**: 49-59.

Baker, S. P. & P. A. Grant, (2007) The SAGA continues: expanding the cellular role of a transcriptional co-activator complex. *Oncogene* **26**: 5329-5340.

Balasubramanian, R., M. G. Pray-Grant, W. Selleck, P. A. Grant & S. Tan, (2002) Role of the Ada2 and Ada3 transcriptional coactivators in histone acetylation. *J Biol Chem* **277**: 7989-7995.

Bartels, C., C. Klatt, R. Luhrmann & P. Fabrizio, (2002) The ribosomal translocase homologue Snu114p is involved in unwinding U4/U6 RNA during activation of the spliceosome. *EMBO Rep* **3**: 875-880.

Bartels, C., H. Urlaub, R. Luhrmann & P. Fabrizio, (2003) Mutagenesis suggests several roles of Snu114p in pre-mRNA splicing. *J Biol Chem* **278**: 28324-28334.

Batsche, E., M. Yaniv & C. Muchardt, (2006) The human SWI/SNF subunit Brm is a regulator of alternative splicing. *Nat Struct Mol Biol* **13**: 22-29.

Bauren, G., W. Q. Jiang, K. Bernholm, F. Gu & L. Wieslander, (1996) Demonstration of a dynamic, transcription-dependent organization of pre-mRNA splicing factors in polytene nuclei. *J Cell Biol* **133**: 929-941.

Bauren, G. & L. Wieslander, (1994) Splicing of Balbiani ring 1 gene pre-mRNA occurs simultaneously with transcription. *Cell* **76**: 183-192.

Belotserkovskaya, R., D. E. Sterner, M. Deng, M. H. Sayre, P. M. Lieberman & S. L. Berger, (2000) Inhibition of TATA-binding protein function by SAGA subunits Spt3 and Spt8 at Gcn4-activated promoters. *Mol Cell Biol* **20**: 634-647.

Bennett, M. R. & J. Hasty, (2009) Microfluidic devices for measuring gene network dynamics in single cells. *Nat Rev Genet* **10**: 628-638.

Bennett, M. R., W. L. Pang, N. A. Ostroff, B. L. Baumgartner, S. Nayak, L. S. Tsimring & J. Hasty, (2008) Metabolic gene regulation in a dynamically changing environment. *Nature* **454**: 1119-1122.

Beyer, A. L. & Y. N. Osheim, (1988) Splice site selection, rate of splicing, and alternative splicing on nascent transcripts. *Genes Dev* **2**: 754-765.

Beyer, A. L. & Y. N. Osheim, (1991) Visualization of RNA transcription and processing. *Semin Cell Biol* **2**: 131-140.

Biswas, D., A. N. Imbalzano, P. Eriksson, Y. Yu & D. J. Stillman, (2004) Role for Nhp6, Gcn5, and the Swi/Snf complex in stimulating formation of the TATA-binding protein-TFIIA-DNA complex. *Mol Cell Biol* **24**: 8312-8321.

Black, D. L., (2000) Protein diversity from alternative splicing: a challenge for bioinformatics and post-genome biology. *Cell* **103**: 367-370.

Brenner, T. J. & C. Guthrie, (2006) Assembly of Snu114 into U5 snRNP requires Prp8 and a functional GTPase domain. *RNA* **12**: 862-871.

Bres, V., N. Gomes, L. Pickle & K. A. Jones, (2005) A human splicing factor, SKIP, associates with P-TEFb and enhances transcription elongation by HIV-1 Tat. *Genes Dev* **19**: 1211-1226.

Brookes, E. & A. Pombo, (2009) Modifications of RNA polymerase II are pivotal in regulating gene expression states. *EMBO Rep* **10**: 1213-1219.

Brow, D. A., (2002) Allosteric cascade of spliceosome activation. *Annu Rev Genet* **36**: 333-360.

Burke, D., D. Dawson, T. Stearns & Cold Spring Harbor Laboratory., (2000) *Methods in yeast genetics : a Cold Spring Harbor Laboratory course manual,* p. xvii, 205 p. Cold Spring Harbor Laboratory Press, Plainview, N.Y.

Candau, R. & S. L. Berger, (1996) Structural and functional analysis of yeast putative adaptors. Evidence for an adaptor complex in vivo. *J Biol Chem* **271**: 5237-5245.

Candau, R., J. X. Zhou, C. D. Allis & S. L. Berger, (1997) Histone acetyltransferase activity and interaction with ADA2 are critical for GCN5 function in vivo. *Embo J* **16**: 555-565.

Carmen, A. A., P. R. Griffin, J. R. Calaycay, S. E. Rundlett, Y. Suka & M. Grunstein, (1999) Yeast HOS3 forms a novel trichostatin A-insensitive

homodimer with intrinsic histone deacetylase activity. *Proc Natl Acad Sci U S A* **96**: 12356-12361.

Caspary, F. & B. Seraphin, (1998) The yeast U2A'/U2B complex is required for pre-spliceosome formation. *Embo J* **17**: 6348-6358.

Cech, T. R., N. K. Tanner, I. Tinoco, Jr., B. R. Weir, M. Zuker & P. S. Perlman, (1983) Secondary structure of the Tetrahymena ribosomal RNA intervening sequence: structural homology with fungal mitochondrial intervening sequences. *Proc Natl Acad Sci U S A* **80**: 3903-3907.

Chan, S. P., D. I. Kao, W. Y. Tsai & S. C. Cheng, (2003) The Prp19p-associated complex in spliceosome activation. *Science* **302**: 279-282.

Chen, J. Y., L. Stands, J. P. Staley, R. R. Jackups, Jr., L. J. Latus & T. H. Chang, (2001) Specific alterations of U1-C protein or U1 small nuclear RNA can eliminate the requirement of Prp28p, an essential DEAD box splicing factor. *Mol Cell* **7**: 227-232.

Chen, M. & J. L. Manley, (2009) Mechanisms of alternative splicing regulation: insights from molecular and genomics approaches. *Nat Rev Mol Cell Biol* **10**: 741-754.

Cheng, S. C. & J. Abelson, (1987) Spliceosome assembly in yeast. *Genes Dev* **1**: 1014-1027.

Choi, J. K., J. B. Bae, J. Lyu, T. Y. Kim & Y. J. Kim, (2009) Nucleosome deposition and DNA methylation at coding region boundaries. *Genome Biol* **10**: R89.

Cookson, S., N. Ostroff, W. L. Pang, D. Volfson & J. Hasty, (2005) Monitoring dynamics of single-cell gene expression over multiple cell cycles. *Mol Syst Biol* **1**: 2005 0024.

Cote, J., M. J. Simard & B. Chabot, (1999) An element in the 5' common exon of the NCAM alternative splicing unit interacts with SR proteins and modulates 5' splice site selection. *Nucleic Acids Res* **27**: 2529-2537.

Dai, J., E. M. Hyland, D. S. Yuan, H. Huang, J. S. Bader & J. D. Boeke, (2008) Probing nucleosome function: a highly versatile library of synthetic histone H3 and H4 mutants. *Cell* **134**: 1066-1078.

Damgaard, C. K., S. Kahns, S. Lykke-Andersen, A. L. Nielsen, T. H. Jensen & J. Kjems, (2008) A 5' splice site enhances the recruitment of basal transcription initiation factors in vivo. *Mol Cell* **29**: 271-278.

de la Mata, M., C. R. Alonso, S. Kadener, J. P. Fededa, M. Blaustein, F. Pelisch, P. Cramer, D. Bentley & A. R. Kornblihtt, (2003) A slow RNA polymerase II affects alternative splicing in vivo. *Mol Cell* **12**: 525-532.

Dellaire, G., E. M. Makarov, J. J. Cowger, D. Longman, H. G. Sutherland, R. Luhrmann, J. Torchia & W. A. Bickmore, (2002) Mammalian PRP4 kinase copurifies and interacts with components of both the U5 snRNP and the N-CoR deacetylase complexes. *Mol Cell Biol* **22**: 5141-5156.

Dybkov, O., C. L. Will, J. Deckert, N. Behzadnia, K. Hartmuth & R. Luhrmann, (2006) U2 snRNA-protein contacts in purified human 17S U2 snRNPs and in spliceosomal A and B complexes. *Mol Cell Biol* **26**: 2803-2816.

Eisenmann, D. M., K. M. Arndt, S. L. Ricupero, J. W. Rooney & F. Winston, (1992) SPT3 interacts with TFIID to allow normal transcription in Saccharomyces cerevisiae. *Genes Dev* **6**: 1319-1331.

Eperon, I. C., O. V. Makarova, A. Mayeda, S. H. Munroe, J. F. Caceres, D. G. Hayward & A. R. Krainer, (2000) Selection of alternative 5' splice sites: role of U1 snRNP and models for the antagonistic effects of SF2/ASF and hnRNP A1. *Mol Cell Biol* **20**: 8303-8318.

Faustino, N. A. & T. A. Cooper, (2003) Pre-mRNA splicing and human disease. *Genes Dev* **17**: 419-437.

Feaver, W. J., J. Q. Svejstrup, N. L. Henry & R. D. Kornberg, (1994) Relationship of CDK-activating kinase and RNA polymerase II CTD kinase TFIIH/TFIIK. *Cell* **79**: 1103-1109.

Fong, Y. W. a. Q. Z., (2001) Stimulatory effect of splicing factors on tracriptional elongation. *Nature* **414**: 929-933.

Fromont-Racine, M., J. C. Rain & P. Legrain, (1997) Toward a functional analysis of the yeast genome through exhaustive two-hybrid screens. *Nat Genet* **16**: 277-282.

Ginsburg, D. S., C. K. Govind & A. G. Hinnebusch, (2009) NuA4 lysine acetyltransferase Esa1 is targeted to coding regions and stimulates transcription elongation with Gcn5. *Mol Cell Biol* **29**: 6473-6487.

Goossens, A., J. Forment & R. Serrano, (2002) Involvement of Nst1p/YNL091w and Msl1p, a U2B'' splicing factor, in Saccharomyces cerevisiae salt tolerance. *Yeast* **19**: 193-202.

Gornemann, J., K. M. Kotovic, K. Hujer & K. M. Neugebauer, (2005) Cotranscriptional spliceosome assembly occurs in a stepwise fashion and requires the cap binding complex. *Mol Cell* **19**: 53-63.

Govind, C. K., F. Zhang, H. Qiu, K. Hofmeyer & A. G. Hinnebusch, (2007) Gcn5 promotes acetylation, eviction, and methylation of nucleosomes in transcribed coding regions. *Mol Cell* **25**: 31-42.

Grant, P. A., A. Eberharter, S. John, R. G. Cook, B. M. Turner & J. L. Workman, (1999) Expanded lysine acetylation specificity of Gcn5 in native complexes. *J Biol Chem* **274**: 5895-5900.

Grant, P. A., L. Duggan, et al., (1997) Yeast Gcn5 functions in two multisubunit complexes to acetylate nucleosomal histones: characterization of an Ada complex and the SAGA (Spt/Ada) complex. *Genes and Development* **11**: 1640-1650.

Groisman, A., C. Lobo, H. Cho, J. K. Campbell, Y. S. Dufour, A. M. Stevens & A. Levchenko, (2005) A microfluidic chemostat for experiments with bacterial and yeast cells. *Nat Methods* **2**: 685-689.

Gunderson, F. Q. & T. L. Johnson, (2009) Acetylation by the transcriptional coactivator Gcn5 plays a novel role in co-transcriptional spliceosome assembly. *PLoS Genet* **5**: e1000682.

Guthrie, C., H. Nashimoto & M. Nomura, (1969) Studies on the assembly of ribosomes in vivo. *Cold Spring Harb Symp Quant Biol* **34**: 69-75.

Hampsey, M., (1997a) A review of phenotypes in Saccharomyces cerevisiae. *Yeast* **13**: 1099-1133.

Hampsey, M., (1997b) A SAGA of histone acetylation and gene expression. *Trends Genet* **13**: 427-429.

Hampsey, M., (1998) Molecular genetics of the RNA polymerase II general transcriptional machinery. *Microbiol Mol Biol Rev* **62**: 465-503.

Hassan, A. H., S. Awad, Z. Al-Natour, S. Othman, F. Mustafa & T. A. Rizvi, (2007) Selective recognition of acetylated histones by bromodomains in transcriptional co-activators. *Biochem J* **402**: 125-133.

Hawkins, J. D., (1988) A survey on intron and exon lengths. *Nucleic Acids Res* **16**: 9893-9908.

Henry, K. W., A. Wyce, W. S. Lo, L. J. Duggan, N. C. Emre, C. F. Kao, L. Pillus, A. Shilatifard, M. A. Osley & S. L. Berger, (2003) Transcriptional activation

via sequential histone H2B ubiquitylation and deubiquitylation, mediated by SAGA-associated Ubp8. *Genes Dev* **17**: 2648-2663.

Holstege, F. C., E. G. Jennings, J. J. Wyrick, T. I. Lee, C. J. Hengartner, M. R. Green, T. R. Golub, E. S. Lander & R. A. Young, (1998) Dissecting the regulatory circuitry of a eukaryotic genome. *Cell* **95**: 717-728.

Horiuchi, J., N. Silverman, G. A. Marcus & L. Guarente, (1995) ADA3, a putative transcriptional adaptor, consists of two separable domains and interacts with ADA2 and GCN5 in a trimeric complex. *Mol Cell Biol* **15**: 1203-1209.

Hossain, M. A., J. M. Claggett, T. Nguyen & T. L. Johnson, (2009) The cap binding complex influences H2B ubiquitination by facilitating splicing of the SUS1 pre-mRNA. *RNA* **15**: 1515-1527.

Howe, K. J., C. M. Kane & M. Ares, Jr., (2003) Perturbation of transcription elongation influences the fidelity of internal exon inclusion in Saccharomyces cerevisiae. *RNA* **9**: 993-1006.

Huang, S. & D. L. Spector, (1996) Intron-dependent recruitment of pre-mRNA splicing factors to sites of transcription. *J Cell Biol* **133**: 719-732.

Huisinga, K. L. & B. F. Pugh, (2004) A genome-wide housekeeping role for TFIID and a highly regulated stress-related role for SAGA in Saccharomyces cerevisiae. *Mol Cell* **13**: 573-585.

Huppler, A., L. J. Nikstad, A. M. Allmann, D. A. Brow & S. E. Butcher, (2002) Metal binding and base ionization in the U6 RNA intramolecular stem-loop structure. *Nat Struct Biol* **9**: 431-435.

Imoberdorf, R. M., I. Topalidou & M. Strubin, (2006) A role for gcn5-mediated global histone acetylation in transcriptional regulation. *Mol Cell Biol* **26**: 1610-1616.

Ingvarsdottir, K., N. J. Krogan, N. C. Emre, A. Wyce, N. J. Thompson, A. Emili, T. R. Hughes, J. F. Greenblatt & S. L. Berger, (2005) H2B ubiquitin protease Ubp8 and Sgf11 constitute a discrete functional module within the Saccharomyces cerevisiae SAGA complex. *Mol Cell Biol* **25**: 1162-1172.

Jankowsky, E., C. H. Gross, S. Shuman & A. M. Pyle, (2001) Active disruption of an RNA-protein interaction by a DExH/D RNA helicase. *Science* **291**: 121-125.

Johnson, T. L. & J. Abelson, (2001) Characterization of U4 and U6 interactions with the 5' splice site using a S. cerevisiae in vitro trans-splicing system. *Genes Dev* **15**: 1957-1970.

Johnsson, A., M. Durand-Dubief, Y. Xue-Franzen, M. Ronnerblad, K. Ekwall & A. Wright, (2009) HAT-HDAC interplay modulates global histone H3K14 acetylation in gene-coding regions during stress. *EMBO Rep* **10**: 1009-1014.

Kalari, K. R., M. Casavant, T. B. Bair, H. L. Keen, J. M. Comeron, T. L. Casavant & T. E. Scheetz, (2006) First exons and introns--a survey of GC content and gene structure in the human genome. *In Silico Biol* **6**: 237-242.

Kohler, A., P. Pascual-Garcia, A. Llopis, M. Zapater, F. Posas, E. Hurt & S. Rodriguez-Navarro, (2006) The mRNA export factor Sus1 is involved in Spt/Ada/Gcn5 acetyltransferase-mediated H2B deubiquitinylation through its interaction with Ubp8 and Sgf11. *Mol Biol Cell* **17**: 4228-4236.

Kohler, A., E. Zimmerman, M. Schneider, E. Hurt & N. Zheng, (2010) Structural basis for assembly and activation of the heterotetrameric SAGA histone H2B deubiquitinase module. *Cell* **141**: 606-617.

Kolasinska-Zwierz, P., T. Down, I. Latorre, T. Liu, X. S. Liu & J. Ahringer, (2009) Differential chromatin marking of introns and expressed exons by H3K36me3. *Nat Genet* **41**: 376-381.

Konarska, M. M. & P. A. Sharp, (1987) Interactions between small nuclear ribonucleoprotein particles in formation of spliceosomes. *Cell* **49**: 763-774.

Konarska, M. M., J. Vilardell & C. C. Query, (2006) Repositioning of the reaction intermediate within the catalytic center of the spliceosome. *Mol Cell* **21**: 543-553.

Konforti, B. B., M. J. Koziolkiewicz & M. M. Konarska, (1993) Disruption of base pairing between the 5' splice site and the 5' end of U1 snRNA is required for spliceosome assembly. *Cell* **75**: 863-873.

Kornblihtt, A. R., M. de la Mata, J. P. Fededa, M. J. Munoz & G. Nogues, (2004) Multiple links between transcription and splicing. *RNA* **10**: 1489-1498.

Kotovic, K. M., D. Lockshon, L. Boric & K. M. Neugebauer, (2003) Cotranscriptional recruitment of the U1 snRNP to intron-containing genes in yeast. *Mol Cell Biol* **23**: 5768-5779.

Kristjuhan, A., and Svejstrup, J.Q., (2004) Evidence for distinct mechanisms facilitating transcript elongation through chromatin i*in vivo*. *The EMBO Journal* **23**: 4243-4252.

Kristjuhan, A., Walker, J., Suka, N., Grunstein, M., Roberts, D., Cairns, B.R., and Svejstrup, J.Q., (2002) Transcriptional Inhibition of Genes with Severe Histone H3 Hypoacetylation in the Coding Region. *Molecular Cell* **10**: 925-933.

Kuo, M. H., J.E. Brownell, et al., (1996) Transcription-linked acetylation by Gcn5p of histones H3 and H4 specific lysines. *Nature* **383**: 269-272.

Kuo, M. H., J. Zhou, P. Jambeck, M. E. Churchill & C. D. Allis, (1998) Histone acetyltransferase activity of yeast Gcn5p is required for the activation of target genes in vivo. *Genes Dev* **12**: 627-639.

Kwek, K. Y., S. Murphy, A. Furger, B. Thomas, W. O'Gorman, H. Kimura, N. J. Proudfoot & A. Akoulitchev, (2002) U1 snRNA associates with TFIIH and regulates transcriptional initiation. *Nat Struct Biol* **9**: 800-805.

Lacadie, S. A. & M. Rosbash, (2005) Cotranscriptional spliceosome assembly dynamics and the role of U1 snRNA:5'ss base pairing in yeast. *Mol Cell* **19**: 65-75.

Lacadie, S. A., D. F. Tardiff, S. Kadener & M. Rosbash, (2006) In vivo commitment to yeast cotranscriptional splicing is sensitive to transcription elongation mutants. *Genes Dev* **20**: 2055-2066.

Lamond, A. I., M. M. Konarska, P. J. Grabowski & P. A. Sharp, (1988) Spliceosome assembly involves the binding and release of U4 small nuclear ribonucleoprotein. *Proc Natl Acad Sci U S A* **85**: 411-415.

Laprade, L., D. Rose & F. Winston, (2007) Characterization of new Spt3 and TATA-binding protein mutants of Saccharomyces cerevisiae: Spt3 TBP allele-specific interactions and bypass of Spt8. *Genetics* **177**: 2007-2017.

Larschan, E. & F. Winston, (2005) The Saccharomyces cerevisiae Srb8-Srb11 complex functions with the SAGA complex during Gal4-activated transcription. *Mol Cell Biol* **25**: 114-123.

Li, S. & M. A. Shogren-Knaak, (2009) The Gcn5 bromodomain of the SAGA complex facilitates cooperative and cross-tail acetylation of nucleosomes. *J Biol Chem* **284**: 9411-9417.

Liao, X. C., H. V. Colot, Y. Wang & M. Rosbash, (1992) Requirements for U2 snRNP addition to yeast pre-mRNA. *Nucleic Acids Res* **20**: 4237-4245.

Lim, S. R. & K. J. Hertel, (2004) Commitment to splice site pairing coincides with A complex formation. *Mol Cell* **15**: 477-483.

Lin, S., G. Coutinho-Mansfield, D. Wang, S. Pandit & X. D. Fu, (2008a) The splicing factor SC35 has an active role in transcriptional elongation. *Nat Struct Mol Biol* **15**: 819-826.

Lin, Y. Y., Y. Qi, J. Y. Lu, X. Pan, D. S. Yuan, Y. Zhao, J. S. Bader & J. D. Boeke, (2008b) A comprehensive synthetic genetic interaction network governing yeast histone acetylation and deacetylation. *Genes Dev* **22**: 2062-2074.

Listerman, I., A. K. Sapra & K. M. Neugebauer, (2006) Cotranscriptional coupling of splicing factor recruitment and precursor messenger RNA splicing in mammalian cells. *Nat Struct Mol Biol* **13**: 815-822.

Longo, D. & J. Hasty, (2006) Dynamics of single-cell gene expression. *Mol Syst Biol* **2**: 64.

Longtine, M. S., A. McKenzie, 3rd, D. J. Demarini, N. G. Shah, A. Wach, A. Brachat, P. Philippsen & J. R. Pringle, (1998) Additional modules for versatile and economical PCR-based gene deletion and modification in Saccharomyces cerevisiae. *Yeast* **14**: 953-961.

Lopez-Bigas, N., B. Audit, C. Ouzounis, G. Parra & R. Guigo, (2005) Are splicing mutations the most frequent cause of hereditary disease? *FEBS Lett* **579**: 1900-1903.

Luco, R. F., Q. Pan, K. Tominaga, B. J. Blencowe, O. M. Pereira-Smith & T. Misteli, (2010) Regulation of alternative splicing by histone modifications. *Science* **327**: 996-1000.

MacDonald, V. E. & L. J. Howe, (2009) Histone acetylation: where to go and how to get there. *Epigenetics* **4**: 139-143.

Maeder, C., A. K. Kutach & C. Guthrie, (2009) ATP-dependent unwinding of U4/U6 snRNAs by the Brr2 helicase requires the C terminus of Prp8. *Nat Struct Mol Biol* **16**: 42-48.

Maniatis, T., and Reed, R., (2002) An extensive network of coupling among gene expression machines. *Nature* **41**: 499-506.

Marcus, G. A., N. Silverman, S. L. Berger, J. Horiuchi & L. Guarente, (1994) Functional similarity and physical association between GCN5 and ADA2: putative transcriptional adaptors. *EMBO J* **13**: 4807-4815.

Marks, P., R. A. Rifkind, V. M. Richon, R. Breslow, T. Miller & W. K. Kelly, (2001) Histone deacetylases and cancer: causes and therapies. *Nat Rev Cancer* **1**: 194-202.

Martinez, E., Palhan, V.B., Tjernberg, A., Lymar, E.S., Gamper, A.M., Kundu, T.K., Chiat, B.T., and Roeder, R.G., (2001) Human STAGA Complex Is a Chromatin- Acetylating Transcription Coactivator That Interacts with Pre-mRNA Splicing and DNA-Damage-Binding Factors In Vivo. *Molecular and Cellular Biology* **21**: 6782-6795.

Mohibullah, N. & S. Hahn, (2008) Site-specific cross-linking of TBP in vivo and in vitro reveals a direct functional interaction with the SAGA subunit Spt3. *Genes Dev* **22**: 2994-3006.

Munoz, M. J., M. de la Mata & A. R. Kornblihtt, (2010) The carboxy terminal domain of RNA polymerase II and alternative splicing. *Trends Biochem Sci*.

Nahkuri, S., R. J. Taft & J. S. Mattick, (2009) Nucleosomes are preferentially positioned at exons in somatic and sperm cells. *Cell Cycle* **8**: 3420-3424.

Navaratnam, D. S., T. J. Bell, T. D. Tu, E. L. Cohen & J. C. Oberholtzer, (1997) Differential distribution of Ca2+-activated K+ channel splice variants among hair cells along the tonotopic axis of the chick cochlea. *Neuron* **19**: 1077-1085.

Nilsen, T. W. & B. R. Graveley, (2010) Expansion of the eukaryotic proteome by alternative splicing. *Nature* **463**: 457-463.

O'Mullane, L. & I. C. Eperon, (1998) The pre-mRNA 5' cap determines whether U6 small nuclear RNA succeeds U1 small nuclear ribonucleoprotein particle at 5' splice sites. *Mol Cell Biol* **18**: 7510-7520.

Orphanides, G., T. Lagrange & D. Reinberg, (1996) The general transcription factors of RNA polymerase II. *Genes Dev* **10**: 2657-2683.

Osheim, Y. N., O. L. Miller, Jr. & A. L. Beyer, (1985) RNP particles at splice junction sequences on Drosophila chorion transcripts. *Cell* **43**: 143-151.

Pan, Q., O. Shai, L. J. Lee, B. J. Frey & B. J. Blencowe, (2008) Deep surveying of alternative splicing complexity in the human transcriptome by high-throughput sequencing. *Nat Genet* **40**: 1413-1415.

Pandya-Jones, A. & D. L. Black, (2009) Co-transcriptional splicing of constitutive and alternative exons. *RNA* **15**: 1896-1908.

Parker, R., P. G. Siliciano & C. Guthrie, (1987) Recognition of the TACTAAC box during mRNA splicing in yeast involves base pairing to the U2-like snRNA. *Cell* **49**: 229-239.

Pleiss, J. A., G. B. Whitworth, M. Bergkessel & C. Guthrie, (2007) Rapid, transcript-specific changes in splicing in response to environmental stress. *Mol Cell* **27**: 928-937.

Pray-Grant, M. G., D. Schieltz, S. J. McMahon, J. M. Wood, E. L. Kennedy, R. G. Cook, J. L. Workman, J. R. Yates, 3rd & P. A. Grant, (2002) The novel SLIK histone acetyltransferase complex functions in the yeast retrograde response pathway. *Mol Cell Biol* **22**: 8774-8786.

Prochasson, P., K. E. Neely, A. H. Hassan, B. Li & J. L. Workman, (2003) Targeting activity is required for SWI/SNF function in vivo and is accomplished through two partially redundant activator-interaction domains. *Mol Cell* **12**: 983-990.

Rando, O. J. & H. Y. Chang, (2009) Genome-wide views of chromatin structure. *Annu Rev Biochem* **78**: 245-271.

Rino, J. & M. Carmo-Fonseca, (2009) The spliceosome: a self-organized macromolecular machine in the nucleus? *Trends Cell Biol* **19**: 375-384.

Ritchie, D. B., M. J. Schellenberg & A. M. MacMillan, (2009) Spliceosome structure: piece by piece. *Biochim Biophys Acta* **1789**: 624-633.

Roberts, S. M. & F. Winston, (1997) Essential functional interactions of SAGA, a Saccharomyces cerevisiae complex of Spt, Ada, and Gcn5 proteins, with the Snf/Swi and Srb/mediator complexes. *Genetics* **147**: 451-465.

Rosbash, M. & B. Seraphin, (1991) Who's on first? The U1 snRNP-5' splice site interaction and splicing. *Trends Biochem Sci* **16**: 187-190.

Rosenblatt, K. P., Z. P. Sun, S. Heller & A. J. Hudspeth, (1997) Distribution of Ca2+-activated K+ channel isoforms along the tonotopic gradient of the chicken's cochlea. *Neuron* **19**: 1061-1075.

Ruby, S. W., T. H. Chang & J. Abelson, (1993) Four yeast spliceosomal proteins (PRP5, PRP9, PRP11, and PRP21) interact to promote U2 snRNP binding to pre-mRNA. *Genes Dev* **7**: 1909-1925.

Sanders, S. L., K. A. Garbett & P. A. Weil, (2002) Molecular characterization of Saccharomyces cerevisiae TFIID. *Mol Cell Biol* **22**: 6000-6013.

Schmucker, D., J. C. Clemens, H. Shu, C. A. Worby, J. Xiao, M. Muda, J. E. Dixon & S. L. Zipursky, (2000) Drosophila Dscam is an axon guidance receptor exhibiting extraordinary molecular diversity. *Cell* **101**: 671-684.

Schwartz, S., E. Meshorer & G. Ast, (2009) Chromatin organization marks exon-intron structure. *Nat Struct Mol Biol* **16**: 990-995.

Seraphin, B. & M. Rosbash, (1989) Identification of functional U1 snRNA-pre-mRNA complexes committed to spliceosome assembly and splicing. *Cell* **59**: 349-358.

Sermwittayawong, D. & S. Tan, (2006) SAGA binds TBP via its Spt8 subunit in competition with DNA: implications for TBP recruitment. *EMBO J* **25**: 3791-3800.

Shepard, P. J. & K. J. Hertel, (2009) The SR protein family. *Genome Biol* **10**: 242.

Sims, R. J., 3rd, S. Millhouse, C. F. Chen, B. A. Lewis, H. Erdjument-Bromage, P. Tempst, J. L. Manley & D. Reinberg, (2007) Recognition of trimethylated histone H3 lysine 4 facilitates the recruitment of transcription postinitiation factors and pre-mRNA splicing. *Mol Cell* **28**: 665-676.

Sjolinder, M., P. Bjork, E. Soderberg, N. Sabri, A. K. Farrants & N. Visa, (2005) The growing pre-mRNA recruits actin and chromatin-modifying factors to transcriptionally active genes. *Genes Dev* **19**: 1871-1884.

Spies, N., C. B. Nielsen, R. A. Padgett & C. B. Burge, (2009) Biased chromatin signatures around polyadenylation sites and exons. *Mol Cell* **36**: 245-254.

Staley, J. P. & C. Guthrie, (1998) Mechanical devices of the spliceosome: motors, clocks, springs, and things. *Cell* **92**: 315-326.

Staley, J. P. & C. Guthrie, (1999) An RNA switch at the 5' splice site requires ATP and the DEAD box protein Prp28p. *Mol Cell* **3**: 55-64.

Sterner, D. E., R. Belotserkovskaya & S. L. Berger, (2002a) SALSA, a variant of yeast SAGA, contains truncated Spt7, which correlates with activated transcription. *Proc Natl Acad Sci U S A* **99**: 11622-11627.

Sterner, D. E. & S. L. Berger, (2000) Acetylation of histones and transcription-related factors. *Microbiol Mol Biol Rev* **64**: 435-459.

Sterner, D. E., P. A. Grant, S. M. Roberts, L. J. Duggan, R. Belotserkovskaya, L. A. Pacella, F. Winston, J. L. Workman & S. L. Berger, (1999) Functional organization of the yeast SAGA complex: distinct components involved in structural integrity, nucleosome acetylation, and TATA-binding protein interaction. *Mol Cell Biol* **19**: 86-98.

Sterner, D. E., X. Wang, M. H. Bloom, G. M. Simon & S. L. Berger, (2002b) The SANT domain of Ada2 is required for normal acetylation of histones by the yeast SAGA complex. *J Biol Chem* **277**: 8178-8186.

Storici, F., L. K. Lewis & M. A. Resnick, (2001) In vivo site-directed mutagenesis using oligonucleotides. *Nat Biotechnol* **19**: 773-776.

Suka, N., Y. Suka, A. A. Carmen, J. Wu & M. Grunstein, (2001) Highly specific antibodies determine histone acetylation site usage in yeast heterochromatin and euchromatin. *Mol Cell* **8**: 473-479.

Sun, H. & L. A. Chasin, (2000) Multiple splicing defects in an intronic false exon. *Mol Cell Biol* **20**: 6414-6425.

Syntichaki, P., I. Topalidou & G. Thireos, (2000) The Gcn5 bromodomain co-ordinates nucleosome remodelling. *Nature* **404**: 414-417.

Tang, J., N. Abovich & M. Rosbash, (1996) Identification and characterization of a yeast gene encoding the U2 small nuclear ribonucleoprotein particle B" protein. *Mol Cell Biol* **16**: 2787-2795.

Tardiff, D. F., S. A. Lacadie & M. Rosbash, (2006) A genome-wide analysis indicates that yeast pre-mRNA splicing is predominantly posttranscriptional. *Mol Cell* **24**: 917-929.

Tardiff, D. F. & M. Rosbash, (2006) Arrested yeast splicing complexes indicate stepwise snRNP recruitment during in vivo spliceosome assembly. *RNA* **12**: 968-979.

Tilgner, H., C. Nikolaou, S. Althammer, M. Sammeth, M. Beato, J. Valcarcel & R. Guigo, (2009) Nucleosome positioning as a determinant of exon recognition. *Nat Struct Mol Biol* **16**: 996-1001.

Timmers, H. T. & L. Tora, (2005) SAGA unveiled. *Trends Biochem Sci* **30**: 7-10.

Valadkhan, S. & J. L. Manley, (2001) Splicing-related catalysis by protein-free snRNAs. *Nature* **413**: 701-707.

Venter, J. C., M. D. Adams, E. W. Myers, P. W. Li, R. J. Mural, G. G. Sutton, H. O. Smith, M. Yandell, C. A. Evans, R. A. Holt, J. D. Gocayne, P. Amanatides, R. M. Ballew, D. H. Huson, J. R. Wortman, Q. Zhang, C. D. Kodira, X. H. Zheng, L. Chen, M. Skupski, G. Subramanian, P. D. Thomas, J. Zhang, G. L. Gabor Miklos, C. Nelson, S. Broder, A. G. Clark, J. Nadeau, V. A. McKusick, N. Zinder, A. J. Levine, R. J. Roberts, M. Simon, C. Slayman, M. Hunkapiller, R. Bolanos, A. Delcher, I. Dew, D.

Fasulo, M. Flanigan, L. Florea, A. Halpern, S. Hannenhalli, S. Kravitz, S. Levy, C. Mobarry, K. Reinert, K. Remington, J. Abu-Threideh, E. Beasley, K. Biddick, V. Bonazzi, R. Brandon, M. Cargill, I. Chandramouliswaran, R. Charlab, K. Chaturvedi, Z. Deng, V. Di Francesco, P. Dunn, K. Eilbeck, C. Evangelista, A. E. Gabrielian, W. Gan, W. Ge, F. Gong, Z. Gu, P. Guan, T. J. Heiman, M. E. Higgins, R. R. Ji, Z. Ke, K. A. Ketchum, Z. Lai, Y. Lei, Z. Li, J. Li, Y. Liang, X. Lin, F. Lu, G. V. Merkulov, N. Milshina, H. M. Moore, A. K. Naik, V. A. Narayan, B. Neelam, D. Nusskern, D. B. Rusch, S. Salzberg, W. Shao, B. Shue, J. Sun, Z. Wang, A. Wang, X. Wang, J. Wang, M. Wei, R. Wides, C. Xiao, C. Yan, et al., (2001) The sequence of the human genome. *Science* **291**: 1304-1351.

Vogelauer, M., J. Wu, N. Suka & M. Grunstein, (2000) Global histone acetylation and deacetylation in yeast. *Nature* **408**: 495-498.

Voth, W. P., Y. W. Jiang & D. J. Stillman, (2003) New 'marker swap' plasmids for converting selectable markers on budding yeast gene disruptions and plasmids. *Yeast* **20**: 985-993.

Wahl, M. C., C. L. Will & R. Luhrmann, (2009) The spliceosome: design principles of a dynamic RNP machine. *Cell* **136**: 701-718.

Wang, A., S. K. Kurdistani & M. Grunstein, (2002) Requirement of Hos2 histone deacetylase for gene activity in yeast. *Science* **298**: 1412-1414.

Wang, E. T., R. Sandberg, S. Luo, I. Khrebtukova, L. Zhang, C. Mayr, S. F. Kingsmore, G. P. Schroth & C. B. Burge, (2008) Alternative isoform regulation in human tissue transcriptomes. *Nature* **456**: 470-476.

Wang, L., L. Liu & S. L. Berger, (1998) Critical residues for histone acetylation by Gcn5, functioning in Ada and SAGA complexes, are also required for transcriptional function in vivo. *Genes Dev* **12**: 640-653.

Weidenhammer, E. M., M. Ruiz-Noriega & J. L. Woolford, Jr., (1997) Prp31p promotes the association of the U4/U6 x U5 tri-snRNP with prespliceosomes to form spliceosomes in Saccharomyces cerevisiae. *Mol Cell Biol* **17**: 3580-3588.

Wetterberg, I., J. Zhao, S. Masich, L. Wieslander & U. Skoglund, (2001) In situ transcription and splicing in the Balbiani ring 3 gene. *EMBO J* **20**: 2564-2574.

Wittschieben, B. O., J. Fellows, W. Du, D. J. Stillman & J. Q. Svejstrup, (2000) Overlapping roles for the histone acetyltransferase activities of SAGA and elongator in vivo. *EMBO J* **19**: 3060-3068.

Wu, J. & M. Grunstein, (2000) 25 years after the nucleosome model: chromatin modifications. *Trends Biochem Sci* **25**: 619-623.

Wu, P. Y., C. Ruhlmann, F. Winston & P. Schultz, (2004) Molecular architecture of the S. cerevisiae SAGA complex. *Mol Cell* **15**: 199-208.

Wu, P. Y. & F. Winston, (2002) Analysis of Spt7 function in the Saccharomyces cerevisiae SAGA coactivator complex. *Mol Cell Biol* **22**: 5367-5379.

Xu, D., S. Nouraini, D. Field, S. J. Tang & J. D. Friesen, (1996) An RNA-dependent ATPase associated with U2/U6 snRNAs in pre-mRNA splicing. *Nature* **381**: 709-713.

Yean, S. L. & R. J. Lin, (1991) U4 small nuclear RNA dissociates from a yeast spliceosome and does not participate in the subsequent splicing reaction. *Mol Cell Biol* **11**: 5571-5577.

Yean, S. L., G. Wuenschell, J. Termini & R. J. Lin, (2000) Metal-ion coordination by U6 small nuclear RNA contributes to catalysis in the spliceosome. *Nature* **408**: 881-884.

Yudkovsky, N., J. A. Ranish & S. Hahn, (2000) A transcription reinitiation intermediate that is stabilized by activator. *Nature* **408**: 225-229.

Zapater, M., M. Sohrmann, M. Peter, F. Posas & E. de Nadal, (2007) Selective requirement for SAGA in Hog1-mediated gene expression depending on the severity of the external osmostress conditions. *Mol Cell Biol* **27**: 3900-3910.

Zaug, A. J., P. J. Grabowski & T. R. Cech, (1983) Autocatalytic cyclization of an excised intervening sequence RNA is a cleavage-ligation reaction. *Nature* **301**: 578-583.

Zavanelli, M. I., J. S. Britton, A. H. Igel & M. Ares, Jr., (1994) Mutations in an essential U2 small nuclear RNA structure cause cold-sensitive U2 small nuclear ribonucleoprotein function by favoring competing alternative U2 RNA structures. *Mol Cell Biol* **14**: 1689-1697.